ABSTRACT

Title of Document: *PROTEUS MIRABILIS* SURFACE SENSING SIGNAL TRANSDUCTION PATHWAY

Vanessa Mercee D. Vargas, Master of Science, 2013

Directed By: Dr. Robert Belas
Department of Marine Biotechnology

Proteus mirabilis swarmer cell differentiation is induced by physical conditions that inhibit rotation of vegetative swimmer cell flagella. The protein FliL is important however, signal transduction to induce differentiation is unknown. Defects in differentiation result from mutations in genes involved in cell-wall formation and flagellar genes regulations. I hypothesized that upon surface contact, torsional stress due to inhibition of filament rotation activates stress response, induces swarmer cell differentiation and passes this signal to the protein FliL through a second protein, UmoA. My results show that the expression of stress gene *cpxP* changed over swarming migration with highest levels at zones of initial inoculation and areas where migration stops. I also show that complementation of *fliL* defect is viscosity-, temperature- and wettability–dependent, and *fliL* cells show improved swarming migration compared to wild-type on 0.8% agar. The study gave insight on the role of cell wall stress and *fliL* in swarming.

PROTEUS MIRABILIS SURFACE SENSING SIGNAL TRANSDUCTION PATHWAY

By

Vanessa Mercee D. Vargas

Thesis submitted to the Faculty of the Graduate School of the

University of Maryland, College Park, in partial fulfillment

of the requirements for the degree of

Master of Science

2013

Advisory Committee:

Professor M. Robert Belas, Chair
Professor Harold Schreier
Professor Kevin Sowers

Acknowledgement

I would like to express my deepest gratitude to everyone who helped in my journey through the Marine Estuarine and Environmental Science. The experience, the maturity, and knowledge that I have acquired are all thanks to all of you.

I would like to thank my advisor, Dr. M. Robert Belas for his guidance and mentorship through these years. His award from the National Science Foundation, MCB-0919820, supported this opportunity given to me and the research described in my thesis. Thank you also to my committee members Dr. K. Sowers and Dr. H. Schreier, for recognizing my efforts and providing additional guidance.

My heart-felt thanks to the past and present members of the Belas Lab; the MEES office and my fellow graduate students, and; the faculty and staff of the Department of Marine Biotechnology and the Institute of Marine and Environmental Technology. Specially to Dr. K. Paynter, Ms. Debbie, Dr. R. Hill, Dr. S. Chun, Dr. Y.Y. Li, Dr. P. Sule, Jeanette, Julie, Ryan, Mildred, Tonya and Teresa.

Most of all, thank you to my loved ones who have supported me and gave me strength. To Thong and Ba Ngoai, I would never be able to get this far without your love and confidence. To my family - My Dad, Mom, siblings - RB, Rissa, JR and Yda, and nieces- Doniya and MM, you all are my inspiration and I am very much thankful for all your love and support. To all my friends and KaizenTao family, thank you for all your support.

Table of Contents

List of Tables	**iv**
List of Figures	**v**
Chapter I: Introduction	**1**
Chapter II: *cpxP* changes during swarmer cell differentiation	**27**
Chapter III: The role of the cell wall stress response and the UmoA protein in swarmer cell differentiation	**47**
Chapter IV: Determining regions of *fliL* important in swarming in *Proteus mirabilis*	**72**
Chapter V: Summary and Conclusion	**109**
Appendix	**114**
References	**117**

List of Tables

Table Title	Page
Table 1. Strains, plasmids and primers used in chapter 2	**29**
Table 2. Homology between *P. mirabilis* and *E. coli* stress genes	**37**
Table 3. Strains and plasmids used in chapter 3	**49**
Table 4. Primers used in chapter 3	**53**
Table 5. Representative Bi-Parental Mating Results between BB2000 and S17-1λpir with pGP704 plus stress genes in varying conditions[1]	**58**
Table 6. Strains and plasmid used in chapter 4	**74**
Table 7. Properties of FliL	**79**
Table 8. XL-1 Red Control	**86**
Table 9. Swarming Assay Condition Tested	**90**
Table 10. Properties of the conserved FliM peptiode in wild-type and mutant	**93**

List of Figures

Figure Title	Page
Fig. 1. Comparison of a wildtype swarmer cell, swimmer cell and *fliL* pseudoswarmer cell.	2
Fig. 2. Schematic representation of the flagellar hook-basal body complex.	5
Fig. 3. Gene hierarchy and flagellar assembly.	9
Fig. 4. The Rcs Phosporelay Signaling Cascade activates a number of cellular processes.	15
Fig. 5. The Cpx System	19
Fig. 6. The Psp Response Pathway	21
Fig. 7. The BaeSR System	23
Fig. 8. The σ^E-dependent extracytoplasmic stress response	25
Fig. 9. Plasmid pYL10	31
Fig. 10. Induction of Cell Envelope Stress Genes	36
Fig. 11. Predicted tertiary structure of *rprA* from *E. coli; Salmonella;* and *Proteus.*	38
Fig. 12. $cpxP_{Ec}$ expression during *P. mirabilis* swarming	39
Fig. 13. β-galactosidase assay of $cpxP_{Ec}$ expression during swarming.	40
Fig. 14. Levels of β-galactosidase activity changes over swarming migration	41
Fig. 15. *cpxP* expression of individual cells during differentiation changed in both β-galactosidase activity and transcription of $cpxP_{Pm}$ as measured by RT-PCR	42
Fig. 16. Alignment of the promoter region of *cpxP* of *E. coli* and *P. mirabilis.*	45
Fig. 17. Map of constructs used in the study to generate mutants via Campbell-style integration	51
Fig. 18. Suicide vector used in the study	52
Fig. 19 Plasmids where Kan^R and Cm^R were amplified.	52
Fig. 20. PspA amplification of two putative PspA mutant	60
Fig. 21. Cm^R CpxR' Transconjugants	63
Fig. 22. PCR amplification of *cpxAR'* transformants from electroporation	65
Fig. 23. PCR amplification of the *cpxR* gene in putative '*cpxAR'* mutants.	65
Fig. 24. Putative *umoA* mutants exhibiting reduce swarming	68
Fig. 25. Plasmid pYL98	76
Fig. 26. Predicted Structure of FliL.	81
Fig. 27. Predicted secondary structure of *in silico*-generated *fliL* mutants	84
Fig, 28. Amplified *fliL* from Swr^+ YL1003/pYL98.	87
Fig. 29. YL1003/pYL98 swarming in different agar concentration	88
Fig. 30. Swarming of BB2000 and YL1003/pYL98 is viscosity dependent	89
Fig. 31. Screening for possible *fliL* mutants	91
Fig.32. Sequence alignment of Swr^- mutant from XL1 Red Mutagenesis	92
Fig.33. Schematic Diagram of XL1-Red Mutageneis of pYL98 and succeeding screens for swarming.	95
Fig. 34. Mutated FliL from XL1-Red Mutagenesis	96

Chapter I: Introduction

Proteus mirabilis. *Proteus mirabilis* is a Gram-negative bacterium, a member of Enterobacteriaceae, is famous for its ability to differentiate from short swimmer cells to long, multinucleated and multi-flagellated swarmer cells (2). Named after the mythological Greek god *Proteus*, Hauser (3) first used the name *Proteus* in 1885 to describe a bacterium isolated from putrefied meat that was able to change its shape. He first identified two species *P. mirabilis* and *P. vulgaris*, based on the speed of their ability to liquify gelatin (3). Currently, the genus *Proteus* contains 5 known species including *P. vulgaris, P. myxofaciens,* and *P. hauseri,* and three unnamed genomospecies designated as *Proteus* genomospecies 4, 5, and 6 (4).

P. mirabilis is the leading cause of catheter-associated urinary tract infections (CAUTIs) and is most common in long-term catherization (5, 6). To establish colonization and subsequent development of protected communities called biofilms (7), bacteria must first gain entry and adhere tightly to the catheter and resist urine flow (8-10). Bacterial fimbriae, which are bacterial appendages with adhesive proteins, are responsible for this adherence. Although its exact role in *P. mirabilis'* catheter adherence and colonization is still unknown, fimbriae are use to mediate attachment to the urinary tract. *P. mirabilis* also produces urease that causes blockage of the catheter by formation of crystalline biofilms (8, 11). *P. mirabilis* has the ability to move across a surface, in a form of flagellum-dependent motility called swarming (12-14). It has been shown that swarming is required for catheter migration and subsequent entry in to the urinary tract (15).

Swarming of *P. mirabilis* is cyclic and can be broken down into four parts (16): (i) swarmer cell differentiation; (ii) the lag period prior to active movement; (iii) swarming colony migration; and (iv) consolidation (where the cells stop moving and de-differentiate to swimmer cell morphology). This cyclic pattern also correlates with the expression of proteins such as ZapA protease, flagellin, urease, and hemolysin (17).

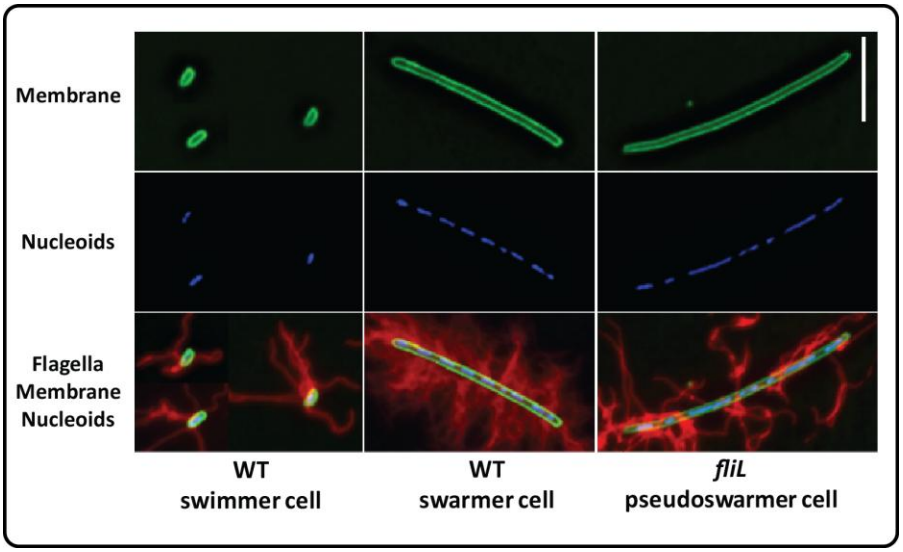

Fig. 1. Comparison of a wildtype swarmer cell, swimmer cell and *fliL* pseudoswarmer cell. *P. mirabilis'* swimmer cells are short vegetative cell with 4-5 flagella. Swarmer cells are long cells with multiple flagella and multiple nucleoids and no septae. Pseudoswarmer cells are similar to swarmer cells but have fewer flagella. Adapted from Lee *et al* (18).

P. mirabilis transitions between two cell morphotypes depends on environmental conditions. In liquid environments, *P. mirabilis* exists as a swimmer cell that is 1.5 to 2.0 μm in length with 4-10 flagella per cell (2). Upon surface contact, swimmer cells differentiate into swarmer cells that are 40 to 80 μm in length, lacks septa and contain

multiple nucleoids and multiple flagella (2, 18). As first reported by Belas and Suvanasuthi (19), conditions that inhibit flagellar rotation induce differentiation from swimmer to swarmer cells. Mutations in three genes associated with the flagellar basal body, *fliL*, *fliF*, and *fliG* result in cells, termed pseudoswarmers, which are swarmer-like cells that are elongated in non-inducing conditions, i.e. broth, or are hyper-elongated on agar media (19). The difference between *fliL* pseudoswarmers and wild-type swarmer cells is that the former has far fewer flagella than the latter (18).

Bacterial motility. Motility allows bacteria to find new environments when nutrients are limiting. Microorganisms have developed a number of motility systems to allow them to move in liquid or viscous media or even on surfaces (20). Bacterial locomotion can be swimming and/or tumbling in liquid, and swarming, twitching, or gliding over surfaces (20-22). In this study, I focused on the surface-induced and the flagella-mediated switch between swimming and swarming.

The Bacterial Flagellum. Bacteria swim and swarm by rotating their helical flagella (23). Flagella are long, thin filaments that protrude from the cell body and are made up of the protein flagellin (Fig. 2). A flagellum consists of three parts: the basal body that anchors the flagellum to the membrane and also serves as the rotary motor, the hook that serves as a universal joint, and the external filament that serves as a helical propeller. The hook and basal body (HBB) spans the bacterial membranes (Fig. 2). Assembly of the structure is a sequential process and the transcription of the flagellar regulon of enteric bacteria is based on three promoter classes temporally regulated in response to assembly.

The basal body, composed of the rod and three rings termed MS, P and L ring, is the first to be constructed, which starts with the insertion of the MS (M=membrane; S=supramembrane) ring into the inner membrane. The MS-ring is embedded in the cytoplasmic membrane and is composed of the protein FliF (24). The P-ring is associated with the peptidoglycan layer and is composed of FlgI, while the L ring is associated with the outer membrane (lipopolysaccharide; LPS) and is composed of FlgH (25, 26). The proteins FlgB, FlgC, and FlgF constitute the proximal rod, while FlgG that of the distal rod (27). Individual extracytoplasmic flagellar subunits are secreted through the MS ring after the assembly of an associated type III secretion system (TTSS) (28). The flagellar TTSS is composed of six transmembrane proteins that form an export channel (FlhA, FlhB, FliO, FliP, FliQ and FliR) and three cytosolic proteins (FliH, FliI and FliJ) that interact with the channel (27) (Fig.2). The hook structure of *Salmonella* is composed of about 120 copies of a single protein FlgE, and its length is controlled at 55±6 nm by FliK, a protein that determines flagellar hook length. FliK also functions in changing the secretion-specificty substrate to prevent the premature export of late flagellar substrates (29, 30). The hook-associated proteins, HAP1 and HAP3, consisting of FlgK and FlgL, respectively, serve as a junction between the hook and the filament (31).

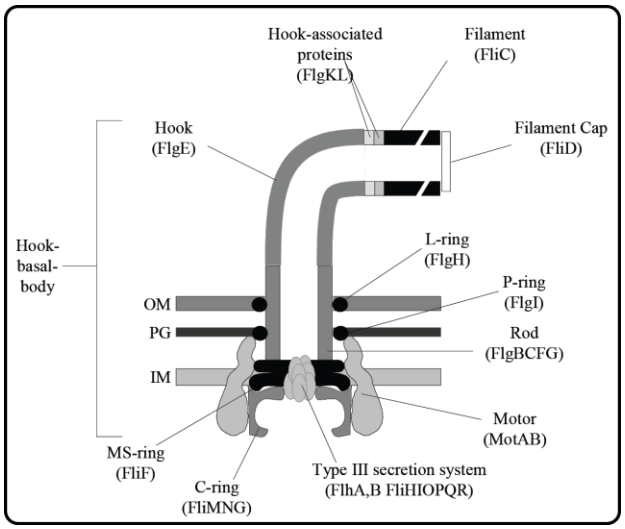

Fig. 2. Schematic representation of the flagellar hook-basal body complex. (Adapted from Aldridge and Hughes (1))

The C-ring (composed of proteins FliM, FliN and FliG) is mounted on the cytoplasmic face of the MS ring (32-35) and forms the switch complex that functions in the rotation/switching/assembly of the flagellum (36, 37). The clockwise-counter clockwise switching is mainly attributed to FliM (38). The N-terminal domain of FliM contains a conserved peptide (LSQXEIDALL) where CheY-P directly binds to switch flagellar rotation direction (39). CheY-P is the phosphorylated response regulator that is controlled by the histidine kinase CheA in response to chemoreceptor occupancy (40). The C-terminal of FliM binds FliN to form a stable FliM-FliN complex (41). FliN is suggested to have a more of a structural role in the C-ring of the flagellum (42).

MotA and MotB exists in the cytoplamic membrane, assemble around the rotor, together conduct the flow of H^+ across the membrane, and are involve in torque generation (43-45). The proton motive force (PMF) powers the Mot complex by creating an inwardly directed electrochemical potential of hydrogen across the bacterial cell membrane due to a concentration gradient. The C-ring and the motor proteins, MotA and

MotB, which forms the stator, achieve rotation of the HBB structure. FliG, in particular its C-terminal domain, is directly involved in rotation, its conserved charged residues gives FliG two orientations (46) that interacts with MotA (47, 48) which could be important in switching rotational direction.

Bacterial Swimming. The helical shape of a flagellum is suited to locomotion of microorganisms as they operate at a low Reynolds number, where the viscosity of the surrounding water is much more important than the cell's mass or inertia (49). If a bacterium is slower than 1 μm/s, moving is useless as nutrient would diffuse faster than the cell can move (49). The length and number of flagella, as well as the maximum motor rotation rate dictates the fastest speed that a bacterium can physically attain (49). The direction of rotation can switch almost instantaneously, caused by a slight change in the position of a protein in the rotor. Swimming gives bacteria a survival advantage in different environmental conditions and gives them a competitive advantage in acquiring nutrients (50).

Bacterial Swarming. The operational definition of swarming motility is a rapid multicellular bacterial surface movement powered by rotating flagella (51). Swarming differs from swimming in that it is a movement of a group of bacteria over a surface, rather than swimming motility of individual cells in liquid. Swarming can play a role in the bacteria's colonization of natural niches. Bacteria living as a group in surface colonies have distinct cell types with specialized functions that contribute to growth and survival,

with better access to nutrients and greater defense mechanisms from desiccation and antagonists (22).

The most important requirement for swarming is the flagella. Mutations targeting flagella synthesis or flagella functions result in a non-swarming (Swr^-) phenotype (52, 53). Swarmer cells have an increased number of flagella (2, 54). Most swarming bacteria develop characteristic peritrichous/lateral flagella in which multiple flagella are randomly distributed on the cell surface (54). There are species, like *V. parahaemolyticus,* that swim with a polar flagella and then induce lateral (peritrichous) flagella when swarming (55). Other species, such as *P. aeruginosa,* swarms while retaining its polar flagellum but requires the expression of an alternative motor to facilitate its movement over surfaces (54). In general, swarming requires multiple flagella on the cell surface. Even *P. aeroginosa* may produce two polar flagella when swarming.

Swarming bacteria move side-by-side in cell groups called rafts. It has been suggested that movement as a group likely increases fluid retention around the cells (22). Water content is an important factor when inducing swarming in laboratory conditions, too little results in poor swarming, while too much might induce cellular dedifferentiation and swimming motility (54, 56). Different swarming bacteria can swarm over a range of surface viscosities, and some require surface-active agents or surfactants, ampiphatic molecules that the bacteria synthesize and secrete to reduce surface tension (54, 57-60).

Another requirement for swarming motility is contact with a surface (61, 62). The mechanism of how a bacteriaum senses and determines it is on a surface and the molecular signaling that follows remains poorly understood. In *V. parahaemolyticus* and *P. mirabilis,* flagella are the surface sensors (19, 55). In *P. mirabilis,* inhibition of

flagellar rotation induces differentiation of swimmer to swarmer cell, and the protein FliL assesses the health of, or torsional constraint on, the flagellar motor through interactions with other flagellar proteins and passes this signal through a still unknown mechanism (18, 19, 63). This will be discussed more in a later section.

Swarming migration is often associated with bioflim formation, two events that are reversely regulated. Genes required for swarming are turned off in biofilms and vice-versa. It has been suggested that swarming is important when cells re-colonize a new surface, and hence its regulation is a target to control biofilm formation. Swarming has also been correlated with pathogenicity in *P. mirabilis* (19). Often, toxin secretion was also found to be co-regulated with swarming motility (54). It has also been observed that swarming of *Salmonella enteric* serovar *Typhimurium* (herein *Salmonella*) shows an elevated resistance to certain antibiotics. This can also be due to the fact that surfactants that promote swarming are also potent antimicrobials (54).

FlhDC. The production of a flagellum is sequential and tightly regulated. Flagellar proteins are only synthesized once they are needed for assembly. Transcriptional control is based on three flagellar promoter classes (64). The flagellar master operon *flhDC* controls flagellum production and is transcribed from a class 1 promoter. Their protein product forms a heteromultimeric complex, $FlhD_4C_2$, that promotes σ^{70}-dependent transcription from the class 2 flagellar promoters (65). Class 2 promoters then direct transcription of genes needed for HBB assembly and the gene for the flagellum specific sigma factor FliA (σ^{28}). Once HBB is completed, σ^{28} RNA polymerase (64) transcribes the class 3 promoters that are specific for later assembled components. Class 3A genes

require both σ^{28} and FlhDC while class 3B genes only require σ^{28}. FlgM, which is a class 3A gene, is a σ^{28}- specific anti-sigma factor (66). Once the HBB is completed, the cell secretes FlgM and σ^{28} transcription ensues.

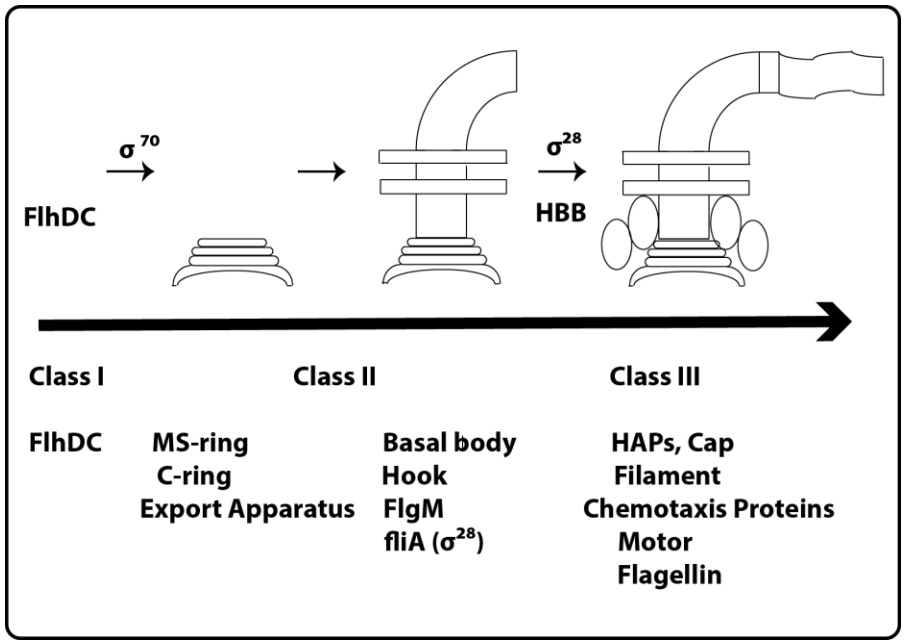

Fig. 3. Gene hierarchy and flagellar assembly. Assembly of the flagellum is based on a three class gene hierarchy temporally regulated to ensure that genes are expressed as their products are needed for assembly. The sole class I gene encodes the master regulator *flhDC*. Class II genes encode the regulatory protein σ^{28} and the anti-sigma factor FlgM. They also facilitate completion of the hook-basal body structure, which serves as key checkpoint for coordinating assembly and regulates Class III genes. Figure adapted from Smith and Hoover (67).

Regulation of FlhDC. Defects in *flhDC* in *P. mirabilis* result in non-swimming, non-swarming cells that do not elongate (19). Expression of *flhDC* is negatively regulated by the RcsBCD phosphorelay, which represses swarming and differentiation (68). Other

regulators include the leucine-responsive regulatory protein, Lrp (69), the flagellar secretion apparatus component FlhA (70, 71), post-transciptional binding of the protein CsrA (72), proteolytic regulation by the Lon protease (73) and over-expression of the amino acid decarboxylase, DisA (74, 75).

Other important regulators are the Umo proteins (**u**pregulator of the **m**aster **o**peron) discovered by Dufour *et al* (76). The *umo* loci in *P. mirabilis* were identified as genes that when over-expressed could suppress the swarming defect of a mutation in the secretion chaperone for hook-associated proteins, *flgN* (76, 77). There are four *umo* genes: *umoA, umoB, umoC,* and *umoD*, which can increase expression of *flhDC* when over expressed. UmoA and UmoC proteins appear to be unique to *P. mirabilis.* UmoD protein is similar to YcfJ of *Escherichia coli* while UmoB is similar to YrfF in *E. coli* and IgaA in *S. Typhimurium* (76). Loss of *umoD* and *umoB* results in a non-swarming phenotype while mutation in *umoA* and *umoC* has little effect on swarming in *P. mirabilis* (76). Expression of *umoA* and *umoD* increases in swarmer and pseudoswarmer cells, suggesting a link between the Umo proteins and surface sensing through *fliL* (63).

FliL. Physical conditions that inhibit the rotation of the peritrichous flagella of the swimmer cell triggers differentiation of swimmer cells to swarmer cells (19). A mutation in *fliL*, the first gene in the class 2 *fliLMNOPQR* operon results in an inappropriate production of swarmer cells, termed pseudoswarmer cells, in normally non-inducing conditions (19). Formation of pseudoswarmers indicates that this defect affects the surface-sensing mechanism. However, the molecular mechanism of the signal

transduction from the flagella to *fliL* and its relation to swarmer cell differentiation is still unknown.

For a long time, the function of FliL remained mysterious. FliL is ubiquitous among the genomes of flagellated bacteria and appears to have species-specific function. As mentioned, it is the first gene in the class 2 operon that encodes proteins of the C-ring of the flagella (FliM and FliN) and of the flagellar export apparatus (FliO, FliP, FliQ and FliR) (78). Null mutations in *fliL* in alphaproteobacteria results in a non-motile phenotype (79-81) while in Enteric bacteria, *i.e. P. mirabilis*, *E. coli*, and *Salmonella*, the loss of FliL does not dramatically affect swimming, but has a major effect on swarming (19, 82, 83). In *C. crescentus* and *Salmonella*, a defect in *fliL* results in flagella detachment (79, 82). In the case of *Salmonella*, this breakage occurs between the proximal and distal rod proteins (FlgF and FlgG) (82). This suggests that one of the functions of FliL is to maintain the integrity and stability of the flagellar rod.

Mutations in *P. mirabilis fliL* also confer a non-swarming phenotype and production of pseudoswarmer cells in non-inducing conditions (broth). There are 3 published *fliL* strains of *P. mirabilis*: BB2204 (*fliL*::Tn*5*-Cm), which is non-motile; YL1001, which is a motile revertant of BB2204; and YL1003 (*fliL*::*kan*-nt30), which swims but does not swarm (18, 19, 63). All three however produces pseudoswarmer cells in broth and are complemented by $fliL^{+}$ *in trans* resulting in wild-type cell elongation. The non-motile phenotype of BB2204 is attributed to polar effects, as shown in YL1001, however both strains show an alteration of the C terminus of FliL suggesting that the C terminus of FliL may be responsible for the pseudoswarmer cell phenotype. YL1003 on the other hand has an insertion at nt 30 of the *fliL* coding region generating a protein that

is truncated. Lee *et al.* (18) reported that in YL1003 (*fliL::kan*-nt30), the Swr$^-$ phenotype can be complemented but it requires three elements: the *P. mirabilis fliL* promoter, *fliL* coding region, and a portion of *fliM* 5' sequence (18). Interestingly, it was found that expression of *umoA* and *umoD* is increased in wildtype swarmer cells and *fliL* pseudoswarmer cells suggesting a role of *umoA* and *umoD* in surface sensing and swarmer cell differentiation (63).

Mechanisms of surface sensing and swarmer cell differentiation. In a study by Belas *et al.* (84), aside from flagellar defects, *P. mirabilis* mutants defective in swarmer cell elongation also arises from mutations in genes involved in cell wall formation. As previously mentioned, the flagella serves as the surface sensor and in *P. mirabilis*, evidence suggests that the protein FliL is central to this interaction as discussed earlier (19).

The outer membrane of gram-negative bacteria contains LPS and also, in the case, of enteric bacteria, the enterobacterial common antigen (ECA) (85). LPS contains a lipid A region, a core region, and the O-antigen region (86). The major form of ECA is ECA_{PG} which is covalently linked to phosphoglyceride (85). The two minor forms are ECA_{LPS}, which is ECA attached to the LPS core region, and ECA_{CYC}, which are water-soluble cyclic forms of ECA (85), both are only found in certain enteric bacteria. Both LPS and ECA play a role in bacterial motility. O-antigen mutants have been shown to exhibit motility defects in *Myxococcus xanthus, Salmonella, and E. coli* (87-89). In *P. mirabilis,* LPS plays a role in swarming (84). Specifically, transposon insertions in the *waaL (rfaL)*

gene that encodes O-antigen ligase prevents an increase in *flhDC* expression (90). In *Serratia marcescens,* ECA is important for swarming by upregulating *flhDC* (91).

The molecular mechanism and signal transduction pathway from surface contact to swarming, specifically swarmer cell differentiation in *P. mirabilis*, remain unknown. Two-component systems (TCS) are the most common ways that bacteria utilize in response to environmental signals (92). They typically include a sensor histidine kinase (HK) and a response regulator (RR). Upon sensing a specific environmental signal, the sensor HK autophosphorylates and transfers phosphoryl group from ATP to a histidine residue. The phosphate is then transferred to a specific aspartate residue on the RR protein causing a conformational change. This phosphorylation and dephosphorylation of the response regulator modulates the protein activity by affecting its DNA binding ability and acting as a transcription regulator.

The cell envelope stress response system. Integrity of the bacterial cell wall is pertinent to the organisms survival, thus the bacteria have mechanisms that can sense perturbations in the cell wall (93). There are five extracytoplasmic stress signaling mechanisms in *E. coli*: σ^E, Psp (phage shock protein), Cpx (conjugative plasmid expression, Bae (bacterial adaptive response), and the Rcs system (93).

The Rcs phosphorelay system. The Rcs (for regulator of capsular synthesis) phosphorelay is composed of the sensor RcsC, an intermediary phosphotransferase (RcsD), and the response regulator RcsB (94). Originally identified for its role in colanic

acid biosynthesis (95), the RCS system has now been reported to be involved in a number of bacterial cell processes such as flagellar synthesis (96), O-antigen chain length determination (97) and ECA structure alteration (91), motility (98), cell wall stress response, and antibiotic resistance (99) among others. Remarkably, the Rcs phosphorelay is found to be specific to enteric pathogens (*Enterobacteriaceae*) (100). Homologs of associated genes have been mapped in some enterics, and the *rcsC, rcsD*, and *rcsB* gene loci appear to be conserved across these species (101).

The Rcs system was initially recognized as a TCS composed of the RcsC as the sensor HK, which autophosphorylates at a conserved His residue, and transfers its phosphoryl group to an Asp residue on RcsB, the cognate RR (95). Recent identification of a phosphorelay protein, YojN, later renamed RcsD, led to the distinction of the Rcs system from a typical two-component system to a more complex phosphorelay system with signal (phosphate) traveling from RcsC→RcsD→RcsB (102). RcsA is degraded by the Lon protease and its apparent instability has implication in regulation (94). RcsA serves as auxiliary protein to RcsB, the primary regulator. In the absence of RcsA, over expression of RcsB is sufficient to activate the *cps* gene. However, no *cps* gene is detected in the absence of RcsB (103).

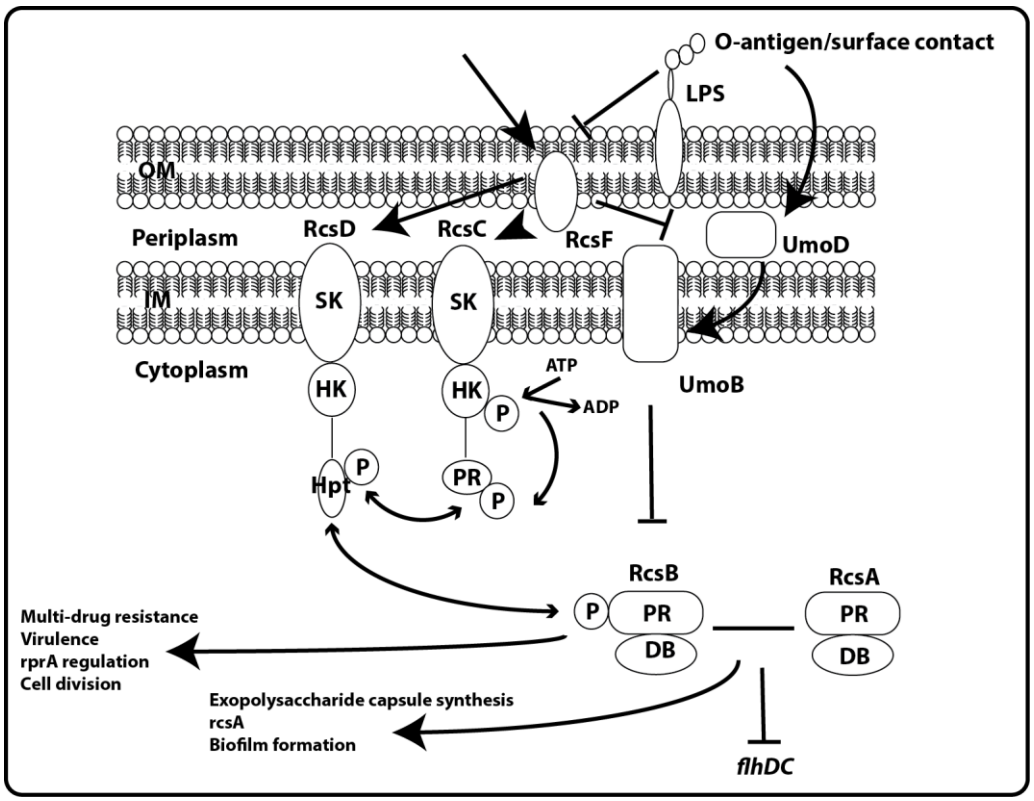

Fig. 4. The Rcs Phosporelay Signaling Cascade activates a number of cellular processes. Flow of signal is from RcsF→RcsC→RcsD→RcsB. RcsB may or may not complex with RcsA for signal transduction. Adapted form Rogov *et al.*(103) and Morgenstein et al (104).

Another target of RcsB is the small RNA RprA discovered in connection with the stationary phase sigma factor, RpoS (105). Regulation of RprA synthesis is by the Rcs system, established through mutation studies wherein *rcsB* null mutations abolishes RprA basal levels (106). Mutations in RcsC activate capsule synthesis and activate *rprA* expression. Consequently, activation of the Rcs system leads to increased RpoS synthesis. It was later found that *rprA* activation is an RcsA-independent process (94). Another outer membrane lipoprotein, the small protein RcsF has been implicated in the Rcs system (107). RcsF activates RprA and its RcsB-dependent promoter. RcsF also

plays a role in sensing cell surface perturbation and then passing the signal to RcsC, such that it has been suggested that signaling proceeds through RcsF→RcsC→RcsD→RcsB, with RcsF transferring signal from the cell surface to the Rcs system (94, 107).

The Rcs system induces expression of a number of pathways, but in the case of the *flhDC* master operon, it is a repressor. Regulation of FlhDC is dependent on RcsA and RcsB, by directly binding to the RcsAB box of the *flhDC* promoter region (96). Also, it has been demonstrated that in an *rcsB* mutant, there is up-regulation of *flgC, flgG* and *flgl* flagellar genes (108). Furthermore, *rcs* gene mutants of *Erwinia amylovora* showed irregular and reduced motility in swarming plates (109). In *P. mirabilis*, mutations in a gene called *rsbA* (regulator of swarming behavior) exhibited a precocious swarming phenotype (68). This gene was later identified as a homolog of RcsD, indicating a role of the Rcs system in swarming which FlhDC directly regulates.

A strong RcsCBD response, manifested by flagellum production inhibition and overproduction of capsule materials were found in mutants affecting *Salmonella* IgaA (Intracellular Growth Attenuator A) stability (110). IgaA is a negative repressor of the Rcs system by favoring the switch from RcsB-P (active) to the dephosphorylated state (inactive), suggesting a role for the dephosphorylated form of RcsB in regulation (111). In *P. mirabilis*, IgaA is the homolog of UmoB, which is part of the *umo* loci.

Work by the Rather group at Emory University (90) also demonstrated that O-antigen is important in surface-sensing in *P. mirabilis* through the Rcs phosphorelay system. They proposed a model for Rcs inhibition by surface contact wherein O antigen mediates a perturbation or torsional change in the outer membrane that results in two opposing effects: RcsF inhibition and an increase in UmoD activity (104). UmoB (IgaA)

is activated by UmoD reducing the levels of phosporylated RcsB removing repression of *flhDC* expression (104).

Peptidoglycan stress activates the Rcs pathway and subsequently contributes to its intrinsic antibiotic resistance (99). Different β-lactam antibiotics, cefsulodin, amdinocilin and cef-amd, activate the Rcs system, indicating that inhibition of peptidoglycan synthesis is an activator, which enhances bacterial survival independent of capsule production (99). In *S. marcescens*, disruptions of ECA, results in an envelope disturbance that induces the Rcs regulatory system (91). Aside from peptidoglycan, it was reported that the Rcs phosphorelay also responds to perturbations in MDO (membrane-derived oligosaccharides) and LPS.

The role of the Rcs system in biofilm formation has been actively investigated, although it has been shown that initial attachment does not depend on *rcsC* or *rcsB,* suggesting a much later role (94). The transfer of *E. coli* from liquid to an agar surface causes induction of Rcs genes, particularly, RcsC dependent genes.

The CpxAR TCS. The Cpx (conjugative plasmid expression) envelope stress response in *E. coli* is activated by a variety of stressors to the bacterial cell envelope and activates a number of genes including periplasmic protein folding (DsbA, PpiA, PpiD) and degradation factors (DegP) (112). It mainly responds to alterations in the cell envelope composition i.e. changes in NlpE levels and over-expression of misfolded envelope proteins (113). It was shown to be activated by adhesion to abiotic surfaces through the NlpE and has been implicated in biofilm formations in *E. coli* (114). Cpx also responds to osmolarity, chemical signals such as ethanol and indole, and changes in pH (115).

Cpx is a TCS consisting of a sensor histidine kinase CpxA and a cytoplasmic response regulator CpxR (115). Both CpxA and CpxR display homology to the conserved phosphotransfer domains of other two component systems. CpxA localizes in the inner membrane and contains both a periplasmic and cytoplasmic domain while CpxR is predicted to encode an OmpR-like transcriptional activator (115). CpxA autophosphorylates on a conserved histidine in the cytoplasmic kinase domain in the presence of a stress signal. Phosphate is transferred to a conserved aspartate domain in the N-terminal of CpxR. Phosphorylated CpxR activates the transcription of genes involved in periplasmic protein folding (DsbA, PpiA, PpiD) and degradation factors (DegP) (116), as well as genes involved in lipid and lipopolysaccharide metabolism (117).

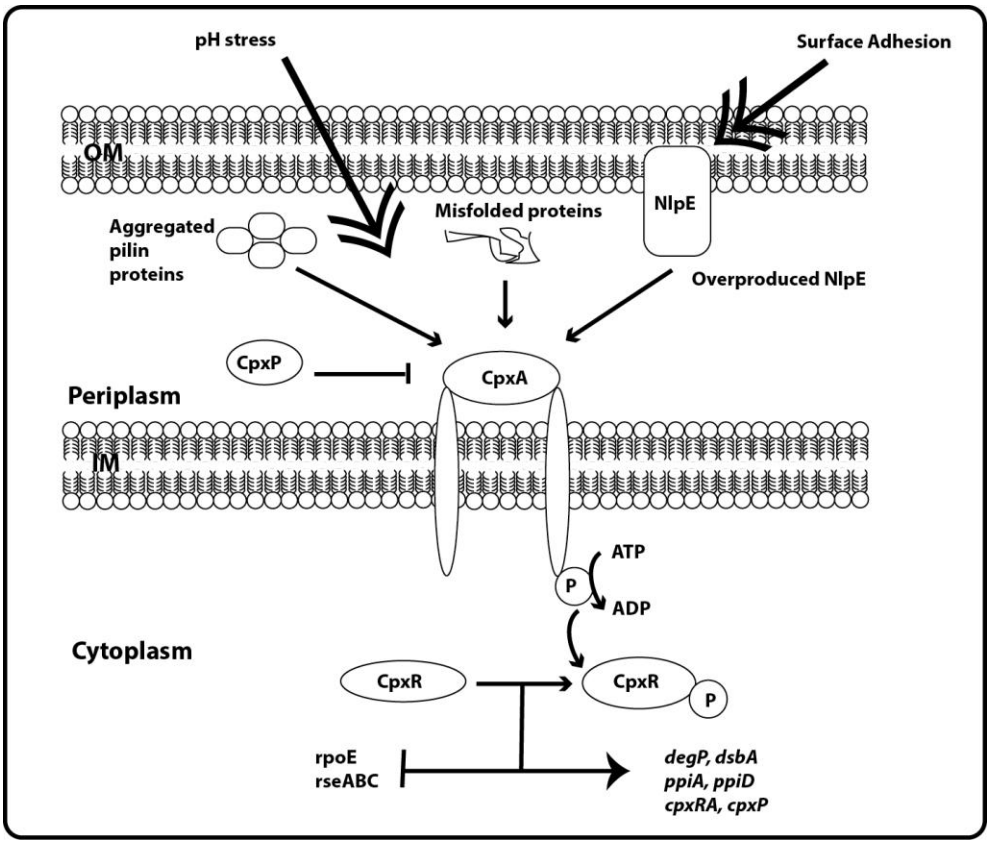

Fig. 5. The Cpx System. Envelope stress signals are sense by the sensor kinase CpxA, which in turn autophosphorylates and then passes the phosphate group to CpxR. CpxR-P then activates transcription of the Cpx regulon, a gene of which is *cpxP* whose protein product CpxP binds and inhibits CpxA via a feedback inhibition. CpxP dissociates from CpxA in the presence of envelope stress (118). Figure adapted from Rowley et al (118).

Another member of the *cpx* regulon is the protein CpxP that was originally identified as an up-regulated product of the Cpx pathway in *E. coli* (119). It serves as a negative regulator of the Cpx system by binding to the periplasmic sensor domain of CpxA. It responds to protein misfolding, acting as a stress sensor of the pathway and facilitates the degradation of misfolded proteins (115). Alkaline conditions induce CpxP in a CpxA-dependent fashion. CpxP is required for suppressing misfolded P pilus

subunits-associated toxicity by degradation of DegP with these misfolded subunits (119). CpxP is a small periplasmic protein made up of 147 amino acids (120) and contains a conserved LTXXQ motif shared by a large family of proteins of which CpxP and Spy are included (120, 121). Mutations in and near these motifs disrupt the regulatory function of CpxP and it is suggested that this motif has a structural role in stabilizing the protein based on its crystal structure (120).

The Psp regulatory pathway. The phage-shock protein or PSP response pathway is induced by conditions that may cause dissipation of the proton-motive force (PMF) i.e. proton ionophores such as CCCP and mislocalization of secretin proteins (122-124). It was originally discovered in *E. coli* as a protein produced at high concentrations during filamentous phage infection, thus named phage-shock protein A or PspA (125). The PSP system consists of six proteins, PspA, PspB, PspC, PspD, PspF and PspG (126, 127). In non-inducing conditions, PspA binds to PspF (a member of the enhancer binding protein family of transcriptional regulators) preventing transcriptional activation.

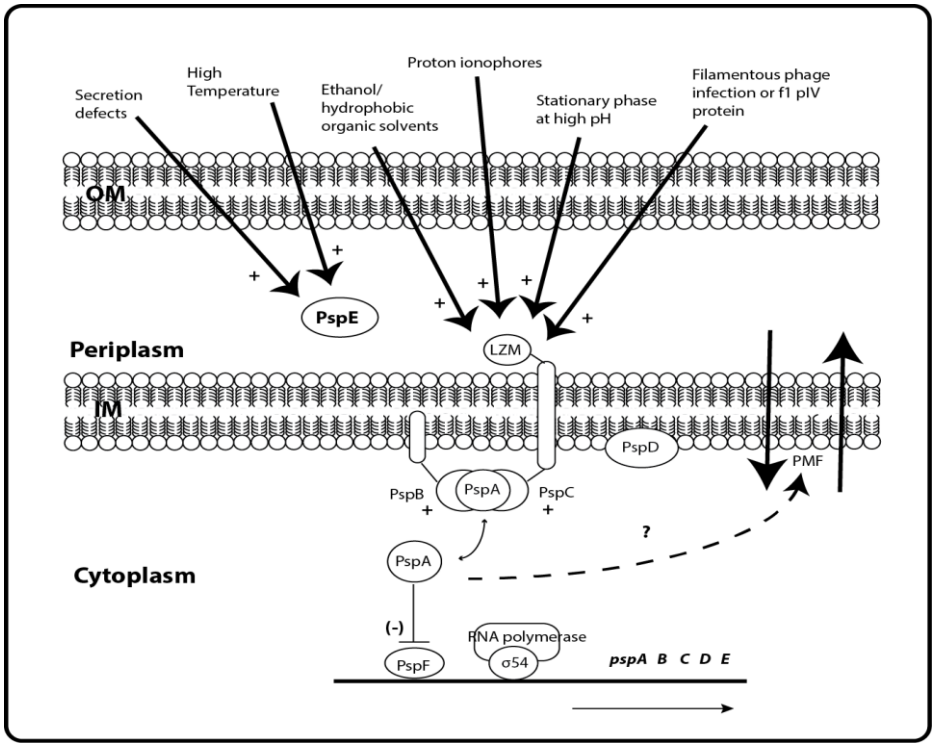

Fig. 6. The Psp Response Pathway. In non-inducing conditions, PspF is inhibited by PspA binding. PspC and PspB, located in the inner membrane sense inducers such as mislocalize secretins and PMF dissipation. They then bind to PspA, freeing PspF to activate transcription of the *pspA* operon and the *pspG* gene. PspA is then over-expressed and serves several physiological function such as maintaining the PMF. Figure adapted from Rowley *et al.*(118).

Upon induction, cytoplasmic membrane proteins PspB and PspC binds to PspA freeing PspF to activate transcription of the *pspA* operon and *pspG* gene, predicted to encode a small hydrophobic protein that traverses the cytoplasmic membrane (127). PspA reduces dissipation of the PMF while the roles of PspD and PspG remain unknown (128, 129). Little is known about the physiological role of the Psp response. All the inducing conditions and associated phenotype with *pspA* null mutants all point to PMF maintenance (130). Psp also supports virulence in *Yersinia enterocolitica* and *Salmonella*

(131). In *E. coli*, it was observed that the Psp response is induced during biofilm formation and that *pspF* null mutants have biofilm-formation defect (132).

The BaeSR TCS. The BaeSR (bacterial adaptive response) pathway is a classical TCS consisting of a sensor HK, BaeS, and a response regulator, BaeR. It was initially identified in the search for the additional pathway in the spheroplast induction of *spy* expression acting in conjunction with the *cpxAR* system (133). It was later found that Spy expression via the Cpx system is caused by copper ions while zinc ions, tannin, and indole caused/enhanced its expression via the Bae pathway (121). Over expression of the pilin subunit, PapG also induces the Bae pathway as well as the CpxAR and σ^E stress response systems. Other compounds such as sodium tungstate, zinc, flavonoids myricetin, quercetin, and morin also strongly induce the Bae pathway (134). The BaeR regulon consists of *arcD*, *spy*, and the *mdtABCDbaeSR* operon. MdtABC and ArcD are RND (resistance, nodulation and cell division) multidrug efflux pumps, while MdtD is a predicted MFS (major facilitator division) multidrug efflux pump (133). Spy is a periplasmic protein whose function is relatively unknown, deletion mutant showed no defect under both normal and stress conditions (121). However, Spy shares 25% identity to CpxP, implying that the function of BaeSR is related to the stress response system. Analysis of the Spy crystal structure showed that Spy and CpxP have similar structures (121). LeBlanc *et al.* (134) concluded that the Bae pathways restore envelope homeostasis in response to specific envelope –damaging MdtABC substrates and removes these compounds by up regulating the MdtABC efflux pump.

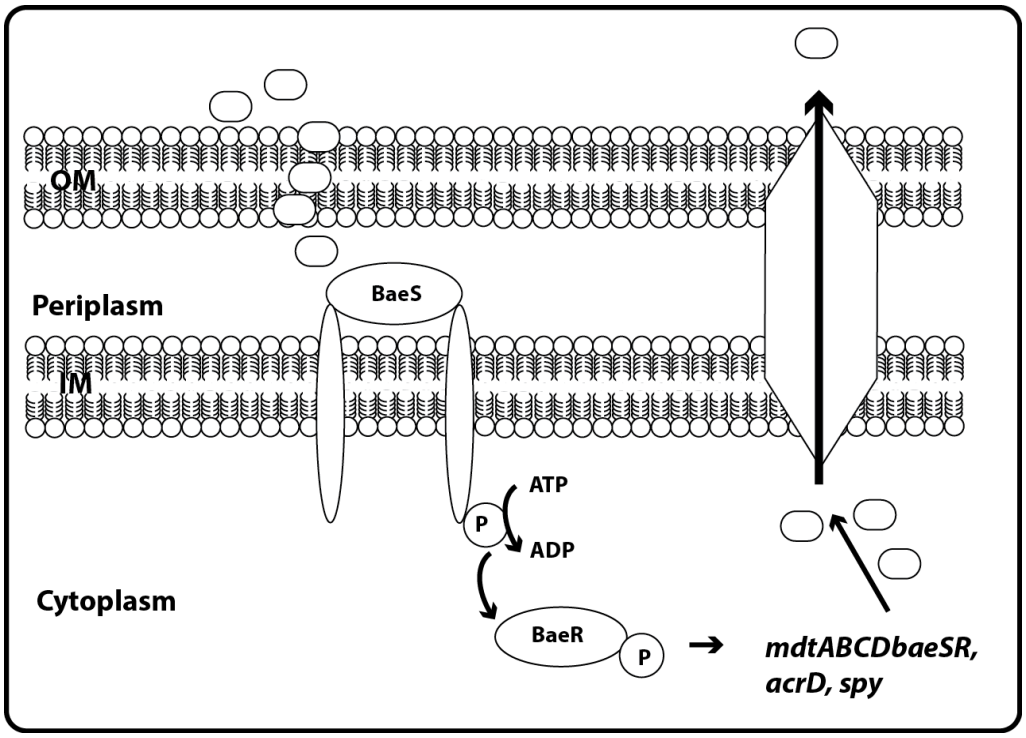

Fig. 7. The BaeSR System. The BaeSR is an atypical two-component system with BaeS as the sensor kinase that sense environmental signals and BaeR as the response regulator that facilitates the transcription of the Bae regulon upon induction.

σ^E (ECF sigma factor). The sigma factor σ^E (also called σ^{24}), encoded by *rpoE*, is the most studied member of ExtraCytoplasmic Function or ECF sigma factors that are implicated in sensing stress in the cell envelope of Gram-negative bacteria. It was initially discovered as a new heat shock sigma factor in *E. coli* that recognizes and transcribed the P3 promoter of *rpoH*, whose product is the heat shock sigma factor, σ^{32} (135). σ^E is induced by misfolding of the outer membrane proteins (OMPs), heat shock, OMP genes over-expression, and mutations in chaperones genes required for OMP folding (113, 136-141). In non-inducing conditions, σ^E is bound to the anti-sigma factor RseA at the inner membrane preventing its interaction with RNA Polymerase (136, 142).

RseB binds to RseA to protect it from proteolysis. In inducing conditions, misfolded OMPs activates the protease DegS, which then cleaves RseA. RseA is further cleaved by RseP. This releases the cytoplasmic domain of Rse- bound σ^E, which ClpXP degrades. σ^E is then released to the cytoplasm allowing it to interact with the RNA polymerase and subsequently transcribe genes in its regulon.

In *P. mirabilis*, mutation in *ugd* (UDP-glucose dehydrogenase) and *galU* (UDP-glucose pyrophosphorylase) activates the promoter activity of *rpoE* (143). These genes are involved in LPS synthesis, and mutants of these have a lower ability to swarm (84, 143). Further, over-expression and constitutive active expression of *rpoE* resulted in lower *flhDC* expression and a decrease in swarming (143). On the other hand, in *Salmonella*, a deletion mutant of *rpoE* is non-motile and causes a down-regulation of some class 2 and class 3 genes while *flhDC* expression remained the same (144).

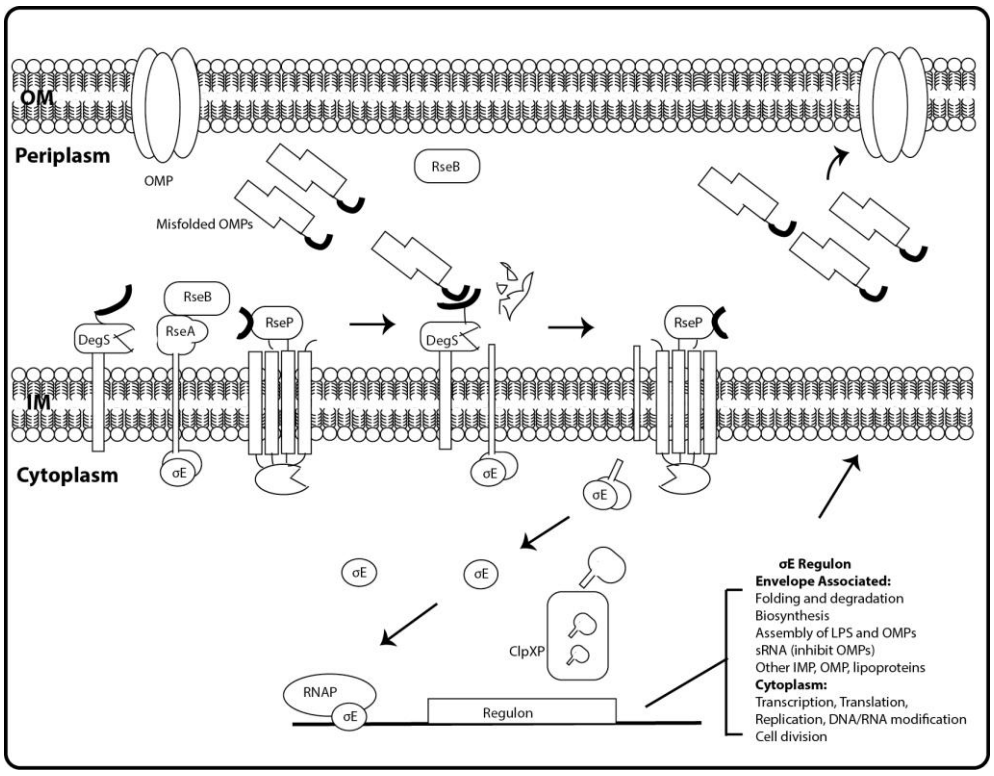

Fig. 8. The σ^E-dependent extracytoplasmic stress response. σ^E is bound by RseA and RseB in the membrane. Misfolded OMPs then activate DegS that cleaves RseA, followed by subsequent degradation by RseP and ClpXP releasing σ^E to the cytoplasm where it can interact with RNA polymerase and direct transcription of its regulon. Figure adapted from Hayden and Ades (145).

Cell envelope stress response and swarmer cell differentiation. The central question of this study revolves around the molecular mechanism of signal transduction upon surface contact as the signal passes through the flagella, *fliL*, and *flhDC* to induce swarmer cell differentiation. Armitage *et al*. (146, 147) first suggested the possible relation between alternations in the cell envelope and swarmer cell differentiation in *P. mirabilis.* They reported that there is a change in the proportion of LPS with O-antigen side chains between swimmer cells and swarmer cells. As was discussed previously, evidence now links the cell envelope, particularly LPS, with swarming and flagellar

control (63, 84, 90, 143). Furthermore, it has been shown that in *fliL* pseudoswarmers and wild-type swarmer cells, genes involved in outer membrane fluidity, membrane permeability, and cell wall function are up regulated (63). Perturbations in the cell envelope are sensed by five known cell envelope stress system (93). The role of the Rcs system and RpoE stress response has now been directly linked to *fllhDC* control and swarming in *P. mirabilis* (68, 90, 104, 143). The Cpx system on the other hand, has been implicated in motility and biofilm formation in *E. coli* (114). The Psp system responds to changes in the PMF (124), which is directly related to flagella function. It was also implicated in biofilm formation in *E. coli* (132). Homologs of both Cpx and Psp genes exist in *P. mirabilis*. Another group of related proteins, the Umo proteins appears to be also important in this signal transduction (63, 76, 104).

In this study, I hypothesize that (1) upon surface contact torsional stress due to inhibition of filament rotation activates a cell-envelope stress response and induces swarmer cell differentiation; (2) the regulator UmoA is part of this signal transduction; and, (3) the protein FliL is central to this function.

Chapter 2: *cpxP*$_{Ec}$ Expression Changes During Swarmer Cell Differentiation

Abstract

Proteus mirabilis swarmer cell differentiation is induced by physical conditions that inhibit rotation of vegetative swimmer cell flagella. The molecular mechanisms that transduce the signal from the flagella to induce differentiation are unknown. Defects in differentiation result from many different types of mutations, particularly in genes involved in cell wall formation. Recent transcriptomic analyses of swarmer cells indicate major changes in the expression of these genes. Furthermore, defects in Rcs cell envelope stress response genes results in precocious swarming behavior, suggesting a link between cell envelope stress and swarmer cell differentiation. I hypothesized that upon surface contact torsional stress due to inhibition of filament rotation activates a cell-envelope stress response and induces swarmer cell differentiation. I measured heterologous *cpxP* expression, a gene that is highly expressed during envelope stress, using a *cpxP*$_{Ec}$*::lacZ* transcriptional fusion. A series of Lac^{+} zones that correlated with areas of consolidation were observed when wild-type *P. mirabilis* carrying *cpxP*$_{Ec}$*::lacZ* swarmed over LB agar. β-galactosidase measurements using the Miller assay confirmed that expression of *cpxP*$_{Ec}$ changes during swarming, with the highest levels occurring at the initial inoculation point and in consolidation zones (when cells are in the swimmer phase), while the lowest levels were found in areas predominated by swarmer cells. *cpxP*$_{Ec}$ expression of individual cells during differentiation and over swarming migration changed in β-galactosidase activity while transcription of *cpxP*$_{Pm}$ as measured by RT-PCR still needs to be validated. These results suggest a possible link between cell envelope stress, inhibition of flagellar rotation, and swarmer cell differentiation.

Introduction

Proteus mirabilis is a Gram-negative bacterium and a member of the Enterobacteriaceae. Swarming of *P. mirabilis* is cyclic and can be broken down into four parts (16), (i) swarmer cell differentiation; (ii) the lag period prior to active movement; (iii) swarming colony migration; and (iv) consolidation (where the cells stop moving and de-differentiate to swimmer cell morphology). Differentiation of swimmer cells to swarmer cells is triggered by physical conditions that inhibit the rotation of the peritrichous flagella of the swimmer cell (19). A mutation in *fliL*, the first gene in the class 2 *fliLMNOPQR* operon results in inappropriate production of swarmer cells, termed pseudoswarmer cells, in normally non-inducing conditions (19). However, the molecular mechanism of how the signal transmits from the flagella to *fliL* and how these affect swarmer cell differentiation is still unknown. Transcriptome analyses of swarmer cells showing major changes in the expression of genes involved in the cell envelope (63) and the precocious phenotype of cells defective in *rcsD* (68), a gene in the Rcs cell wall stress pathway suggest involvement of the extracytoplasmic stress signaling pathways.

There are five extracytoplasmic stress signaling mechanisms in Enterics, these are the σ^E, Psp (phage shock protein), Cpx (conjugative plasmid expression), Bae (bacterial adaptive response), and the Rcs (regulator of capsule synthesis) system (93). As was discussed in the earlier section, all but the Bae system directly or indirectly affects surface sensing and flagella function. In order to determine if cell wall stress plays a role in swarmer cell differentiation, the Belas Laboratory (Department of Marine Biotechnology, University of Maryland Baltimore County and Institute of Marine and Environmental Technology) obtained *E. coli* reporter strains for all five stress systems

that were used by Bury-Mone *et al* (93). I was only able to express heterologously the *E. coli* $cpxP_{Ec}$*::lacZ* transcriptional fusion in *P. mirabilis* to monitor $cpxP_{Ec}$ expression changes during *P. mirabilis* swarming migration. I tested the hypothesis that swimmer cells placed on an agar surface have torsional stress on their flagellar motors. Torque on the motors generates envelope stress, which, through a currently unknown mechanism, increases the transcription of *flhDC,* resulting in swarmer cell differentiation.

Materials and Methods

Bacterial strains and culture conditions. All strains and plasmids used are listed in Table 1. *P. mirabilis* BB2000 and *E. coli* strains were grown in LB broth, at 37°C, and agitated at 200 rpm. Colonies were grown in LSW^- (10 g $liter^{-1}$ Bacto tryptone, 5 g $liter^{-1}$ yeast extract, 0.4 g liter−1 NaCl, 5 ml $liter^{-1}$ glycerol, 20 g $liter^{-1}$ Bacto agar) plates for BB2000 strains and 1.5% LB agar (LB medium containing 15 g $liter^{-1}$ Bacto agar) plates for *E. coli* strains at 37°C. Selective media contained ampicillin (Amp 100) at 100μg/ml. Swarming assays were performed on 1.5% LB agar plates at 37°C and 30°C.

Table 1. Strains and plasmids used in the study

Strains	**Genotype/Properties/Sequence**	**Source**
BB2000	wild-type *Proteus mirabilis*	Lab strain[1], (53)
DH5α($cpxP_{Ec}$*::lacZ*)	*E. coli* (cpxP_{Ec}*::lacZ*)	This study
BB2000($cpxP_{E}c$*::lacZ*)	*P. mirabilis* ($cpxP_{Ec}$*::lacZ)*	This study
TR323	MC4100 (pLONG $cpxP_{Ec}$*-lacZ*)	(115)
T350	MC4100 λRS88 ($cpxP_{Ec}$*::lacZ*)	(115)
TR530	MC4100 λRS88 (spy_{Ec}*::lacZ*)	(148)
MC3	MC4100 λRS88 ($pspA_{Ec}$*::lacZ*)	(123)
GEB658	MC4100 λRS88 (*rprA142*p_{Ec}*::lacZ*)	(149)

CAG16037	MC1061 φλ (*RPOH3$_{Ec}$::lacZ*)		(150)
Plasmid			
pLONG	*cpxP$_{Ec}$::lacZ*		(115)
pDH300	*rprA142p$_{Ec}$::lacZ*		(106)
pYL10	*lacZ*		Y.Y. Lee[2]
pVV1	*cpxP$_{Ec}$::lacZ*		This study
Primers			
FpcpxP$_{Ec}$	5'-TTGAATTCTGCACGTACGCTAGCAGA-3'	PCR primer for cloning *E. coli cpxP* promoter; contains the Ecor1 site at 5' end	(115)
RpcpxP$_{Ec}$	5'-TAGAATTCGGCTTTCAGCTCAGCAAACT-3'	PCR primer for cloning *E. coli cpxP* promoter; contains the Ecor1 site at 5' end	(115)
FPrpraA$_{Ec}$	5'-TTAGAATTCCTTGATATTGCTTGCTC	PCR primer for cloning *E. coli rprA* promoter; contains the Ecor1 site at 5' end	(106)
RPrprA$_{Ec}$	5'-CTGGAATTCGAGCTAATAGTAGGCA	PCR primer for cloning *E. coli rprA* promoter; contains the Ecor1 site at 5' end	(106)
FcpxP$_{Pm}$	5'-CAGCCAATTCCTATCCG-3'	RT-PCR primer for cloning *P. mirabilis cpxP* coding region	This study
RcpxP$_{Pm}$	5'-GCATGGTTATCCCAGTT-3'	RT-PCR primer for cloning *P. mirabilis cpxP* coding region	This study
FrpoA$_{Pm}$	5'-TAGAATTCTTAATGTTGTGCTCGCC-3'	RT-PCR primer for cloning *P. mirabilis rpoA* coding region	This study
RrpoA$_{Pm}$	5'-CTGAATTCAATCGCTCTATCAAAAGGT-3'	RT-PCR primer for cloning *P. mirabilis rpoA* coding region	This study

[1] Belas Laboratory, Department of Marine Biotechnology, UMBC and Institute of Marine and Environmental Technology, University Systems of Maryland
[2]Dr. Yi-Ying Lee, post-doctoral fellow at the Belas Laboratory

Cloning. *E. coli* reporter strains for the five CES genes were obtained from the corresponding author of Bury-Mone *et al.* (93). The promoter region was amplified and ligated to the *EcoR1* site of plasmid pYL10 (Fig. 9), a low-copy-number, Amp^R,

pWSK29 derivative (151, 152) harboring a promoterless *lacZ*. BB2000 was then transformed by electroporation with the resulting plasmid. Strain BB2000/pVV1 (*cpxP*$_{Ec}$::*lacZ*) was generated and used for succeeding experiments. Each reaction mixture (50 µl) contained 10× ThermoPol buffer, 25 ng DNA, a 200 nM concentration of each primer, 200 µM deoxynucleoside triphosphates (dNTPs), and 5 U Taq polymerase (NEB). Thermocycling conditions were as follows: 94°C for 5 min; 30 cycles of 94°C for 1 min, 62°C for 30 s, and 72°C for 30 s; and 72°C for 5 min. All plasmid and primers used and generated are Table 1.

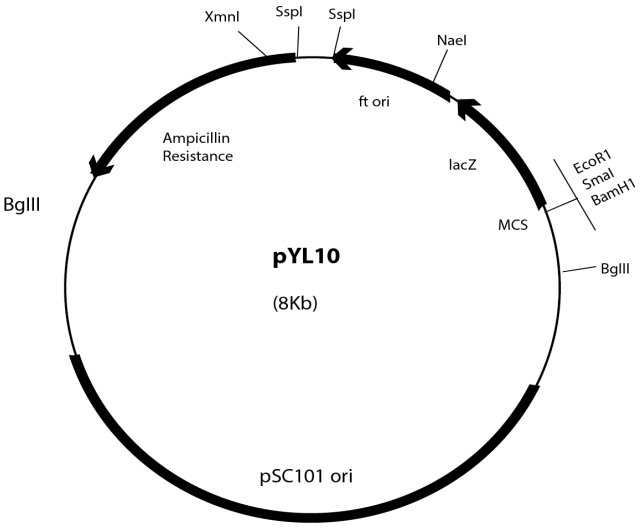

Fig. 9. Plasmid pYL10.

pYL10 is a low-copy-number, Amp^{R}, pWSK29 derivative harboring a promoterless *lacZ.*

DNA Purification and Electroporation. Prior to electroporation, DNA was purified by ammonium acetate precipitation following the Belas Laboratory protocol. Briefly, 10 µl of stock 100x tRNA was added to 20 µl of ligation mixture and 20 µl of 7.5M ammonium acetate, mixing thouroughly by vortexing. One-hundred µl of absolute ethanol was added and the solution is then chilled on ice for 15 min. Using a refrigerated centrifuge set at

4°C, the mixture was centrifuge at 14000 x g for 15 min and then the supernatant was carefully decanted. The pellet was then washed with 1 ml 70% ethanol and centrifuge at 14000 x g for 15 min at RT. The supernatant was removed and the pellet dried in the speed vac for 15 min. The DNA is resuspended in sterile distilled de-ionized water.

Purified DNA at a concentration of 100 ng/ul was added to a pre-chilled sterile 1.5 ml microcentrifuge tube and then 50 µl of ice-thawed competent cells were pipeted in. The mixture was placed into a clean, sterile and ice-cold 0.2 cm electroporation cuvettes (BTX) and pulsed at 2.5 kV and a time constant ideally between 4.2 to 4.9 msec. Pre-warmed 1 ml LB broth was immediately added and gently mixed with the electroporated cells. The mixture was then placed in pre-warmed 1.5 ml microcentrifuge tubes and allowed to recover at 37°C without agitation for 30 min, and then incubated for an additional 1 - 1.5 h with agitation. Cells were then spread-plated with dilution in the appropriate media with Amp - 1.5% LB agar for *E. coli* and LSW^- agar for *P. mirabilis*. Succesful electroporation/cloning is checked by plasmid extraction using the Qiagen Miniprep Kit and RE digestion.

Swarming Assay. BB2000/pVV1 cells were grown overnight in 2 ml LB broth plus Amp 100 from a single colony. The overnight culture was then washed and diluted 1:100 with 1% Phosphate buffer saline (PBS, pH 7.4; 8 g $liter^{-1}$ NaCl, 0.2 g $liter^{-1}$ KCl, 1.44 g $liter^{-1}$ Na_2HPO_4, 0.24 g $liter^{-1}$ KH_2PO_4). Five microliters of which was drop-inoculated at the center of 1.5% LB agar with Amp (100 µg per mL) and XGal (5-bromo-4-chloro-3-indolyl-β-d-galactopyranoside) at a final concentration of 40 µg per mL. Swarming migration was observed at 37°C for 24 h; for documentation, plates were incubated at

30°C. Samples for β-galactosidase measurements were taken from an overnight swarm plates grown in 1.5% LB agar with XGal and Amp, 37°C at consolidation and swarming zones. Samples were also taken every 5 mm from initial point of inoculation after swarming on 1.5% LB agar with XGal and Amp, 30°C.

β-galactosidase Assay. β-galactosidase was measured using the Thermo Scientific Yeast β-galactosidase Assay Kit (Thermo Scientific) following the manufacturer's protocol for Microplates (stopped). Optical densities were measured using the Spectramax M5. β-galactosidase activity was measured using the following equation:

$$\mathbf{(1000 \times A_{420})/(t \times V \times OD_{600}) = \beta\text{-galactosidase activity}}$$

t = time of incubation (in minutes); V = volume of cells (ml) used in the assay

***cpxP*$_{Ec}$ expression during swarmer cell differentiation.** BB2000 (*cpxP*$_{Ec}$*::lacZ)* was grown overnight in 2 ml LB broth plus Amp from a single colony at 37C, 200 rpm. Overnight cells were then washed with 1% PBS and diluted 1:1000. One-hundred microliters of the diluted culture was then spread-plated in parallel pre-warmed 1.5% LB-agar plates incubated at 37°C. The remaining diluted cultures served as time 0. Samples were then harvested at times 1.5, 4 and 5 hour by washing the plate with 5ml 1% PBS and scraping the cells with disposable, sterile spreader. Cells are then analyzed for β-galactosidase activity as a proxy for *cpxP*$_{Ec}$ expression.

RNA extraction, cDNA synthesis, and RT-PCR. Total RNA was extracted and purified from bacterial samples using Ribopure (Ambion) following the manufacturer's instructions, with a 1-h DNAse treatment. RNA was converted to cDNA using High-capacity cDNA Reverse Transcription Kit and RNAse inhibitor (Applied Biosystems), with a 25°C for 10 min, 37°C for 2 h, and 85°C for 5 min thermocycling regime. RT-PCR was performed with *rpoA* (RNA polymerase subunit alpha) serving as a control.

Statistical Analysis. The mean and standard deviation of the mean of β-galactosidase activity were calculated using Prism, version 4.0, software (GraphPad). Graphs were made using Origin 6.1 (OriginLab) and error bars show standard error of the mean with n = 3.

Results

There are five major cell envelope stress (CES) systems in enterics: Bae, Cpx, Psp, Rcs and σ^E pathways, that may be monitored by *spy::lacZ, cpxP::lacZ, pspA::lacZ, rprA::lacZ* and P3*rpoH::lacZ*, respectively (93). I initially obtained reporter plasmids pDH300 (*rprA::lacZ*) (106) and pLONG ($cpxP_{Ec}$*::lacZ*) (115) with *E. coli* promoters in pRS415 plasmid backbone. The plan was to use these plasmids in wild-type BB2000 and BB2204 (*fliL*::Tn5-Cm ;the only *fliL* mutant being used in the lab at that time) to measure expression of each promoter during swarmer cell differentiation. However, after repeated attempts to transform pDH300 into BB2000, reviewing and troubleshooting the protocols from competent cells to electroporation to antibiotics concentration, I have found that

pRS415 with its colE1 origin was simply not compatible for use in BB2000. At the same time I have received from the corresponding author (93) *E. coli* chromosomal reporter strains for each of five stress genes that was used in their study.

Induction of *E. coli* CES genes. As a preliminary test, I made sure that the induction results for each *E. coli* strain were reproducible using the Miller assay for β-galactosidase activity (Fig. 10a). I then PCR-amplified the $rprA_{Ec}$ and $cpxP_{Ec}$ promoters and then ligated into pYL10, a low-copy-number, Amp^R, pWSK29 derivative (151, 152) harboring a promoterless *lacZ*, thereby constructing a transcriptional fusion between $rprA_{Ec}$ gene promoter and *lacZ*. I started with $rprA_{Ec}$ for the RCS system and followed this cloning with $cpxP_{Ec}$ for the Cpx system. Upon construction, I tested the induction of the $rprA_{Ec}$*::lacZ* fusion in *E. coli* DH5α using indole (Fig. 10b). Using the original MC4100/pDH300(*rprA::lacZ)* reporter strain and DH4α as controls, I compared DH5α/pYL10 ($rprA_{Ec}$*::lacZ)* and BB2000/pYL10 ($rprA_{Ec}$*::lacZ*). The two strains showed different fold-change induction pattern and were even lower than the DH5α strain without a reporter plasmid. MC4100/pDH300, on the other hand, did not show any induction. I decided to move along with *cpxP*, having shown that $cpxP_{Ec}$ can be induced in *E. coli* (Fig. 10a) and check if the $cpxP_{Ec}$*::lacZ* can be induced in BB2000. Using the known inducers of the *cpx* system, $CuCl_2$ and indole, I was able to show that $cpxP_{Ec}$ can be induced in BB2000 with 2.0 to 2.5-fold induction (Fig. 10c). Once this was established, I then monitored $cpxP_{Ec}$ expression during swarming.

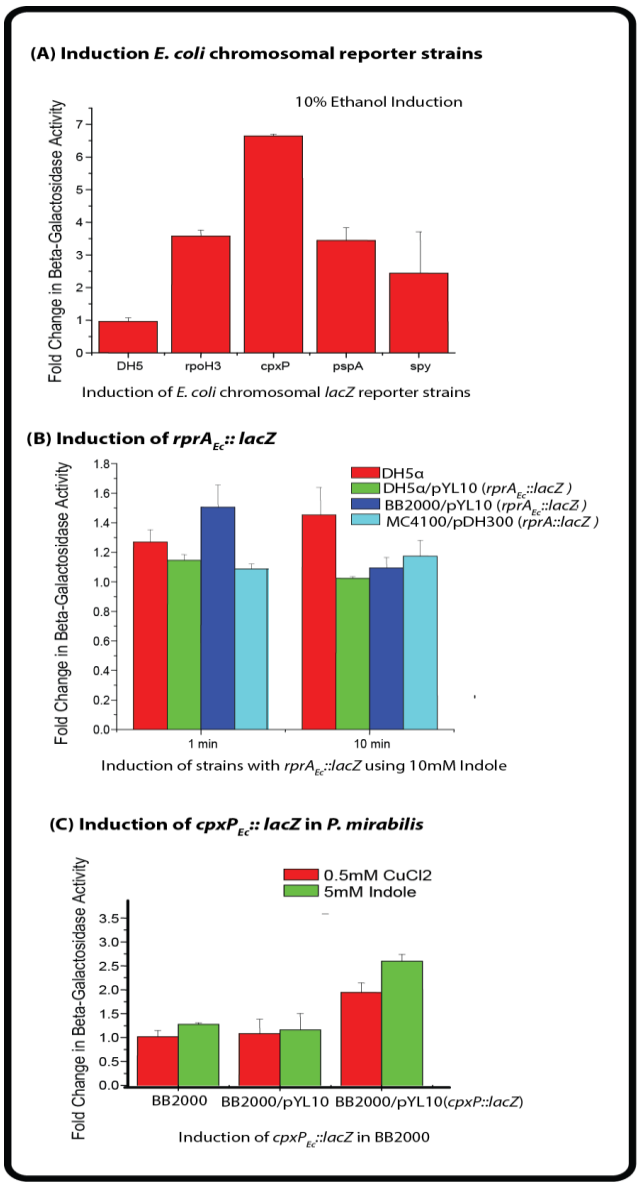

Fig. 10. Induction of Cell Envelope Stress Genes. The induction of the five CES genes was tested using: (A) *E. coli* chromosomal fusion for rpoH, Cpx, Psp and Bae (*spy)* systems with 10% ethanol while (B) a plasmid reporter pDH300 ($rprA_{Ec}$*::lacZ)* for the RCS system was used with 10mM indole. The induction of (B) $rprA_{Ec}$ and (C) $cpxP_{Ec}$ was also tested by constructing a reporter plasmid using pYL10, a plasmid harboring a promoterless *lacZ*. Error bars show standard error of the mean; n = 3.

Homology of CES genes between *P. mirabilis and E. coli.* Using the NCBI-BLAST database, I have determined the homology of the different stress genes between *E. coli* and *P. mirabilis* (Table 2). All the *E. coli* stress genes except for the Bae circuit have homology to *P. mirabilis* genes. (Due to lack of homology, Bae is not included in Table 2). Also, the predicted tertiary structure (RNAfold webserver (153); http://rna.tbi.univie.ac.at/cgi-bin/RNAfold.cgi) of the small RNA *rprA*, which is induced by *rcsB* independent of *rcsA* is very different from that of *E. coli and Salmonella* (Fig. 11).

Table 2. Homology between *P. mirabilis* and *E. coli* stress genes

Stress genes	Nucleic Acid/Amino Acid[1] composition		homology[2]	e-value
	E. coli	*P. mirabilis*		
rprA	105	106	62%	2.00E-11
rpoH	284	284	82%	9.00E-175
cpxA	457	455	79%	0
cpxR	232	232	87%	5.00E-148
cpxP	166	188	41%	3.00E-33
pspA	222	222	69%	1.00E-111
PspB	74	74	64%	2.00E-34
pspF	335	335	70%	6.00E-37

[1] Nucleic acid composition for the small RNA *rprA;* the rest are amino acid composition
[2]Homology and E-value based on NCBI-BLASTp

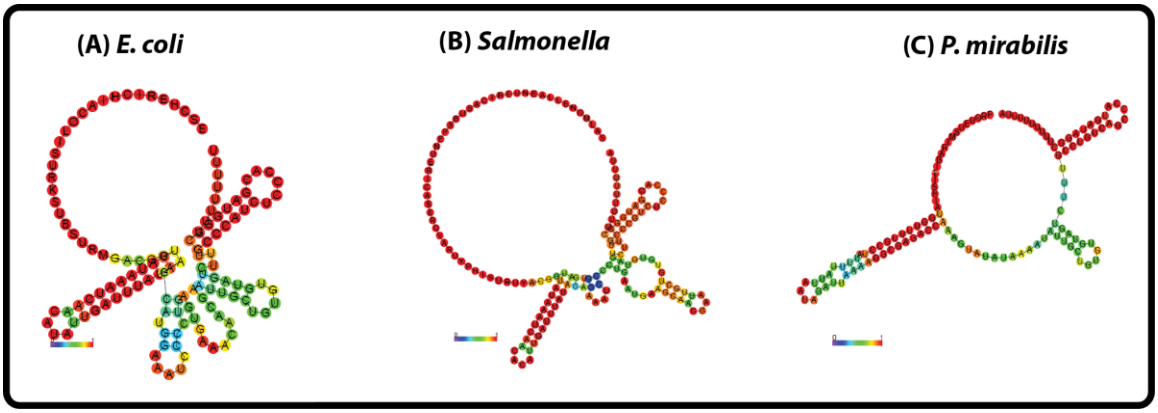

Fig. 11. **Predicted tertiary structure of *rprA* from (A) *E. coli;* (B) *Salmonella;* and (C) *P. mirabilis.*** The predicted tertiary structure of *P. mirabilis rprA* is very different from that of *E. coli* and *Salmonella*. Structures were derived using the RNAfold webserver available at http://rna.tbi.univie.ac.at/cgi-bin/RNAfold.cgi ((153).

***cpxP*$_{Ec}$*::lacZ* is expressed at consolidation zones during swarming**. In *E. coli,* the Cpx pathway plays a key role in the regulation of adhesion-induced genes (154). Here, I attempted to correlate the Cpx pathway with *P. mirabilis* swarmer cell differentiation by using heterologous expression system employing an *E. coli cpxP*$_{Ec}$*::lacZ* transcriptional fusion in BB2000. I observed that when BB2000/pVV1 (*cpxP*$_{Ec}$*::lacZ*) swarmed over 1.5% LB agar plus XGal and Amp, a periodic series of blue rings formed, perhaps at areas where swarming migration stopped, i.e., zones of consolidation (Fig. 12b). β-galactosidase activity was highest at the initial inoculation point and areas where swarming migration appeared to have stopped (Fig. 13). The initial inoculum showed a very high level of β-galactosidase activity, and this could possibly be explained by the presence of XGal in the plate that can cause high β-galactosidase activity. Nonetheless, these data suggest that the surface contact/adhesion induces the Cpx system.

Transcriptomic results reported by Pearson *et al* (155) also showed that stress genes such as the general stress response sigma factor RpoS and *rcsB* are up-regulated in *P. mirabilis* cells isolated during consolidation phase. This indicates a possible linkage among the different CES genes.

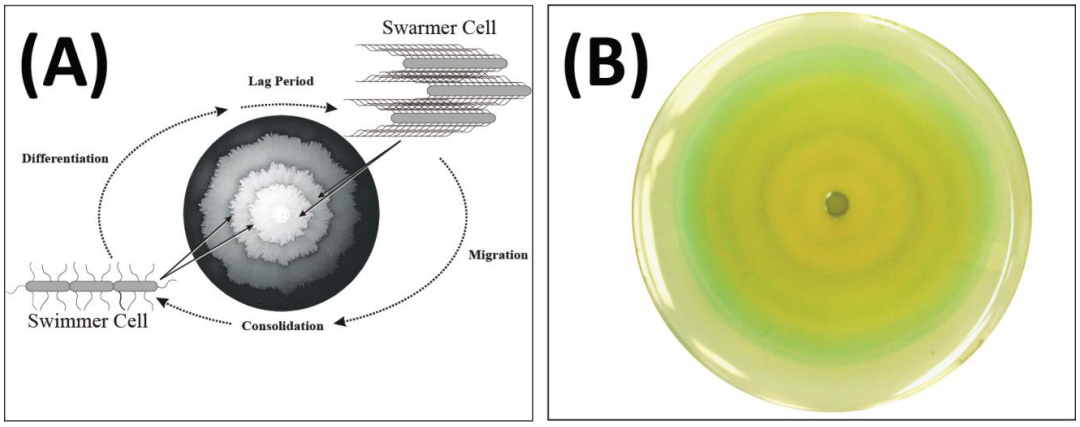

Fig. 12. *cpxP*$_{Ec}$ expression during *P. mirabilis* swarming. (A) Cyclic nature of *P. mirabilis* swarming (16). (B) When cells containing *cpx*$_{Ec}$*::lacZ* swarm over LB agar containing XGal and Amp, a series of blue rings result at the areas where swarming migration appeared to have stopped. Washed diluted overnight cultures were drop inoculated at the center of the plate and grown at 30^{o}C for 36 h.

β-galactosidase activity changes over swarming migration. In order to verify the observed pattern of *cpxP*$_{Ec}$ expression over swarming migration, BB2000/pVV1 was allowed to swarm for 36 h at 30 ^{o}C on 1.5% LB agar plus XGal and Amp. I took samples every 5 mm from initial point of inoculation and measured β-galactosidase activity. This "randomized" sampling removed the bias towards a particular zone and showed how *cpxP*$_{Ec}$ expression temporally correlates with swarming migration. The levels of β-

galactosidase changed over swarming migration following a decreasing-increasing cyclic pattern (Fig. 14). This is consistent with the data that activity is highest at zones where migration stopped and lowest during active swarming (Fig. 13). However, I have yet to establish that $cpxP_{Ec}$ expression is correlated with cell-differentiation since cell morphology, i.e., swimmer and swarmer cells, was not measured.

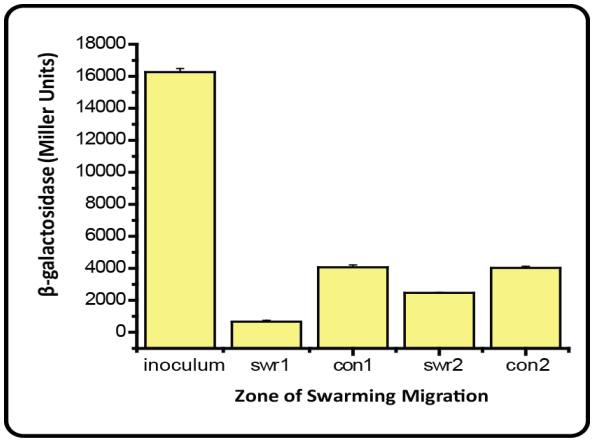

Fig. 13. β-galactosidase assay of *cpxP*$_{Ec}$ expression during swarming. β-galactosidase activity over swarming migration at zones where swarming migration stopped, refered here as consolidation (con), and zones where swarming migration was active (sw) were measured. Highest levels of β-galactosidase activity occur at the initial inoculation point and at consolidation zones. Cells were grown on 1.5% LB agar plus XGal 40 and Amp 100 at 37^{C}C overnight. Error bars show standard error of the mean; n = 3.

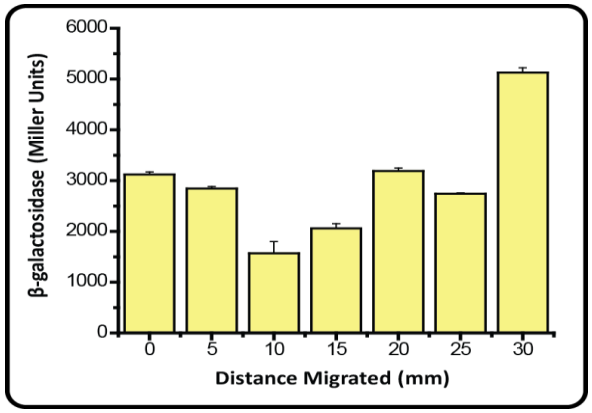

Fig. 14. Levels of β-galactosidase activity changes over swarming migration. β-galactosidase activity was measured using the Miller Assay by sampling every 5 mm from the point of inoculation after swarming on 1.5% LB agar plus XGal and Amp at 30 ^{o}C 36 h. Error bars show standard error of the mean; n = 3.

***cpxP* expression of individual cells during differentiation changes.** Samples taken from a swarm plate may contain a mixture of swimmer and swarmer cells. Upon surface contact, differentiation of swimmer cells to swarmer cells may take about 2 h and active migration starts at about 3.5 h and lasts for about 2 h before cells de-differentiate back to swimmer cells (68). To compare $cpxP_{Ec}$ expression with cell differentiation a diluted overnight culture of BB2000/$cpxP_{Ec}$*::lacZ* was spread evenly on four 1.5% LB agar plus Amp100, and the cells harvested at 0, 1.5, 4.0, and 5 h post-inoculation (t_0, $t_{1.5}$, $t_{4.0}$ and $t_{5.0}$). Both β-galactosidase activity (a proxy for transcription of *E. coli* $cpxP_{Ec}$) and *cpxP* transcription (direct RT-PCR of *P. mirabilis* $cpxP_{Pm}$) were measured (Fig. 15). β-galactosidase activity was highest at $t_{4.0}$ (Fig. 15a) while $cpxP_{Pm}$ transcription using RT-PCR showed that expression was also highest at $t_{4.0}$ (Fig. 15B). The expression profile for *cpxP* expression were mostly parallel sans $t_{5.0}$., where although in both cases it decreased relative to $t_{4.0}$, in the Miller Assay it was higher than t_0 and $t_{1.5}$ while in the RT-PCR it

went lower (Fig. 15). This data suggest that *cpxP* expression changes during cell differentiation, although the RT-PCR data need to be verified.

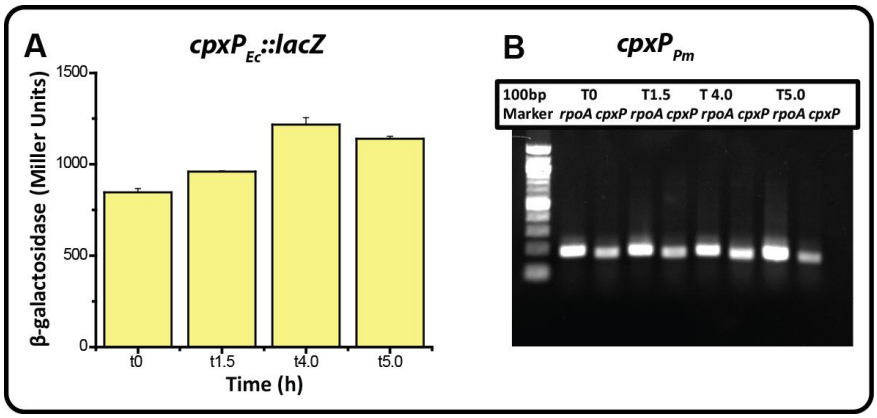

Fig. 15. *cpxP* expression of individual cells during differentiation changed in both β-galactosidase activity and transcription of $cpxP_{Pm}$ as measured by RT-PCR. Cultures were initially grown for 4 h in LB plus Amp then diluted and spread-inoculated in parallel LB agar plates, and grown at 37°C. Cells were sampled at T0 (initial culture), 1.5 h, 4 h and 5 h. RT-PCR expression reference is *rpoA*. Error bars show standard error of the mean; n = 3.

Discussion and Recommendations

My results with $cpxP_{Ec}$*::lacZ*, indicated that expression of $cpxP_{Ec}$ changes during *P. mirabilis* swarming migration, with the highest levels occurring when cells are in the swimmer phase (initial inoculation and presumptive consolidation zones); times when cells have the most torsional stress on their motors. Pearson *et al.* (155) found that more genes are up-regulated in the consolidation phase than in swarming phase. These results suggest that during the consolidation phase, cells prepare for the next swarm cycle, and thus genes that are required for swarming are upregulated and highly expressed at this

time. Consistent with their findings that stress genes (*rpoS and rcsB)* and cell wall remodeling related genes are upregulated during consolidation, I found that $cpxP_{Ec}$ expression is also up-regulated during consolidation.

Thus, the Cpx system is a two-component system activated by adhesion to abiotic surfaces and implicated in surface-induced gene expression and biofilm formations in *E. coli* (115). Inhibition of flagellar rotation upon surface contact induces swarmer cell differentiation in swarming *P. mirabilis*. The initial point of inoculation and the consolidation zones are areas where swimmer cells are predominant, and speculated to be times when flagella motors are inhibited. My results suggest that envelope stress is highest when swimmer cells first contact a surface and at points where the cells stop active migration. This suggests a possible link between inhibition of flagellar rotation, cell envelope stress, and swarmer cell differentiation.

Using samples from a swarm plate, I found that the expression of $cpxP_{Ec}$ was lowest in areas of *P. mirabilis* that appear to be in active migration. However, when I measured $cpxP_{Ec}$ expression of individual cells, I found that at $t_{4.0}$ β-galactosidase activity was highest. At around this time point ($t_{4.5}$), maximal swarming motility had been observed (63) and it is expected to have the highest number of swarmer cells in a population. The difference in $cpxP_{Pm}$ expression observed between cells taken from a swarm plate and spread plate might be due to the difference between their metabolic and physiologic states. Differentiation to a swarmer cell is just one of the requirements for active swarming. And although it's not part of the hypothesis, it is important to note that the process of swarming requires a group of swarmer cells forming multicellular rafts in order to move. The inducing signal for $cpxP_{Ec}$ expression of cells of the same

morphotype might be different between these two conditions. $cpxP_{Ec}$ expression by individual swimmer cells at time 0 and 1.5 could be induce by surface contact, and at times 4.0 and 5.0 increased expression may be due to the increase in the number of flagella in swarmer cells that are now in contact with the surface. The bacteria shares surface-contact or cell stress in actively swarming cells. The colony migration factor or *cmf* that is required for swarming but not in differentiation can help alleviate surface tension. Pearson *et al.* (155) suggested that although cells that are taken from an evenly spread plate and cells taken from the edge of a swarm colony are both short cells, it is unlikely that they are physiologically similar. I used RT-PCR to measure *P.mirabilis* $cpxP_{Pm}$ expression to confirm our results measuring *E. coli* $cpxP_{Ec}$ expression in *P. mirabilis*. Since I have found homologs of the cell envelope stress (CES) genes on the *P. mirabilis* genome with the exception of the Bae system, I did not expect any major differences in expression.

Our result with $cpxP_{Pm}$ showed that expression was highest at $t_{4.0}$, similar to $cpxP_{Ec}$ in the Miller Assay; however, expression did not only decrease at $t_{5.0}$ relative to $t_{4.0}$ but it was actually the lowest point. The difference between using an *E. coli* promoter and directly measuring the *P. mirabilis* gene expression could explain this. The *cpxP* promoter of *E. coli* had already been characterized and upon alignment with that of the upstream sequence of *P. mirabilis cpxP* gene start site, the degree of conservation of the -10 and -35 recognition sequence is different between the two (Fig. 16). Also, I have only done the RT-PCR once and thus optimizing the protocol from RNA extraction to the different PCR conditions would certainly help. In any case, given this caveat, it would be

better to use *P. mirabilis* transcriptional fusion instead. In the following section, I will outline an experimental design that could be used.

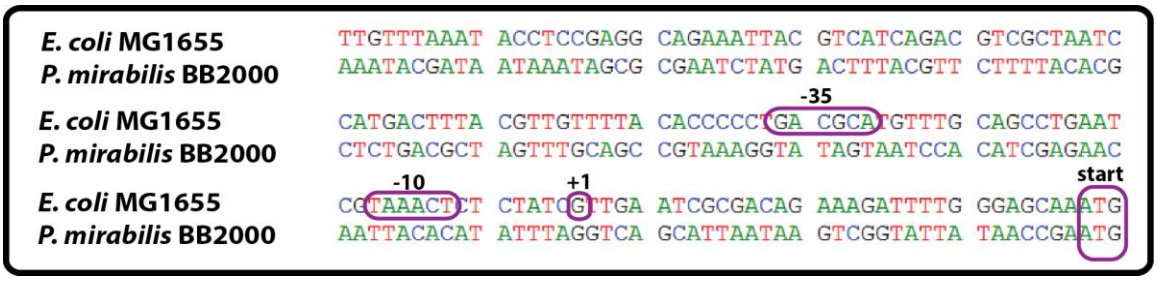

Fig. 16. Alignment of the promoter region of *cpxP* of *E. coli* and *P. mirabilis*. The promoter region of *E. coli cpxP* and its respective σ^{70} recognition site had been characterized (156) as indicated.

To determine the spatial and temporal changes in CES gene expression during swarmer cell differentiation and swarming colony formation, PCR will be used to amplify the respective promoter region of the *Proteus* homolog of each CES gene, which will in turn be ligated into pYL10. While our results show that pYL10 provides strong data, I can also PCR the CES promoter::*lacZ* DNA along with DNA flanking BB2000_3115 (c-di-GMP gene) and insert this cassette in the suicide plasmid pGP704 (157). This plasmid, once conjugated into *P. mirabilis*, will produce a Campbell (single crossover) integration in PMI3101 yielding a single copy of the CES promoter transcriptional fusion.

A central premise of our hypothesis was cell-envelope stress results from inhibition of filament rotation. Aside from using LB agar, I can also test this hypothesis

by using LB plus 10% polyvinylpyrrolidone (PVP) or anti-FlaA antisera that inhibit rotation of the flagella in liquid media (19). A series of increasing concentrations of each agent will be used. The prediction is that as the concentration of agar, PVP, or anti-FlaA antiserum increases, I should see an increase in LacZ expression (proxy to CES promoter transcription).

The expression of each CES genes will also be measured in mutant backgrounds with defects in the following genes: *fliL, fliL-C, fliF, fliG,* and *motB*. The prediction is that CES gene expression will decrease in mutants resulting in no filament (*fliF* and *fliG*) or paralyzed filaments (*motB*) since these mutations eliminate motor stress. An increase in LacZ activity is predicted for cells with *fliL* defects (YL1003 and FliL-C defective strains) since FliL mutants were predicted to have weak rod/motor thus cell envelope stress will be magnified by flagellar inhibition.

Conclusion

In conclusion, I have shown that $cpxP_{Ec}$ expression changes over swarming migration with the highest levels at zones of initial inoculation and where active migration stops. I proposed that *cpx* expression, i.e., cell wall stress, is highest when a swimmer cell is immobilized on the agar surface, and where torque on flagellar motors is highest due to inhibition of filament rotation. Cell wall stress is relieved once the bacterium differentiates into a swarmer cell, with flagellar motors operating with less torsional constraint. Our results suggest a possible link between cell envelope stress, inhibition of flagellar rotation, and swarmer cell differentiation.

Chapter 3: The Role of Cell Wall Stress Response and UmoA in Swarmer Cell Differentiation

Abstract

Swarmer cell differentiation in *Proteus mirabilis* is triggered by physical conditions that inhibit the rotation of the peritrichous flagella of the swimmer cell. Signal transduction mechanism from the flagella to cell differentiation is still unknown. Evidence links genes involve in cell wall formation and envelope stress response to surface sensing. I hypothesized that upon surface contact torsional stress due to inhibition of filament rotation activates a cell-envelope stress response and induces swarmer cell differentiation. This study attempted to introduce mutations in the cell wall stress genes *pspA*, *cpxR* and *rpoH* via Campbell integration. Various attempts and cloning strategies were employed to achieve mutation. However, I have observed plasmid replication but not successful chromosomal integration. This suggests that mutations in these genes might not be favorable to the cell and could be lethal. A different target, *umoA*, a known regulator of swarmer cells with no lethal phenotype in *Proteus* was also explored but successful mutation was also not achieved. The initial experimental design did not work because of the inactivation/loss of the *ClaI* site in *umoA* that was supposed to be used to insert Cm^R to disrupt *umoA* gene function. Subsequent attempts to use both inverse PCR and site-directed mutagenesis to introduce an internal restriction site and the use of Campbell integration to introduce mutation were also not successful. This was due to the inability to optimize the protocol and experimental design because of time limitations i.e. possible incorrect primer design, PCR conditions, bi-parental mating conditions etc.

Introduction

Physical conditions that inhibit rotation of vegetative swimmer cell flagella induce *P. mirabilis'* swarmer cell differentiation and involve the protein FliL (19). However, the molecular mechanisms that transduce the signal from the flagella to induce differentiation are currently unknown. I hypothesized that upon surface contact torsional stress due to inhibition of filament rotation activates a cell-envelope stress response and induces swarmer cell differentiation. Of the five cell envelope stress (CES) signaling mechanisms in enterics the σ^E, Psp (phage shock protein), Cpx (conjugative plasmid expression), and the Rcs (regulator of capsule synthesis) system are highly conserved in *P. mirabilis.*

Aside from the CES genes, increases in *umoA* and *umoD* expression were observed in wild-type (wt) swarmer cells and *fliL* strains (63), suggesting that UmoA and UmoD are part of the surface-sensing pathway. Loss of function mutations in *umo* genes decrease *flhDC* expression resulting in poorly swarming cells (76). Recent reports have also shown linkage between the Rcs pathway and portions of the 'Umo' pathway (104).

This series of experiments attempted to introduce mutations in the three cell wall stress genes, *pspA, cpxR, rpoH,* and the *flhDC* regulator *umoA* by Campbell integration. The main objective was to correlate cell wall stress (CES) and/or *umoA* expression with swarmer cell differentiation and determine the role FliL plays in mediating the response.

Materials and Methods

Bacterial strains and culture conditions. All strains and plasmids used are listed in Table 3. BB2000 and *E. coli* strains were grown in LB broth (10 g liter^{-1} Bacto tryptone, 5 g liter^{-1} yeast extract, 10 g liter^{-1} sodium chloride) at 37 ^{o}C, 200 rpm. Colonies were grown in LSW^{-} (10 g liter^{-1} Bacto tryptone, 5 g liter^{-1} yeast extract, 0.4 g liter−1 NaCl, 5 ml liter^{-1} glycerol, 20 g liter^{-1} Bacto agar) plates for BB2000 strains and LB agar (LB medium containing 15 g liter^{-1} Bacto agar) plates for *E. coli* strains at 37 ^{o}C. Selective media contained antibiotics at the following concentrations: ampicillin (Amp), 100 μg/ml; tetracycline (Tet), 15 μg/ml; streptomycin (Sm), 35 μg/ml, chloramphenicol (Cm), 40 μg/ml; kanamycin (Kan), 50 μg/ml; rifampicin (Rif), 100 μg/ml. Swarming assays were performed on 1.5% LB agar plates and urease was measured using Urea agar (Difco).

Table 3. Strains and plasmids used in the study

Strains	**Genotype**		**Source**
BB2000	*Wild-type, Rfr Tcr*		(53)
DH5αλpir			
SM10-1λpir	Rec^{-} RP4-2Tc::Mu λpir		(158)
S17-1λpir	Rec^{-} RP4-2Tc::Mu λpir		(158)
Plasmid			
pGP704	Suicide vector; R6K ori	Amp	(157)
pKNG101	Suicide vector; R6K ori	Sm	(159)
pACYC177	Low copy vector; p15A ori	Kan	(160)
pACYC184	Low copy vector; p15A ori	Cm	(160)
pVV1	pGP704 (*'pspA'*)	Amp	This study
pVV2	pGP704 *('cpxR')*	Amp	This study
pVV3	pGP704 *('rpoH')*	Amp	This study

pVV4	pKNG101 *('pspA')*	Sm	This study
pVV5	pKNG101 ('*cpxR'*)	Sm	This study
pVV6	pKNG101 ('*rpoH'*)	Sm	This study
pVV7	pGP704 ('*pspA'*)	Amp Cm	This study
pVV8	pGP704 ('*cpxR'*)	Amp Cm	This study
pVV9	pGP704 ('*rpoH'*Cm^R)	Amp Cm	This study
pVV10	pGP704 ('*pspA'* Kan^R)	Amp Kan	This study
pVV11	pGP704 ('*cpxR'* Kan^R)	Amp Kan	This study
pVV12	pGP704 ('rpoH' Kan^R)	Amp Kan	This study
pVV13	pKNG101 ('*pspA'* Cm^R)	Sm Cm	This study
pVV14	pKNG101('*cpxR'* Cm^R)	Sm Cm	This study
pVV15	pKNG101 ('*rpoH'*)	Sm Cm	This study
pVV16	pGP704 ('*cpxAR')*	Amp	This study
pVV17	pGP704 ('*cpxAR'*)	Amp Cm	This study
pVV18	pGP704 (Cm^R)	Amp Cm	This study
pVV20	pGP704 (*umoA*)	Amp	This study
pVV21	PGP704 (*umoA cm*)	AmpCm	This study

[1] Amp Ampicillin resistance
[2] Sm Streptomycin resistance
[3] Kan Kanamycin resistance
[4] Cm Chloramphenicol resistance

Cloning. Internal gene fragments of *pspA*, *cpxR*, *rpoH*, *cpxAR*, and *umoA* (Fig. 17) were PCR amplified from BB2000 genomic DNA and were each cloned into suicide vector pGP704 (Fig. 18a) using *EcoRI* site added to the gene through PCR. For suicide vector pKNG101 (Fig. 18b) based construct, internal gene fragments were cloned using blunt-end ligation to the *SmaI* site. Cm^R and Kan^R were achieved by amplifying the Cm^R and Kan^R gene from pACYC184 (Fig. 19a) and pACYC177 (Fig. 19b), respectively, and cloning into the vector using SalI site added to the gene through PCR. For the *cpxAR* and *umoA* internal fragments, the *XbaI* site was used. Each reaction mixture (50 µl) contained 10× ThermoPol buffer, 25 ng DNA, a 200 nM concentration of each primer, 200 µM deoxynucleoside triphosphates (dNTPs), and 5 U Taq polymerase (NEB). Thermocycling conditions were as follows: 94 °C for 5 min; 30 cycles of 94 °C for 1 min, 62 °C for 30 s,

and 72 °C for 30 s; and 72 °C for 5 min. All constructs were made using *E. coli* DH5α λpir as a host, and plasmid carriage and fragment insertion was confirmed by colony PCR and plasmid digestion. All plasmid used and generated are listed in Table 3 and all the primers used are listed in Table 4.

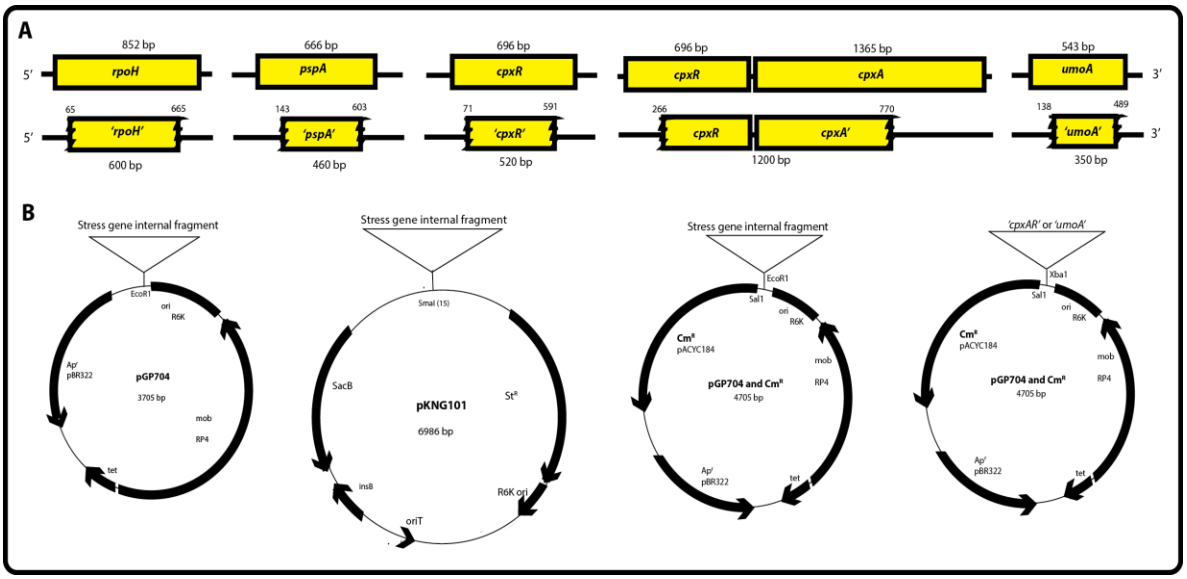

Fig. 17. Map of constructs used in the study to generate mutants via Campbell-style integration. (A) Internal fragments from *rpoH*, *pspA*, *cpxR*, *cpxAR* and *umoA* were amplified and ligated into (B) suicide vectors pGP704, pKNG101 and pGP704 with Cm^R. Corresponding sizes of coding regions and internal fragments are also illustrated in (A).

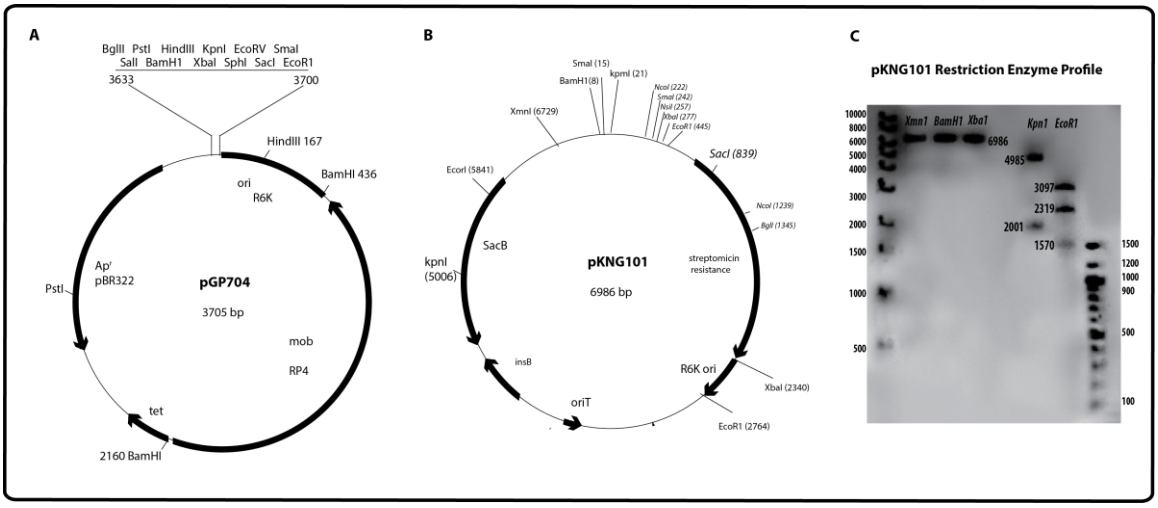

Fig. 18. Suicide vectors used in the study. Suicide vectors (A) pGP704 and (B) pKNG101 were used to generate mutants. Both are non-replicating plasmid in the absence of the *pir* gene. (C)The restriction profile of pKNG101 using *Xmn1*, *BamH1*, *XbaI*, *Kpn1* and *EcoR1* generated the expected bands except for *XbaI*. The *XbaI* near the 3' end of the Sm^R gene can only be cut in a *dam*$^-$ strain according to CABRI (Common Access to Biological Resources and Information, (http://www.cabri.org/CABRI/srs-bin/wgetz?-newId+-e+-page+qResult+[BCCM_LMBP-id:%27LMBP%205246%27])

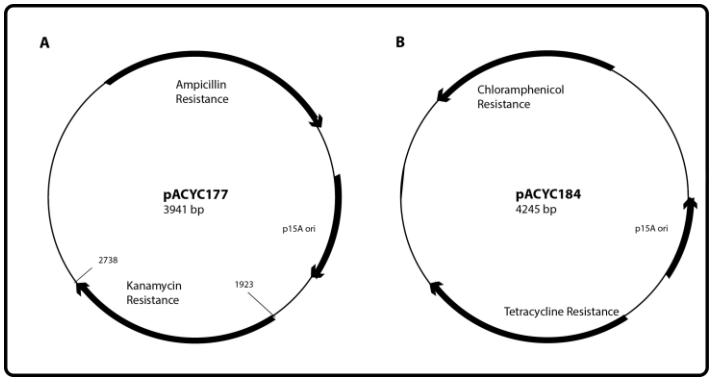

Fig. 19 Plasmids where Kan^R and Cm^R were amplified. Plasmids (A) pACYC177 and (B) pACYC184 were used to amplify the Kan^R and Cm^R gene respectively.

Table 4. Primers used in the study

Primer	Oligonucleotide	Description	Source
FpspA'	5'-TTGAATTCTGCACGTACGCTAGCAGA-3'	PCR primer for cloning 460 bp *P, mirabilis pspA* internal fragment; contains the Ecor1 site at 5' end	This study
RpspA'	5'-TAGAATTCGGCTTTCAGCTCAGCAAACT-3'	PCR primer for cloning 460 bp *pspA* internal fragment; contains the Ecor1 site at 5' end	This study
FrpoH'	5'-TAGAATTCCAGCCAATTCCTATCCG-3'	PCR primer for cloning 600 bp *P, mirabilis rpoH* internal fragment; contains the Ecor1 site at 5' end	This study
RrpoH'	5'-TAGAATTCGCATGGTTATCCCAGTT-3'	PCR primer for cloning 600 bp *rpoH* internal fragment; contains the Ecor1 site at 5' end	This study
FcpxR'	5'-TAGAATTCTTAATGTTGTGCTCGCC-3'	PCR primer for cloning 520 bp *P, mirabilis cpxR* internal fragment; contains the Ecor1 site at 5' end	This study
RcpxR'	5'-CTGAATTCAATCGCTCTATCAAAAGGT-3'	PCR primer for cloning 520 bp *cpxR* internal fragment; contains the Ecor1 site at 5' end	This study
FpspA-3	5'-TGGGTATATTTTCACGTTTTGC-3'	PCR primer for cloning 550 bp *P, mirabilis pspA* gene fragment flanking the internal fragment used	This study
RpspA-3	5'-AGCTTTTAATGCCGCTAATTG-3'	PCR primer for cloning 550 bp *P, mirabilis cpxR* gene fragment flanking the internal fragment used	This study
FrpoH-2	5'-AAGGCAGCATTGAAGCGTAT-3'	PCR primer for cloning 700 bp *P, mirabilis rpoH* gene fragment flanking the internal fragment used	This study
RrpoH-2	5'-CGCTCAGCAGAAACACCATA-3'	PCR primer for cloning 700 bp *P, mirabilis rpoH* gene fragment flanking the internal fragment used	This study
FcpxR-2	5'-ATGACGATCGCGAATTAACCTC-3'	PCR primer for cloning 600 bp *P, mirabilis cpxR* gene fragment flanking the internal fragment used	This study

RcpxR-2	5'-GATAACCACGGCCACGTAAT-'3	PCR primer for cloning 600 bp *P, mirabilis cpxR* gene fragment flanking the internal fragment used	This study
F-kan-SalI	5'-TGTCGACCGATTTATTCAACAAAGCCACG-3'	PCR primer for cloning the Kan^R gene from pACYC177; contains the Sal1 site at 5' end	This study
R-kan-SalI	5'-TGTCGACGCCAGTGTTACAACCAATTAAC-3'	PCR primer for cloning the Kan^R gene from pACYC177; contains the Sal1 site at 5' end	This study
F-cm-SalI	5'-TGTCGACGTAAGTTGGCAGCATCAC-3'	PCR primer for cloning the Cm^R gene from pACYC184; contains the Sal1 site at 5' end	This study
R-cm-SalI	5'-CGTCGACTTATTCAGGCGTAGCACC-3'	PCR primer for cloning the Cm^R gene from pACYC184; contains the Sal1 site at 5' end	This study
F-cpxAR-xbaI	5'-GTCTAGACACTGGCAAGCTGTAAACG-3'	PCR primer for cloning 1200 bp *cpxAR* internal fragment; contains the XbaI site at 5' end	This study
R-cpxAR-xbaI	5'-ATCTAGACCTAGAGCTGGGAGCAGAT-3'	PCR primer for cloning 1200 bp *cpxAR* internal fragment; contains the XbaI site at 5' end	This study
F-umoA-XbaI	5'-GCATATCTAGACACTGGCAGCCATCTCAATA-3'	PCR primer for cloning 543 bp *umoA* gene fragment; contains the XbaI site at 5' end	This study
R-UmoA-XbaI	5'-CCATATCTAGAATTGGTGGTAGCAGCAGGAT-3'	PCR primer for cloning 543 bp *umoA* gene fragment; contains the XbaI site at 5' end	This study
FUmoAInv-NcoI	5'-ATTCTACCATGGGAAATATGGCCCTTATGG-3'	Inverse PCR primer for inserting NcoI site in plasmid-borne *umoA* gene fragment	This study
RUmoAInv-NcoI	5'-GTCCTACCATGGATCGCAATATAGCGAATT-3'	Inverse PCR primer for inserting NcoI site in plasmid-borne *umoA* gene fragment	This study
F-umoA-ncoi	5'-GATGAAATATGGCCCATGGGCAACCTGAAC-3'	Primer for site-directed mutagenesis to insert NcoI site in plasmid-borne *umoA* fragment	This study
R-umoA-ncoi	5'-GTTCAGGTTGCCCATGGGCCATATTTCATC-3'	Primer for site-directed mutagenesis to insert NcoI site in plasmid-borne *umoA* fragment	This study
F-umoA-XbaI-int	5'-ACAGTATCTAGAGCAATCCTTTGCCTGTCCTA-	PCR primer for cloning 350 bp *umoA* internal	This study

	3’	fragment; contains the XbaI site at 5’ end	
R-UmoA-XbaI-int	5’-CCATATCTAGACAGGAAATGGTCTGGTGGAT-3’	PCR primer for cloning 350 bp *umoA* internal fragment; contains the XbaI site at 5’ end	This study

DNA Purification and Electroporation. Prior to electroporation, DNA was purified by ammonium acetate precipitation following the Belas Laboratory protocol. Briefly, 10 µl of stock 100x tRNA was added to 20 µl of ligation mixture and 20 µl of 7.5M ammonium acetate, mixing thouroughly by vortexing. One-hundred µl of absolute ethanol was added and the solution is then chilled on ice for 15 min. With the use of a refrigerated centrifuge set at 4^{o}C, the mixture was centrifuge at 14000 x g for 15 min and then the supernatant was carefully decanted. The pellet was then washed with 1 ml 70% ethanol and centrifuge at 14000 x g for 15 min at RT. The supernatant was removed and the pellet dried in the speed vac for 15 min. The DNA is resuspended in sterile distilled de-ionized water.

Purified DNA at a concentration of 100 ng/ul was added to a pre-chilled, properly labeled sterile 1.5 ml microcentrifuge and then 50 µl of ice-thawed competent cells were pipeted in. The mixture was placed into a clean, sterile and ice-cold 0.2 cm electroporation cuvettes (BTX) and placed into the the pre-chilled white plastic cuvette holder-slide. It was then slid in the BioRad Gene Pulser’s shocking chamber. The mixture was then pulsed at 2.5kV and a time constant ideally between 4.2 to 4.9 msec. Pre-warmed 1 ml LB broth was immediately added and gently mixed to the electroporated cells. The mixture was then placed in pre-warmed 1.5 ml microcentrifuge tubes and allowed to recover at 37^{o}C without agitation for 30 mins and then for 1h to 1.5h with

agitation. Cells were then spread-plated with dilution in the appropriate media with Amp - 1.5% LB agar for *E. coli* and LSW$^-$ agar for *P. mirabilis*.

Construction of mutants. Construction of mutants was achieved by single-crossover homologous recombination via Campbell integration. Constructs were either transformed directly into BB2000 by electroporation as described above or into *E. coli* SM10-1 λpir and/or S17-1 λpir for conjugation with BB2000 by filter mating (53). Briefly, filter mating was achieved by mixing 100 µl each of donor cells (*E. coli* SM10-1 λpir or S17-1 λpir harboring a suicide vector with the desired fragment) and the recipient cells (BB2000) in 1.5 ml microcentrifuge tube. Cells were then spun down for 15 s and the pellet was resuspended in 30 µl 1% PBS and spot inoculated at the center of a sterile25 mm Whatman cellulose nitrate membrane 0.2µm cellulosic filter disk in LSW$^-$ plate. The cells were then incubated at 37 ^oC for 24 h. The filters were resuspended in 1% PBS and plated by spreading dilutions on LSW$^-$ plates with the appropriate selection (Amp for pGP704, Sm for pKNG101 and Cm for pGP704 plus Cm^R) and Tet/Rif as counter-selection. Screening for *Proteus* was done using the urease test and swarming assays (16, 63). Plasmid were extracted using Qiagen Minipreps (Qiagen, Inc., Valencia, Calif.). Confirmation of correct gene insertion was done by PCR using primers flanking the respective internal fragment used. Thermocycling conditions were as follows: 94 °C for 5 min; 30 cycles of 94 °C for 1 min, 62 °C for 30 s, and 72 °C for 2 min ; and 72 °C for 5 min.

Results and Discussion

Mutant construction using pGP704. Electroporation of BB2000 with the pGP704 (Fig 18a) plasmids - pVV1 (pGP704 with 'pspA'), pVV2 (pGP704 with 'cpxR') and pVV3 (pGP704 with 'rpoH') resulted in no colonies on LSW^- plus Amp 100 plates, despite various modifications, e.g., increasing DNA and cell concentration. Initial bi-parental matings between BB2000 and *E. coli* S17-1 λpir harboring plasmid constructs were spread without dilution on LSW^- Rif 100 and Amp 100. These resulted in confluent growth with isolated colonies on the edge of the plate. Typically, 4.5 x 10^3 antibiotic resistant *P. mirabilis* can be obtained from a single mating (53). Re-selection of isolated colonies in LSW^- with Rif 100 and Amp 100 resulted to one possible PspA transconjugant. Examination of the this DNA however resulted in a PCR fragment that was not the predicted size (Fig. 20). Modifications to the bi-parental mating experiments were attempted using a variety of dilution schemes and conditions (time and temperature of incubation for mating, ratio of cells, and concentration of Amp for selection). A representative of one of the four mating experiment is shown in Table 5. The results, described in Table 5, were hampered by consistent problems with 'plating effects', i.e., high density inocula resulted in confluent growth on the plate, while even minor dilutions of these inocula resulted in no colony forming units. The results from direct transformation and conjugation suggested that Amp was killing the cells. Amp-resistant colonies either did not grow after a second round of Amp selection or harbored a wild-type gene upon PCR amplification. *Proteus* is sensitive to ampicillin, and ampicillin is not the best marker for selection, although it has been used successfully in the past (16).

I attempted to correct these earlier problems by switching to another suicide vector, pKNG101 (Sm^R, Fig. 18b), that is also routinely used for their bi-parental mating with *Proteus*, or to use another selection marker like Cm or Kan. pKNG101 is part of our laboratory strain collection and could be quickly tested and used. However, while Cm and Kan are used routinely in our laboratory, the genes encoding these resistances have to be amplified and cloned from suitable plasmids into pGP704. Streptomycin as a selection for BB2000 has not been tested and so primers for Cm and Kan were designed consequently.

Table 5. Representative Bi-Parental Mating Results between BB2000 and S17-1λpir with pGP704 plus stress genes in varying conditions[1]

Varying incubation time in Mating				
PspA	10^{-1}	10^{-2}	10^{-3}	10^{-4}
1h	85			
3h	Lawn[2]	10	1	
6h	Lawn[2]	PE[2]	2	
12h	Lawn[2]	PE[2]	3	0
CpxR				
1h	56			
3h	Lawn[2]	2		
6h	Lawn[2]	PE[3]	18	0
12h	Lawn[2]	PE[3]	35	0
RpoH				
1h	200			
3h	Lawn[2]	14		
6h	Lawn[2]	PE[3]	7	
12h	Lawn[2]	PE[3]	0	
Varying donor:recipient ratio				
PspA				
1:1	Lawn[2]	PE[3]	0	0
3:1	Lawn[2]	PE[3]	0	0
1:3	Lawn[2]	PE[3]	0	0
CpxR				
1:1	Lawn[2]	PE[3]		0

3:1	Lawn[2]	PE[3]		0
1:3	Lawn[2]	0	0	0
RpoH				
1:1	Lawn[2]	PE[3]		0
3:1	Lawn[2]	PE[3]	0	0
1:3	Lawn[2]	0	0	0

[1] Results are representative of one of four mating experiments that was done similarly
[2] lawn- confluent bacterial growth
[3]PE-colonies aggregate on one side, presumably area where Amp lowest due to "plating effect"

Mutant construction using pKNG101. The initial experimental design was to digest the Sm^R gene from pKNG101 (LMBP 5246) with *XbaI* and clone the resulting DNA into the existing plasmids harboring stress gene fragments. However, digestion of the plasmid with XbaI only linearized the vector (Fig. 18b). Analysis of the restriction enzyme profile of pKNG101 (Fig. 18c) showed that one of the *XbaI* site was inactive and this would make cutting out the Sm^R gene not possible. This is supported by the information from the CABRI webpage that states that the *Xba1* located at the 3' end of the Sm^R gene can only be cut in *dam*$^-$ strains. (Common Access to Biological Resources and Information, http://www.cabri.org/CABRI/srs-bin/wgetz?-newId+-e+-page+qResult+[BCCM_LMBP-id:%27LMBP%205246%27]).

After verifying that pKNG101 do not replicate in BB2000, cloning blunt-end ligation using the SmaI site of pKNG101 was done to generate the following constructs for cloning: pVV4 pKNG101('pspA'), pVV5 pKNG101('cpxR'), and pVV6 pKNG101('rpoH'). Streptomycin resistance of BB2000 was tested and the minimum inhibitory concentration (MIC) was at 35 μg/ml. A BB2000-only control for mating in LSW^- plus Tet 15 and Sm 35 yielded no colony growth in 10^{-2} dilutions. Unfortunately, examination of streptomycin resistant colonies from three conjugation experiments using this procedure all yielded wild-type stress genes, with one exception. One possible PspA

transconjugant yielded a PCR band with a size similar to the possible PspA mutant with the pGP704 construct (Fig. 20). This was another unexpected result since pKNG101 and pGP704 differ by 3-KB and should not yield similar band sizes. It is possible that the primer used was able to anneal in another region in pKNG101 and coincidentally generated same-sized fragment. Although the Rather group at the Emory University have been using pKNG101 for their work in *P. mirabilis*, Sm^R in BB2000 is not commonly used in our laboratory. It is likely that the concentration I used is not optimal for filter mating and should have been explored further.

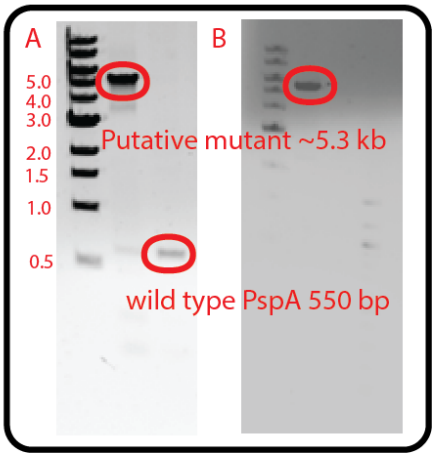

Fig. 20. PspA amplification of two putative PspA mutant. Two PspA mutant were isolated from two different mating experiments and used two different suicide plasmids. (A) pGP704 and (B) pKNG101. The size of the major band for both mutants was identical which was not expected. The two vectors have a 3 kb size difference and should result to different size band, 4831 bp and 8032 bp, respectively upon integration into the *pspA* gene.

Mutant construction using pGP704 with Cm^R. Historically, Cm and Kan are the best antibiotic markers for BB2000. Kan and Cm were cloned into existing pGP704- and

pKNG101-based constructs as described in the Methods section and listed in Table 2. Given that *pspA* had been giving variable results, efforts for mutant generation were focused on making a *cpxR* mutation. The Cpx system is a good target since it has been shown to be activated by adhesion to abiotic surfaces through an outer membrane lipoprotein, and has been implicated in biofilm formations in *E. coli* (154). I also showed that the homology between the *E. coli* and *P. mirabilis cpx* genes was strong (Table 2). Initial conjugation between BB2000 and SM10-1 λpir/pVV8 (pGP704::*cpxR*' Cm) resulted in Cm^R colonies that contained the Cm gene upon colony PCR. These colonies were then checked to determine if they were *Proteus* using urease and swarming assays. Positive *Proteus* colonies were checked for plasmid replication resulting in three colonies, all of which contained a plasmid (respectively). This construct has three possible fates upon entering the cell. First is to die, since a suicide vector such as pGP704 needs the *pir* gene to replicate and BB2000 does not have that gene. Second, to integrate into the chromosome by homologous recombination, since it contained an internal fragment homologous to the *cpxR* gene in the chromosome. Third is to replicate inside the cell, this could be cause by a mutation in the plasmid, specifically in the R6K origin

Initial efforts in mating resulted in Cm^R colonies that were mixed with *E. coli* and *P. mirabilis*. This contamination was eliminated by screening the colonies first using urease and swarming assays. Switching from Tet to Rif as a counter-selection also greatly decreased the growth of *E. coli*. Repeated isolation of plasmids in BB2000 showed that the conjugation was working but, despite the use of a suicide vector, the plasmid did not integrate into the chromosome. I generated and tested a number of hypotheses in efforts to find out what was wrong and correct it. First, that not enough colonies (30 Cm^R

colonies) were tested, and increasing the sample size to 60 would increase the chance of isolating the mutation. Second, that Cm^R selection favored the ones containing the plasmid since they are multi-copy and expected to grow faster. Third, the mutation could be making the cell temperature-sensitive by affecting the cell's ability to adapt to higher temperature. Fourth, the 543 bp internal fragment of *cpxR* was too short to recombine. The first three hypotheses were tested by increasing the sample size to 60, randomly selecting for different colonies of different sizes (small, medium and large) and doing the mating at 37 ^oC, 30 ^oC, and RT. Still, results from various attempts at bi-parental mating were either plasmid replication or wild-type *cpxR* upon PCR amplification. A total of 90 colonies were tested with 11 replicating plasmids and the rest wild-type *cpxR* (representative data shown on Fig 21). Of the ten Cm^R colonies, 6 was shown to have a replicating plasmid. Although the plasmid was not digested by an RE, the upper band corresponds to the expected band size for a linearized plasmid. The four colonies with no plasmid were checked for plasmid integration, but only wt *cpxR* was amplified. The fourth hypothesis was tested by constructing a new clone with a 1.2 kb internal fragment to include both fragments of *cpxA* and *cpxR*.

Mucoid colonies were observed in some 5 day old selection plates left at RT. One characteristics of a cpx mutation in *E. coli* is a mucoid colony (161). These colonies were urease positive and were swarming. Plasmid extraction showed all 6 mucoid colonies contained the plasmid (Fig. 21A). PCR amplification of the genomic DNA of two mucoid colonies yielded wild-type cpxR gene. These colonies, however, did not appear mucoid at 37 oC. Streaked plates in 37 oC, 30 oC and RT showed some differences, specifically, absence of small colonies in 37 oC. Upon isolation of pure, single colonies at 30 oC, it

appeared that these were not *P. mirabilis* by smell and appearance. This suggest that at RT the mucoid colonies were mixed *P. mirabilis* and other bacteria. Upon continued restreaking, I must have isolated the contaminant and lost *P. mirabilis*. When I initially checked for urease and swarming, I did not streaked the colonies, rather I used toothpick to directly pick and transfer to the urease and 1.5% agar plates. Once I streaked and used different temperatures (RT, 30oC, and 37oC), I must have lost the *P. mirabilis*. Another bacteria, *Helicobacter pylori* is also Urea^{+} and is motile at viscous environment (162), however I cannot find a reference that says *H. pylori* swarms at 1.5% agar.

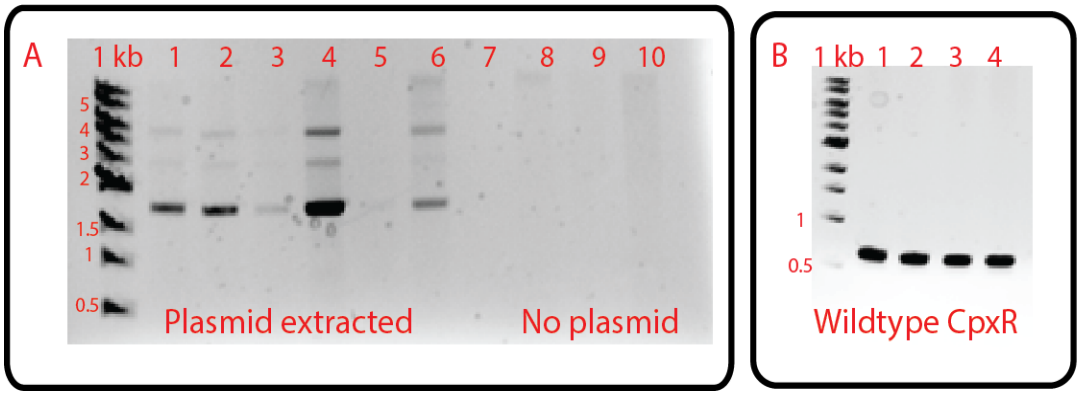

Fig. 21. Cm^{R} CpxR' Transconjugants. Ten putative CpxR transconjugants were analyzed after testing positive to urease and swarming. Lanes 1-6 are colonies that were 'mucoid'. All the colonies were grown at 37 ^{o}C and checked for (A) plasmid replication and (B) plasmid integration. (A) Colonies 1-6 had a replicating a plasmid while colonies 7-10 did not. (B) Genomic DNA of colonies 7-10 was PCR amplified to check for plasmid integration, however all colonies have wild-type CpxR.

These results though suggest that the mutation could actually lead to temperature sensitivity. Another possibility is that the mutation is lethal to the cell, however *cpxR*

mutation in *E. coli* has already been found to be non-lethal. Due to the problems encountered in this approach, I decided to change the focus of my research by analyzing mutations in *umoA*, a gene that is highly up-regulated in *fliL* cells (63). *umoA* has been previously mutated (76) and provides greater assurance of success. This leads to a new research hypothesis that mutations in *umoA* affect swarmer cell differentiation but the chance of successfully getting data and progressing is higher.

Mutant construction with *cpxAR'* insertion. A new construct with the *cpxAR'* internal fragment (Fig. 17a) was constructed by cloning a 1.2 kb '*cpxAR'* fragment into the XbaI site of pGP704, producing pVV16. The Cm^R gene was then cloned into the SalI site on pVV16 yielding pVV17, pGP704 '*cpxAR'*-Cm^R. Direct electroporation of BB2000 with pVV17 yielded Cm^R colonies that were isolated and evenly spread out in the platedunlike in plating effect where colonies are found in only one part of the plate. Twelve colonies were selected and re-streaked in LSW^- plus Cm 40. All 12 colonies retained the Cm^R and were found to have no plasmid. Colony PCR on 20 such Cm^R colonies resulted in two bands that were not wild-type (Fig 22A). PCR amplification of the genomic DNA of six of these colonies resulted in wild-type *cpxAR* (Fig.22B) suggesting false positives in colony PCR. These false positives can be from too much template DNA in the reaction mixture since it can't be controlled when using colony PCR. There could also be contaminating DNA that was easily amplified. The succeeding two transformations and two conjugation experiments again resulted to wild-type *cpxAR* (Fig 23).

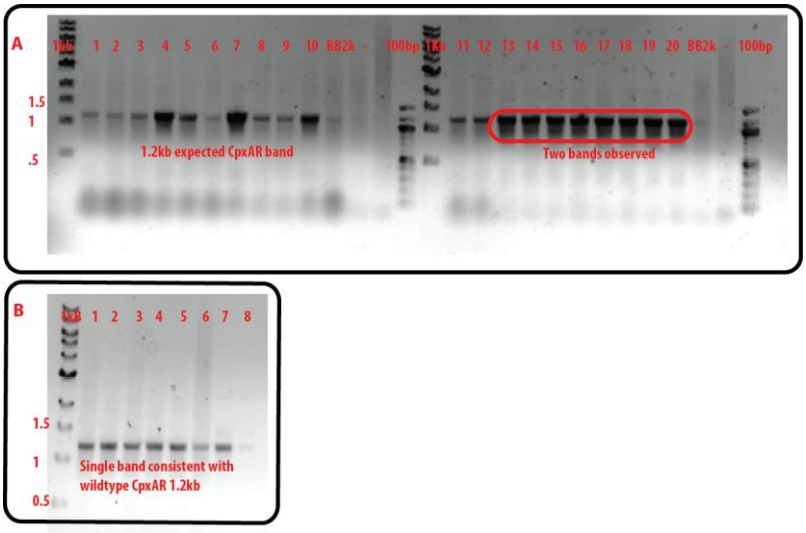

Fig. 22. PCR amplification of *cpxAR'* transformants from electroporation. (A) Colony PCR of '*cpxAR'* transformants showed some colonies having two bands, the first 12 colonies have no plasmid extracted and the last 8 colonies were not tested for plasmids. (B) Genomic DNA of representative colonies (13-18) were amplified for *cpxAR'*, lanes 1-6 were possible mutants, lane 7-pVV17 (pGP704 (*cpxAR'*), and Lane 8-genomic BB2000, all possible mutants harbored a single 1.2 kb fragment of the wild-type *cpxAR'*.

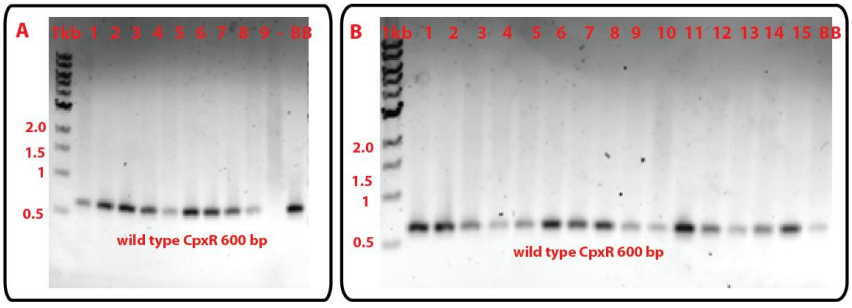

Fig. 23. PCR amplification of the *cpxR* gene in putative '*cpxAR'* mutants. Plasmid-negative colonies from (A) transformation and (B) conjugation experiments were analyzed for plasmid integration using primers for the *cpxR* gene. Expected fragment

sizes for integration were 600 bp and 5.9kb. However, all colonies contained the wild-type 600 bp *cpxR* gene.

UmoA mutant construction. Efforts to mutate the stress genes in BB2000 have so far been unsuccessful despite exhausting a number of hypothesis and methods. Mutation in *umoA* is not lethal, it is a known regulator of swarmer cells (76), and it has been implicated as part of the FliL-FlhDC signaling pathway (63). Construction of an *umoA* mutant in *P. mirabilis* was attempted using homologous recombination with double and single crossovers, respectively. The initial plan for the double recombination was to clone *umoA* into pGP704 (generating pVV20) and then insert the Cm^R gene at the *ClaI* site of *umoA* (pVV21). However, pVV21 seem to be a contaminant plasmid because of the loss of Amp^R and an unexpected restriction enzyme profile. Upon restriction enzyme profiling of both pVV20 and pVV21, the former showed bands consistent with pGP704 but not from *umoA* (*ClaI* and *EcoR1*), and pVV21 did not generate any of the expected band at all. Further analysis showed that *ClaI* can cut *umoA* PCR product but ClaI cannot cut pVV20. This supports the NEBcutter (163) prediction that the *ClaI* recognition site in the gene sequence of *P. mirabilis umoA* is a DAM-methylation site. However, I did not attempt to put the plasmid in a DAM^- *E.coli* and repeat the cut, so this idea is speculative. Upon sequencing pVV20, I found that the *ClaI* site was no longer present and there are four *EcoR1* sites, instead of the expected two. The additional *EcoR1* sites are possibly due to an inaccurate map since they were located right next to the pGP704-published *EcoR1* site within the multiple cloning site. However, as pGP704 is a well-used plasmid, this is highly unlikely unless the map of pGP704 was mapped using RE then multiple *EcoR1* next to each other might not have been detected. This is only possible if the stock

pGP704 in the lab somehow obtained the extra *EcoR1* and was not really significant for single digestion. This has only become relevant since *umoA* has an internal *EcoR1* site. The lost of *Cla1* could be from bad sequencing because when a different primer was used, it was detected. Repeating the pVV20 construction generated the same results. The challenge was then in finding/creating restriction site within *umoA* to insert Cm^R gene for double recombination. I tried to use inverse PCR to introduce an *NcoI* site in pVV20 by designing primers that would result to a linearize pVV20 with an *NcoI* site right in the middle of *umoA.* My first attempt using Taq polymerase resulted in smears once I ran the PCR product on an agarose gel. My next two attempts using *Phusion* DNA polymerase, resulted to an unexpected band-size. I was expecting a 4.3 kb band and was only able to amplify a 3.0 kb band. This could have been caused by errors in primer design or less than optimal PCR conditions. I also tried, unsuccessfully, to use site-directed mutagenesis using the QuickChange Site-directed Mutagenesis kit (Stratagene) to introduce an *NcoI* site in pVV20, once. This resulted to no colony growth. Although this is a kit, I had to use my own competent cells since I needed a *pir* strain for my plasmid to replicate. I did not troubleshoot this experiment. Given more time, I would look more into my primer design since this is the most vital component of the kit. I could also clone *umoA* in a non-suicide plasmid and try introducing an *NcoI* site by Inverse PCR and Site-directed mutagenesis. And once this is successful, put it back into pGP704 with Cm^R and attempt the recombination.

In parallel to the Inverse PCR and Site-directed mutagenesis, I also used Campbell-style integration of *umoA* using pVV22 (pGP704 with Cm^R and *'umoA'* (Fig. 17a). Screening for putative mutants made use of cm^R and reduce swarming phenotype.

Six possible mutants with reduce swarming (Fig. 24) were check for the presence of plasmid and then integration. However, all six generated wild-type *umoA*. I did not pursue the attempt to generate a mutation in *umoA* any further, and instead directed my focus in determining regions in *fliL* necessary for swarming by introducing point mutations in *fliL* using an *E. coli* mutator strain (XL1-Red).

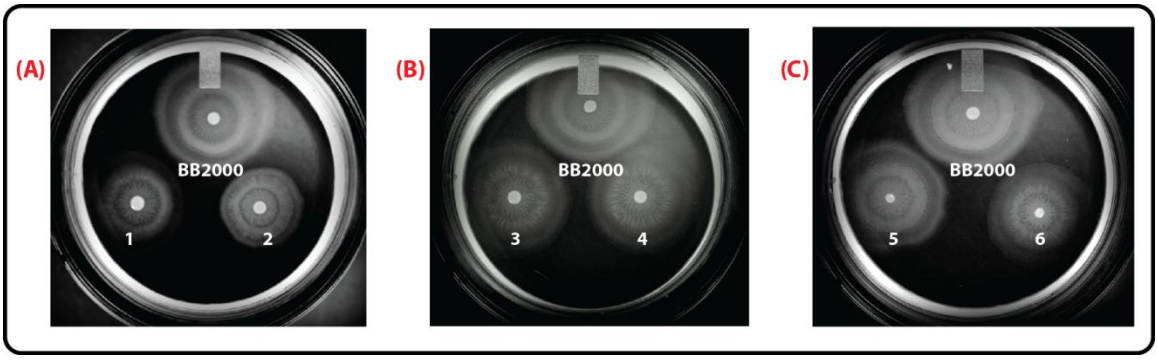

Fig 24. Putative *umoA* mutants exhibiting reduce swarming. Mutation in *umoA* confer reduce swarming phenotype. Panels A, B and C show six possible *umoA* mutant with decrease swarming migration relative to wild-type BB2000 with panel (A) showing the least swarming while panels (B) and (C) show slight decrease of swarming and also differences in swarming patterns compared to the wild type. However, all six contained wild-type *umoA* upon PCR amplification.

Recommendations

The study failed primarily because of the inability to successfully knockout the target genes using homologous recombination, despite many attempt to construct mutations in the stress genes and *umoA* in *P. mirabilis.* Successful chromosomal integration was not observed for any of these genes. While this is a standard protocol in our laboratory and other microbial genetics laboratories, it is recognized that integration is dependent on the

length of the homologous sequence and varies within the same species and particular gene. Specifically, in the case of *B. subtilis*, a minimum of 70 bp homology is to be required for homologous recombination (164); however, in another study (165), at least 150 bp was necessary for plasmid integration and it varied depending on the gene of interest. In *E. coli*, a minimum of 20 bp but at least 75 bp of homologous sequence is needed for efficient recombination (166). Efficiency increases as the length homologous sequence increases (167) and dramatically decreases in the presence of mismatches within the homologous sequence (168). Although my study used at least 350 bp of homologous sequence, I cannot discount the possibility that the length of sequence adversely influenced the outcome. However, Dr. Yi-Ying Lee of the Belas Lab has successfully used homologous recombination to delete approximately 400 bp of the *fliL* gene in *P. mirabilis* (personal communications) which was the minimum length used in this study. Another possibility is that these mutations could have produced a phenotype that inhibit growth, or these mutations could be lethal to the cells. Although the CES genes have been mutated in other enterics, without ill effects, specifically *E. coli*, the effect in *Proteus* is not known. The conditions used in the study might not be favorable, for example, a loss-of-function insertion and deletion mutations in *rpoH* results to extremely temperature sensitive *E.coli* strains that grow only at temperatures less than or equal to 20^{o}C (169). This can explain the observation in the study that colony composition after bi-parental mating between BB2000 and S17-1λpir/pGP704 with 'cpxR' and Cm^{R} differs between cells that were grown at RT, 30 ^{o}C and 37 ^{o}C. Some of the smaller colonies were not present at 37^{o}C, and even the mucoid colonies were only observed at RT.

In the case of *umoA*, mutation in *P. mirabilis* has been shown to be non-lethal (76). The main drawback in creating the *umoA* mutant was primarily in the experimental design where *ClaI* was used as the internal RE digestion site in *umoA* to insert the Cm^R gene. This is based on Dufour et al (76) *umoA* mutant with a Sm^R gene inserted in its internal *EcoR1* site. However, I cannot use *EcoR1* because my vector pGP704 also has an *EcoR1* site. I have spent numerous efforts in trying to make the *ClaI* work and in troubleshooting but failed. The *ClaI* site in the *umoA* sequence is a DAM-methylation site, as predicted by the NEBcutter tool (163). I then decided to use Campbell style/ single-crossover integration to generate an *umoA* mutation, and inverse PCR to introduce an *NcoI* site in *umoA* for double cross-over. As I was waiting for primers, I also tried site-directed mutagenesis to introduce *NcoI* site in *umoA*. All experiments were unsuccessful and were done once. I did not pursue this experiment further, although if the initial troubleshooting effort for *ClaI* was instead concentrated on the single cross-over effort or even the introduction of *NcoI* site in *umoA,* it is possible that success would be achieved.

Another way of introducing mutations that has been used in our laboratory for *P. mirabilis* was the use of the TargeTron Gene Knockout System (Sigma-Aldrich) (18). In the event that successful CES mutants were obtained, they could be examined for their motility phenotype, including swimming, swarmer cell differentiation, and swarming behavior. In parallel, PCR will be used to amplify and clone $baeR_{Pm}$, $cpxR_{Pm}$, $rcsB_{Pm}$, $pspF_{Pm}$, and $rpoE_{Pm}$ (respectively) on plasmids for overexpression of each protein in *Proteus*. This methodology has been previously used to characterize the σ^E regulon (170). I point out a possible limit to this approach, in cases where the regulator requires phosphorylation for its activity (i.e., for *E. coli* BaeR, RcsB, and CpxR); nevertheless,

experimental evidence indicates that overproduction of such regulators can be effectively used in such studies, as a proportion of the molecules is phosphorylated in the absence of signal (171, 172). Expression of genes known to be part of the swarmer cell transcriptome could be measured in the CES mutants and overexpressing strains. These include *flhD*, *fliL*, *flgF*, *flgG*, *flaA*, and *umoA*, other genes may be added to the list such as *zapA* and *hpmB*.

Mutations in *umoA* could be constructed using TargeTron in wild-type, *fliL* defective strains, and CES mutant backgrounds, and the phenotype of the resulting double mutant assessed as a function of medium viscosity (as described earlier). Similarly, *umoA* could be cloned on a low-copy number plasmid downstream from an inducible promoter, which will then be transformed into wt, *fliL* defective strains, and CES mutant backgrounds. Overexpression of *umoA* increases $FlhD_4C_2$ activity and swarming. Our model predicts that defects in *umoA* should dramatically reduce *fliL* pseudoswarmer production. Moreover, if CES activity is higher in the regulatory hierarchy leading to swarmer cell differentiation, then defects in *umoA* should prevent the CES phenotype. Thus, these experiments have a potential to uncover a major part of the surface sensing signal transduction pathway.

Chapter 4: Determining regions of *fliL* essential for swarming by *Proteus mirabilis*

Abstract

Swarmer cell differentiation in *Proteus mirabilis* is induced by physical conditions that inhibit rotation of the flagella. The protein FliL has been implicated in surface induction although the molecular mechanism remains unknown. A mutation in *fliL* results to a Swr^- phenotype and the presence of pseudoswarmer cells in non-inducing condition. The latter can be complemented by expressing *fliL in trans*. However, complementation of the Swr^- phenotype requires *fliL* and some exogenous DNA. This complementation is also viscosity dependent, with an optimum at 0.8% agar, is temperature- and wettability-sensitive, and is characterized by late swarming onset starting with flares, highly motile sectors emerging from an otherwise poorly motile bacterial colony. I have also shown for the first time the complemented *fliL* strain exhibits better swarming than wild type on 0.8% agar, a concentration that normally inhibits active swarming migration. An *E. coli* mutator strain, XL1-Red, was used to introduce mutation in *fliL* to determine which nucleotides and domains are important for FliL function. Using bioinformatics, I predict that mutations adversely affecting FliL function would be found in the promoter region, the transmembrane domain, and a domain from amino acids 61 to 107. This region is predicted to be highly conserved among bacterial species and also homologous to the C-terminal region of FliK. After XL-1 Red mutagenesis, only 2% (2 out of 100) of the putative Swr^- mutants showed mutations in the targeted DNA. Mutations in the plasmid *ori* and Cm^R genes, *fliL* of the Swr^+ colonies and chromosomal *fliL* were also tested, but no mutations in the sequences were found.

Introduction

A mutation in *fliL*, the first gene in the class 2 *fliLMNOPQR* operon results in inappropriate production of swarmer-like cells, termed pseudoswarmer cells, in normally non-inducing conditions, i.e., liquid nutrient broths (19). It also results in a Swr^- phenotype in *P. mirabilis* (18, 19). However, *fliL* mutations cannot be complemented by *in trans* expression of *fliL* alone. Lee et al (18) reported that the Swr^- defect of strain YL1003, *P. mirabilis strain* with a group II intron insertion at nt 30 of *fliL*, could only be complemented by a fragment containing the *fliL* promoter region, the *fliL* coding region, and a portion of *fliM* DNA. Based from their data, they suggest that FliL has a dual role in *P. mirabilis* – sensing a surface and maintaining the integrity of the flagellar rod (18).

In this study, I aimed to determine the regions of *fliL* that are important for swarming by introducing mutations in its coding region. One of the ways to introduce random mutations in a cloned gene is by using an *E. coli* mutator strain e.g. XL1-Red (Agilent Technologies) that is deficient in the three primary DNA repair pathways. This strain lacks the genes *mutS* (error-prone mismatch repair), *mutD* (deficient in 3´- to 5´-exonuclease of DNA polymerase III), and *mutt* (unable to hydrolyze 8-oxo-dGTP). Using XL1-Red, I mutated a plasmid pYL98 containing the *fliL* promoter (200 nt from *fliL* start codon), the *fliL* coding region, and the 400 bp 5' region of *fliM* that was found by Lee *et al* (18) to be the minimum requirement for Swr^- complementation. I found that complementation is not always phenotypically manifested, has delayed onset which starts off as flares of swarming stretching out from the inoculum, and is viscosity-, temperature- and moisture-dependent. After mutagenesis, the Swr^- phenotype was observed, but only 2% of these strains had a mutation in the plasmid's *fliL* locus. I also

tested the hypotheses that (1) Swr^- resulted from mutations in the plasmid *ori* or Cm^R gene, (2) mutations in *fliL* resulted to impaired swarming but not complete loss, and (3) the mutated copy of *fliL* and the chromosomal copy of *fliL* had undergone homologous recombination. However, none of them showed mutations in the genetic sequence.

Materials and Methods

Bacterial strains and culture conditions. Table 6 lists the strains and plasmids used in the study. All strains were grown in LB broth, at 37 ^oC, 200 rpm. Colonies were grown on LSW^- agar (10 g $liter^{-1}$ Bacto tryptone, 5 g $liter^{-1}$ yeast extract, 0.4 g $liter^{-1}$ NaCl, 5 ml $liter^{-1}$ glycerol, 20 g $liter^{-1}$ Bacto agar) for BB2000 strains and LB agar (LB medium containing 15 g $liter^{-1}$ Bacto agar) for *E. coli* strains at 37^oC. Media with selection contained chloramphenicol (Cm), 40 μg/ml or 80 μg/ml and kanamycin (Kan), 50 μg/ml. Swarming assays were performed on 0.85% and 0.9% LB agar plates Costar 24-well clear tc-treated (tissue culture) multiple well plate (Corning Life Sciences) at 37 ^oC.

Table 6. Strains and plasmid used in the study

Strains	**Genotype/Properties**		**Source**
BB2000	wt *Proteus mirabilis*		(53)
YL1003	BB2000 *fliL::kan*-nt30	Amp[1]	(18)
XL1-Red	*mutS, mutD, mutT*	Amp	(173, 174)
XL1-Blue	*E. coli*		Stratagene
DHα5	*E. coli*		Lab[3] stock
Plasmid			
pYL98	*fliLp fliL* $fliM_{400}$	Cm[1]	Y.Y. Lee[4]
pUC18	*lacZ*	Amp	(175)

[1] Amp Ampicillin resistance
[2] Cm Chloramphenicol resistance
[3]Belas Laboratory
[4]Dr. Yi-Ying Lee, post-doctoral fellow Belas Laboratory

Curing of YL1003/pYL98. YL1003/pYL98 was cured of the plasmid by growing Swr^+ YL1003/pYL98 in LB with Kan to select for YL1003 and incubating for a period of four days with re-inoculation every 24 h. After the fourth day, the culture was washed with 1% PBS, diluted 10^{-4} and plated by spreading in LSW^- plus Kan. Cells were grown overnight at 37 ^oC. Forty-nine colonies were selected and picked using sterile toothpicks on parallel LSW^- plates, one with both Kan and Cm selection and the other with Kan only. Colonies that grew on the Kan plates but not the Kan and Cm plates were selected and checked for presence of pYL98 by plasmid extraction using a Qiagen Miniprep Kit. Colonies without a plasmid were screened for swarming using 1.5% LB agar with Kan.

XL1-Red Mutagenesis. Mutagenesis of pYL98 (Fig. 25) was achieved using XL1-Red Competent cells (Agilent Technology) following the manufacturer's protocol. 100 µl of XL1-Red Competent cells were transformed with 50 ng of pYL98 by combining them in 1.5 ml microcentrifuge tubes on ice for 30 min, then heat-shocked at 42 ^oC for 30 s and back on ice for 2 min. 900 µl of LB was then added to the tube and incubated at 37 ^oC, 200 rpm for an hour. 200 µl were then plated by spreading onto 1.5% LB agar with Cm 40, incubated for 48 h at 37 ^oC. Cells were then washed with 5 ml LB and scraped off the plate with sterile disposable spreader. Washed cells were then collected in a 125 ml Erlenmeyer flask (EF) and brought to a volume of 10 ml with LB plus Cm and incubated for 1.5 h at 37 ^oC, 200 rpm. XL1-Red has a doubling time of 90 minutes. This culture represents approximately 20 generations of XL1-Red, some were used as starting inocula for the next incubation (a 1:1000 dilution incubated overnight represents another 10

generations), and then plasmids were extracted from the rest. Cells were incubated for a period of 10 days at 37 ^{o}C, 200 rpm, with re-inoculation everyday at 1:1000 dilution using LB plus Cm 40. An overnight inoculation represents an approximate 10 generations in XL1-Red. Plasmid was then extracted before re-inoculation using the Qiagen Miniprep kit following the manufacturers' protocol. This method would increase the mutation rate with XL1-Red.

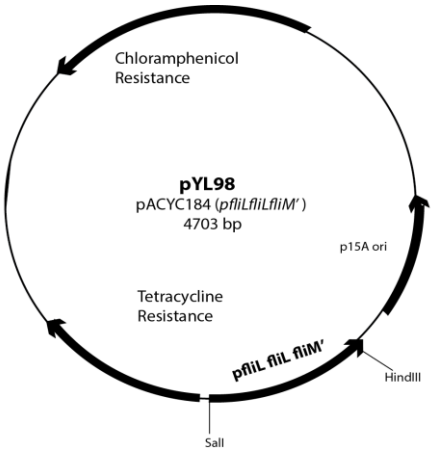

Fig. 25. Plasmid pYL98 derived from pACYC184 with the *fliL* promoter, *fliL* coding region and the 400 bp 5' region of *fliM* can complement the Swr- phenotype of YL1003.

Electroporation. Mutated pYL98 at a concentration of 100 ng/ul was added to a pre-chilled sterile 1.5 ml microcentrifuge tube and then 50 µl of ice-thawed competent cells were pipeted in. The mixture was placed into a clean, sterile and ice-cold 0.2 cm electroporation cuvettes (BTX) and pulsed at 2.5 kV and a time constant ideally between 4.2 to 4.9 msec. Pre-warmed 1 ml LB broth was immediately added and gently mixed with the electroporated cells. The mixture was then placed in pre-warmed 1.5 ml microcentrifuge tubes and allowed to recover at 37^{o}C without agitation for 30 min, and then incubated for an additional 1 - 1.5 h with agitation. One hundred µl of cells were

then spread-plated in LSW$^-$ agar with Kan 50 and Cm 80. The cells were then incubated at 37^{o}C for 36 h. Single colonies were then assayed for possible mutation using Swr$^-$ as the phenotypic screen.

Screening of Swr$^-$ mutants using plates. After incubation, isolated colonies were picked using a sterile toothpick to a 7 x 7 master grid on LSW$^-$ agar with Cm 40 and Kan 50, and incubated at 37 ^{o}C for 18 h. Colonies were then transferred to 0.85% LB agar plus Cm 40 and Kan 50 using a sterile 49-tine metal inoculator 'frog'. Plates were incubated at 37 ^{o}C for ca. 6 h and then incubated at 30 ^{o}C overnight after which swarming motility was assessed. Non-swarming colonies were picked from the master plate using sterile toothpicks to new master plates (7 x 7 LSW$^-$ agar with Cm 40 and Kan 50), incubated using the same conditions, followed by another swarming assay (7 x 7 0.85% LB agar with Cm 40 and Kan 50). This was repeated a total of 3 times to reduce Swr$^-$ false-positives.

Screening Swr$^-$ mutants using 24-well tissue culture plates. A total of 1,000 isolated colonies were selected after transforming YL1003 with a pool of mutated pYL98. Each colony was inoculated into a well of a Costar 24-well clear tc-treated (tissue culture) multiple well plate (Corning Life Sciences) with 1 ml of 0.85% LB agar with Cm 40 and Kan 50. Plates were then incubated at 37 ^{o}C room for about 60 h. Colonies that were Swr$^-$ were re-inoculated into another well of a fresh 24-well tissue culture plate and incubated for another 60 h.

Plasmid preparation and sequencing. Colonies that were consistently Swr^- after successive screening were selected for further analysis. Each colony was streaked on 0.9% LB agar plus Cm 40 and Kan 50 and incubated for 24 h at 37 ^oC. Plasmid were isolated from streaked colonies that have non-swarming isolated colonies by growing them in 2 ml LB plus Cm 40 and Kan 50 overnight and extracting plasmid using the Qiagen Miniprep Kit. Extracted plasmid were retransformed and purified from *E. coli* DH5α then sequenced using the Sanger method on a 16 capillary DNA sequencer, 3130XL Genetic Analyzer (Life Technologies).

Bioinformatics Analysis. Raw sequence chromatograms were checked using Chromas Lite version 2.1 (2012, Technelysium Pty Ltd, South Brisbane, Queensland, Australia). Sequence alignment was done using the ClustalW function of the BioEdit Sequencing Alignment Editor (176). The protein's physical and chemical characteristics were predicted using the ProtParam Tool of the ExPASy server (http://web.expasy.org/protparam/) ((177). Prediction of the effect of amino acid substitution on protein function was generated using the J. Craig Venter Institute's SIFT-BLink tool (http://sift.jcvi.org/www/SIFT_BLink_submit.html) (178). Secondary structure was deduced using the PSIPRED (http://bioinf.cs.ucl.ac.uk/psipred/) secondary structure prediction method (179) while the tertiary/3D structure was predicted using the Phyre2 Protein Fold Recognition server (http://www.sbg.bio.ic.ac.uk/phyre2/html/page.cgi?id=index) (180).

Results

Generation of *fliL* mutants *in silico*

Bioinformatics analysis of *P. mirabilis* FliL predicts that it is a small protein composed of 160 amino acids, with a mass of 18.2 kD (Table 7). It has a theoretical pI of 8.02 and has more positively charged residues than negatively charged ones (Table 2). FliL is predicted to be an inner membrane protein with a single transmembrane region extending from residue 10 to 35, with a predicted secondary structure consisting of 4 alpha helices and 5 beta sheets (Fig. 26).

Table 7. Properties of FliL

Number of amino acids: 160
Molecular weight: 18230.2
Theoretical pI: 8.02
Localization: Inner Membrane
Amino Acid Composition
Ala (A) 10 6.2%
Arg (R) 10 6.2%
Asn (N) 5 3.1%
Asp (D) 6 3.8%
Cys (C) 0 0.0%
Gln (Q) 6 3.8%
Glu (E) 11 6.9%
Gly (G) 7 4.4%
His (H) 5 3.1%
Ile (I) 15 9.4%
Leu (L) 25 15.6%
Lys (K) 8 5.0%
Met (M) 3 1.9%
Phe (F) 5 3.1%
Pro (P) 6 3.8%
Ser (S) 12 7.5%
Thr (T) 12 7.5%
Trp (W) 2 1.2%
Tyr (Y) 5 3.1%

Val (V) 7 4.4%
Pyl (O) 0 0.0%
Sec (U) 0 0.0%

(B) 0 0.0%
(Z) 0 0.0%
(X) 0 0.0%

Total number of negatively charged residues (Asp + Glu): 17
Total number of positively charged residues (Arg + Lys): 18

Atomic composition:
Carbon C 827
Hydrogen H 1335
Nitrogen N 221
Oxygen O 235
Sulfur S 3

Formula: $C_{827}H_{1335}N_{221}O_{235}S_3$
Total number of atoms: 2621
Extinction coefficients:
Extinction coefficients are in units of M^{-1} cm^{-1}, at 280 nm measured in water.
Ext. coefficient 18450
Abs 0.1% (=1 g/l) 1.012
Estimated half-life:
The N-terminal of the sequence considered is M (Met).
The estimated half-life is: 30 h (mammalian reticulocytes, in vitro).
>20 h (yeast, in vivo).
>10 h (*Escherichia coli*, in vivo).
Instability index:
The instability index (II) is computed to be 52.62
This classifies the protein as unstable.
Aliphatic index: 116.44
Grand average of hydropathicity (GRAVY): 0.004

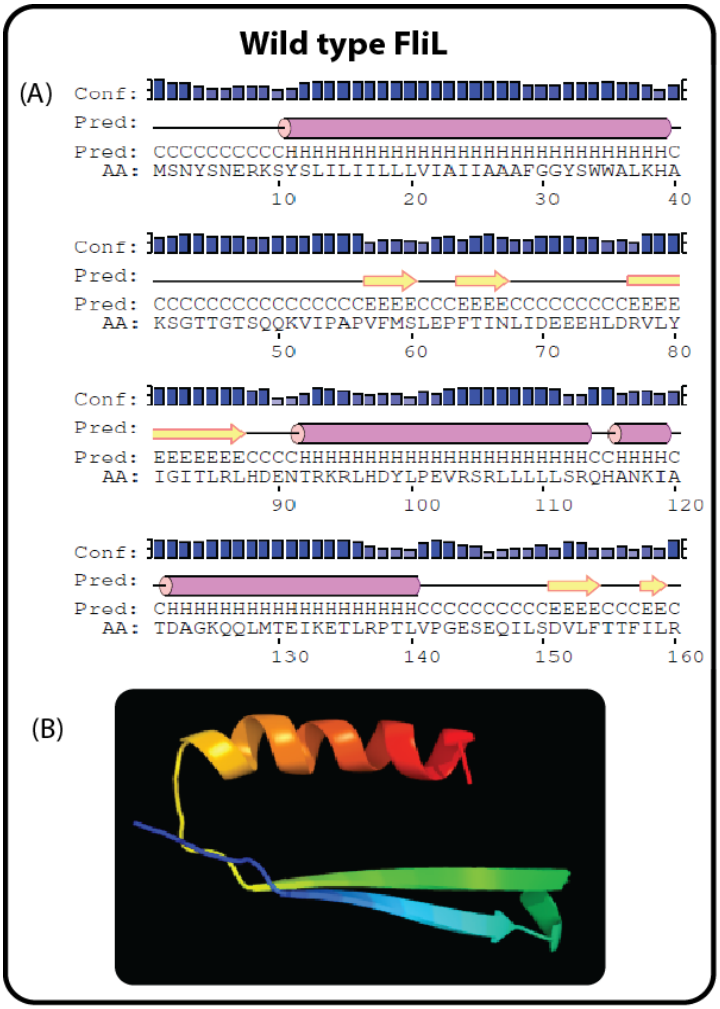

Fig. 26. Predicted Structure of FliL. (A) Secondary structure of FliL predicted using PsiPred server is composed of 4 alpha helices and 5 beta sheets; and (B) Tertiary structure predicted using the Phyre2 Server. The closest homology with 69% confidence was an alignment from position 61-107 to the C-terminal domain of another flagellar protein, FliK.

I used bioinformatics to give a general feel of what to expect in terms of mutations in FliL. A most obvious prediction is that I would see a lot of nonsense mutations that would result in truncation of FliL, as well as mutations in the promoter region and in the transmembrane domain of FliL. I first used the SIFT-BLINK (178) prediction tool to predict which amino acid substitution most strongly affects FliL structure (and perhaps its function). Prediction is based on the degree of conservation of amino acid residues in sequence alignments derived from closely related sequences

collected through PSI-BLAST. This is under the premise that positions in a protein alignment that are important for function are conserved through evolution. The generated list in Appendix 1 showed how a particular amino acid change can potentially affect protein function. Amino acids scoring less than 0.05 means that the change is possibly not tolerated by the cells. Based on this, I predict that mutations in positions 36-55 are more tolerable as compared to mutation in positions 76-160, particularly in the last 10 amino acids from the C-terminal. Also, Cusick et al (63) showed that the last 14 amino acids of the C-terminal of *fliL* is important. There are a number of segments where mutations are predicted to be generally intolerable, implying that the protein FliL has a lot of conserved domain. I used this data as guide in simulating mutation in FliL.

As mentioned earlier, the predicted secondary structure of FliL is composed of 4 alpha helices; the first of which is also predicted to be a transmembrane domain. I simulated mutations that can break each of these helices by changing an amino acid, usually leucine or alanine that are prone to form helices to proline, a known helix breaker. Representatives of mutated FliL secondary structure generated through PSIPRED (179) are shown in Fig. 27. Substitution of P for A_{27} ($FliL_{A27P}$) did not change the predicted secondary structure (Fig. 27B), however, when P was instead substituted to A_{28} ($FliL_{A28P}$) a break in the predicted alpha helix was generated (Fig. 27C). However, the transmembrane domain, protein topology and localization remained unchanged. When leucine at position 63 was substituted to P_{63} ($FliL_{L63P}$) situated between two predicted short beta-sheets, no change on the secondary structure was observed, however, it caused a slight shift of the alpha helix preceding and closest downstream to it (Fig. 27D). A substitution of P for L_{100} ($FliL_{L100P}$) also caused a break of the second predicted

alpha helix (Fig. 27E). Another P substitution, this time to R_{137} ($FliL_{R137P}$) located towards the end of the third alpha helix, caused the helix to end at the substitute P (Fig. 27F). These results show that a base pair mutation can change the secondary structure of the FliL which can potentially affect FliL function by affecting its interaction with other proteins. Based on these simulations, I predict that mutations that would result to a Swr^- phenotype would be most likely be one of these amino acids located in region 76-160,. It was reported by Cusick *et al* (63) that the last 10 amino acid of FliL were most fragile, however, those mutations caused Elo^+ phenotype thus I did not simulate them for Swr^- mutatant.

I also used the program Phyre2 (180) to predict the tertiary structure of FliL (Fig. 26B). The closest homology generated was to the solution structure to the C-terminal domain of FliK, the flagellar hook-length control protein, at 69% confidence. The covered alignment was from position 61-107 (Appendix 2). Interestingly, this region was predicted by SIFT-BLINK (178) to be highly conserved and mutations in these positions were predicted to be generally intolerable. When $FliL_{L100P}$ was modeled using Phyre2 (180) the closest homology became that to a membrane protein with 70% confidence and its predicted homology to FliK dropped to 29% confidence. The same trend went for $FliL_{A28P}$ and $FliL_{L63P}$.

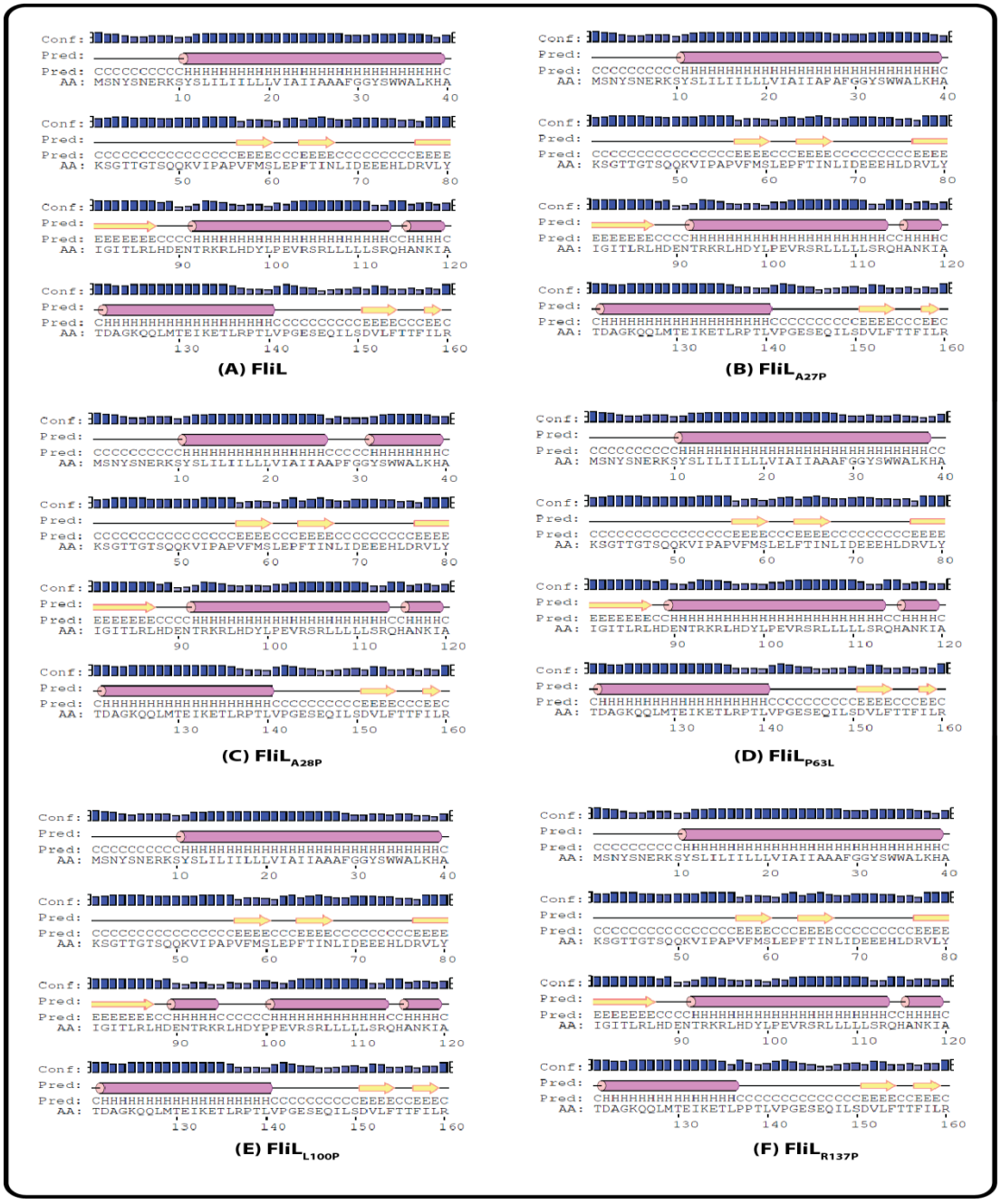

Fig. 27. Predicted secondary structure of *in silico*-generated *fliL* mutants. (A) Wildtype FliL is similar to (B) FliL$_{A27P,}$ which is a single base pair substitution of P to A_{27} however, when P was instead substituted to $A_{28,}$ (C) FliL$_{A28P}$ generated a break in the predicted alpha-helix. When leucine was substituted to P_{63} situated between two predicted short Beta-sheets, no change on the Beta sheets were observed (D) FliL$_{P63L}$ however, it caused a slight shift of the alpha helix preceding and closest downstream to it. A substitution of P to L_{100} (6) FliL$_{L100P}$ caused a break of

the second predicted alpha helix while a substitution of P to R_{137} ($FliL_{R137P}$) located towards the end of the third alpha helix, caused the helix to end at the substitute P (F). Images and prediction generated using PsiPred.

Complementation of the swarming phenotype of *fliL* cells

Mutations in *P. mirabilis* FliL confer a non-swarming phenotype and induce the production of pseudoswarmer cells in non-inducing conditions (broth). Lee *et al.* (2013) reported that in a *fliL* knockout strain YL1003 (*fliL::kan*-nt30) expression of *fliL in trans* can complement the pseudoswarmer phenotype but not the non-swarming phenotype. Complementation requires *P. mirabilis fliL* promoter, *fliL* coding region, and a portion of *fliM* 5' sequence (18).

In this study, my focus was to identify regions of *fliL* important for swarming by mutating a plasmid pYL98 that can complement the non-swarming phenotype of YL1003. Using a mutator strain *E. coli* XL1-Red that lacks DNA repair mechanism a pool of mutated pYL98 was generated. Screening of possible mutants was done by inoculating single colonies of mutated pYL98-transformed YL1003 in a 7 x 7 1.5% LB agar, incubated for 37 ^{o}C and observed for swarming in 12 h. The prediction was that majority of the colonies would be Swr^{+}. However, I observed only an average of 10% swarming colonies (48 of 490) and even the control pYL98-transformed YL1003 did not consistently exhibited the expected Swr^{+} complementation. This unexpected result led me to develop a more efficient assay for determining swarming complementation.

First, the rate of mutation was determined. I performed a control experiment in order to verify *E. coli* XL1-Red activity by making use of pUC18 and *E. coli* XL-1 Blue

in a straight-forward blue-white screening assay. pUC18 was transformed into XL-1 Red and grown for 3 days or approximately 40 generations at 37 ^{o}C with re-inoculation, and plasmids were harvested each day. The pool of mutated plasmid was transformed in XL-1 Blue and spread-plated on LB agar and Amp 100 and XGal 40. White colonies were assumed to contain mutated pUC18 that disrupted the α-complementation of β-galactosidase. I determined that the longer the plasmid was incubated in XL-1 Red, the higher the mutation rate, with 24% mutations after 3 days of incubation/ 40 generations (Table 8). This increasing trend is consistent with the manufacturer's documentation as well as existing literature that made use of XL-1 Red to generate random base pair mutations (173, 174, 181).

Table 8. XL-1 Red Control

pUC18[1]	CFU/10^3	White	%mutation
1	104	14	13
2	115	23	20
3	118	28	24

[1]XL1-Red transformed with pUC18 was grown for 3 days with re-inoculation and plasmid extracted for each day approximate generation is as follows: 1- 20 generations, 2-30 generations and 3-40 generations.

I compared swarming of wild-type BB2000 and YL1003/pYL98 on 1.5% LB agar. YL1003/pYL98 swarmed at a much later time, about 8-10 h after initial inoculation, compared to the wild-type (onset at 3.25 h, Fig. 29 and 30), and most often started with one or more flares (a sector of bacteria swarming ahead of the colony), giving the colony a star-like appearance. Flares could be as the result of a mutation on the chromosome or a

mutation in the plasmid that result in Swr^{+}. A homologous recombination event is also possible between pYL98 *fliL* sequence and YL1003 chromosomal *fliL* given that YL1003 still has all of the *fliL* gene sequence, despite not having witnessed any homologous recombination in previous attempts. I tested this possibility by curing complemented YL1003, and amplifying the *fliL* gene from the genomic DNA. Our results showed that cured YL1003 does not swarm which means that swarming is due to the plasmid not to a secondary mutation in the chromosome. In addition, amplified *fliL* from YL1003/pYL98 were similar to YL1003 (Fig. 28) not wild-type indicating that no recombination event occurred.

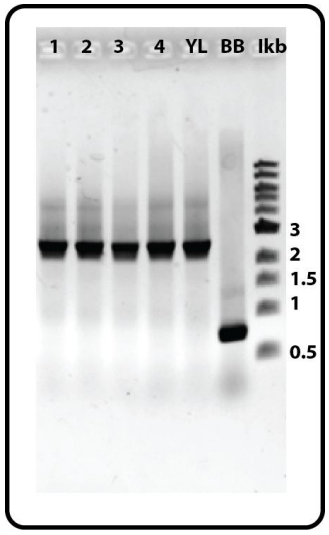

Fig. 28. Amplified *fliL* from Swr^{+} YL1003/pYL98. The Swr^{-} defect of YL1003 is supposed to be complemented by pYL98. However, some colonies were non-swarming at 1.5% LB agar. A possible homologous recombination event can occur between YL1003 and pYL98. Amplification of *fliL* of the genomic DNA of Swr^{+} YL1003/pYL98 (1-4) and YL1003 showed similar bands in contrast to wild-type *fliL* from BB2000.

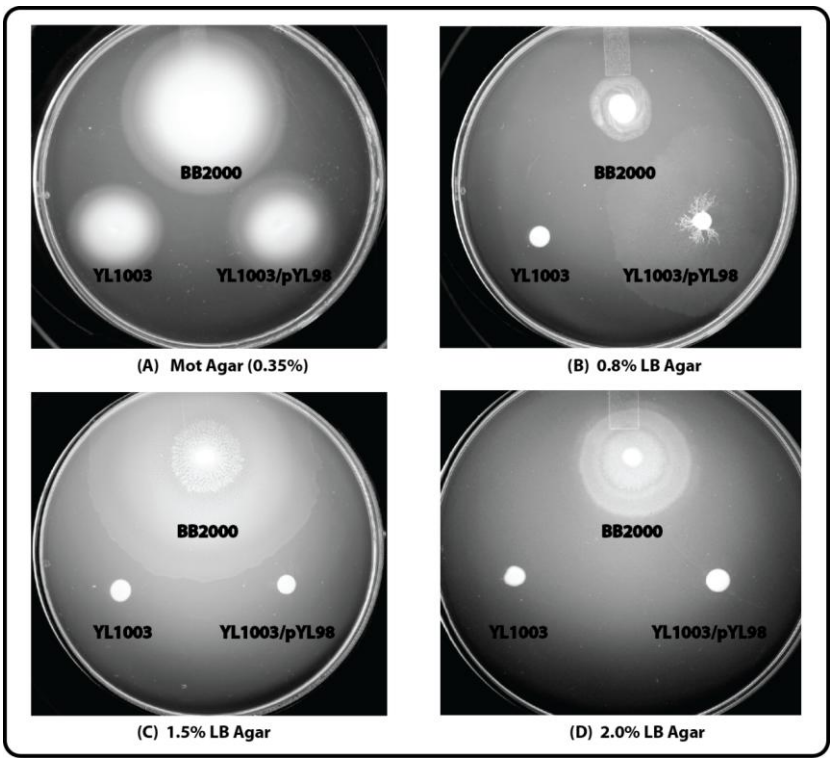

Fig. 29. YL1003/pYL98 swarming in different agar concentration. Swarming of YL1003/pYL98 was compared with BB2000 wt and *fliL* YL1003 in different agar concentrations: 0.35% (Mot agar), 0.8%, 1.5% and 2%. Swarming of YL1003/pYL98 is distinct at 0.8% agar.

With the possibility of secondary mutations ruled out, I concentrated my efforts on determining the best condition for measuring swarming of YL1003. I tested different agar concentrations to see which ones would best discriminate between complemented and non-complemented YL1003 (Fig. 29). Complementation of pYL98 was most apparent and consistent on LB with 0.8% agar as compared to LB with either 1.5% or 2% agar. The migration of YL1003/pYL98 over different agar concentrations in 10 h was also compared with that of YL1003 and BB2000 (Fig. 30). Swarming of YL1003/pYL98 on all agar concentrations started as flares, but swarming migration changed in a viscosity-dependent manner, with the highest swarming seen at 0.8% LB agar. Therefore,

0.8% agar gave the least chance of false-positives and was used in subsequent assays. Interestingly, swarming of YL1003/pYL98 on 0.8% agar was more robust than that of the wild-type. It was also characterized by a thin film of swarming bacteria in contrast to the thicker film and slower migration of the wild-type cells.

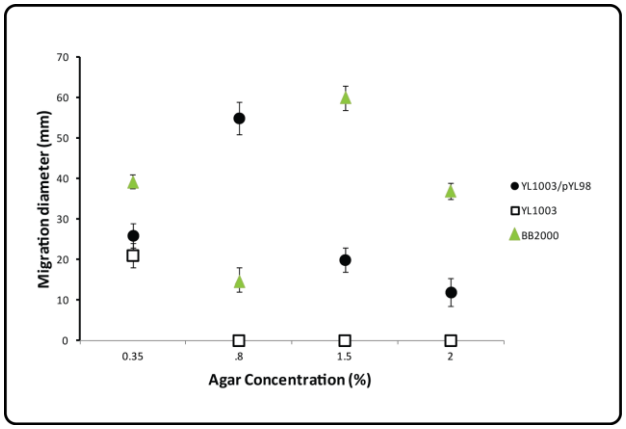

Fig. 30. Swarming of BB2000 and YL1003/pYL98 is viscosity dependent. YL1003/pYL98 swarming is optimal at 0.8% agar concentration while BB2000 wild-type is at 1.5%

Next, I determined the optimal temperature and time of incubation for optimal swarming of YL1003/pYL98. Even in 0.8% agar, YL1003/pYL98 only exhibited swarming after 8-10 h, and even then, not all colonies began to swarm at the same time. This caused problems in the initial screen because over-swarming of some colonies can occur at 37 ^{o}C. At 37 ^{o}C, 15 h of incubation can be too long; however, 8-10 h is not enough. At least 24 h is needed to observe swarming at 30 ^{o}C, while at least 48 h was needed in RT (25 ^{o}C). In the end, a combination of 37 ^{o}C (at least 4 h) and 30 ^{o}C (overnight) was used.

The use of different arrays of cells placed on the agar aside from a 7 x 7 array was also considered. In testing different array configurations, an unexpected result was observed. In overgrown plates, bacteria nearest the edge of the plate swarmed more, possibly due to too much moisture at the center of the plate, which would promote swimming and inhibit swarming motility. I tested the hypothesis that swarming is affected by agar wettability by comparing LB with either 0.75%, 0.8%, or 0.85% agar as well as using parafilm to seal the plate and presumably cause more uniformity of agar surface moisture (Fig. 31). As expected, 0.85% agar generated the most of Swr^+ colonies. I have also tried adding a surfactant (0.001% Tween 20) and removing the selection from swarm plate, but neither improved the assay (Table 9). I have determined that the use of 0.85% agar with selection and incubation at a combination of 37 ^oC and 30 ^oC was the most optimal for the assay. Using the screening procedure described, successive assays using the 7 x 7 grid were screened. Afterwards, to minimize false-positive, Swr^- cultures were assayed in different grid arrays, such as a 2 x 3 grid of colonies.

Table 9. Swarming Assay Condition Tested

Swarm plate condition	Percent of swarming
0.75% agar no parafilm	62%
with parafilm	No swarming
0.8% agar no parafilm	80%
with parafilm	82%
0.85% agar no parafilm	85%
with parafilm	85%
Tween 20 0.001%	Cannot be determined [1]
No selection	Cannot be determined[1]

[1]Cells were over swarming

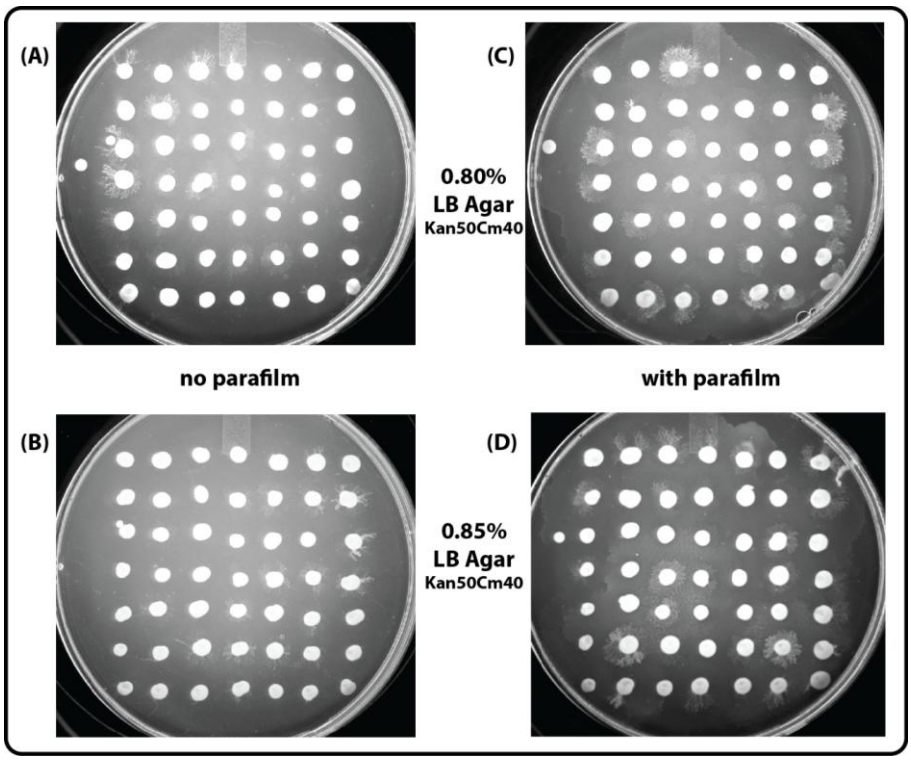

Fig. 31. Screening for possible *fliL* mutants. A 7 x 7 array was used as an initial screen for putative *fliL* mutants. All colonies contained non-mutated pYL98 and should all be Swr^+.

Of the 40 putative Swr^- mutants obtained using this approach, only one manifested a mutation in the insert and it was in the *fliM* region (Fig. 32). In addition, the screening procedure using the agar plate still posed the danger of over-swarming. It is possible that given enough time, those that were putative Swr^- could swarm. Thus, I needed to find a way to isolate each colony at the same time conserving materials without sacrificing the experiment.

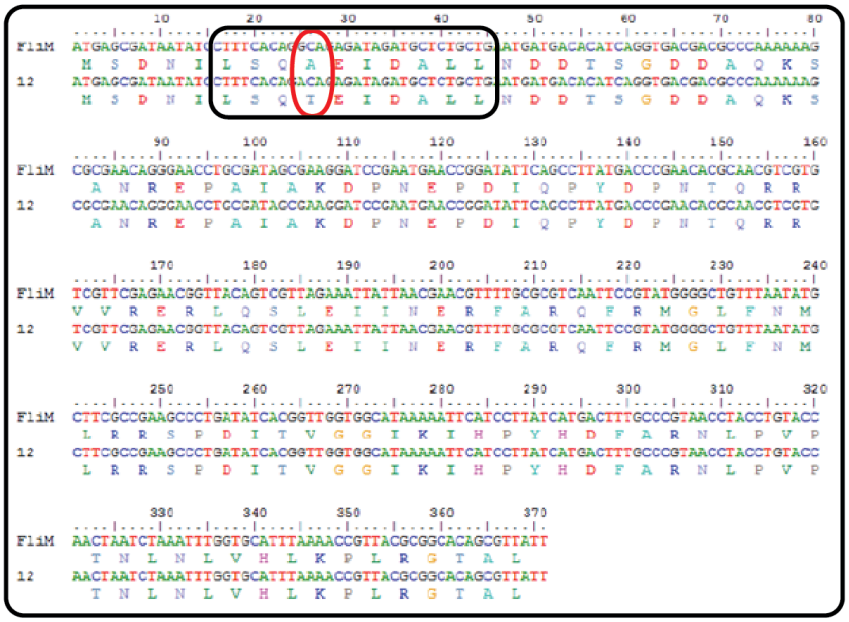

Fig. 32. Sequence alignment of Swr⁻ mutant from XL1 Red Mutagenesis. A putative Swr⁻ mutant showed a single base pair change in position 26 of the *fliM* region resulting to a change from alanine to threonine. This falls within the conserved N terminal peptide LSQXEIDALL in FliM that is important in CheY-P binding. (Image data generated from BioEdit (**175)**)

XL1-Red mutagenesis resulted in a truncated FliL and mutation in the conserved N-terminal LSQXEIDALL domain of FliM that is important in CheY-P binding

I have discussed at great length in the prior section how I tried to optimize my screening procedure. However, even with these optimized conditions, the assay was still problematic in discriminating mutated pYL98-transformed YL1003. This is evident as only one mutation was found in 40 Swr⁻ colonies, and this mutation was in the *fliM* region of the insert. There was base pair substitution from a G to A that resulted in a substitution of threonine for alanine at position 9 (Fig. 32) that falls within the conserved FliM N-terminal domain (LSQXEIDALL), which serves as a binding site for CheY-P

and acts to switch the direction of flagellar rotation (39). This mutation did not change the charge of this conserved peptide but changed its hydropathicity (Table 10). It has already been shown in *Salmonella* that a Mot$^-$ phenotype can occur even with just an amino acid change and that electrostatic interaction plays a role in switching (38). Of course, only a small fragment of *fliM* DNA is carried on pYL98, and it is unlikely that this peptide is active. Moreover, a complete copy of wild-type *fliM* is maintained on the chromosome of YL1003, and is likely dominant over truncated protein. So, it is unlikely that this mutation is affecting the FliM protein. A more reasonable prediction is that the mutation is acting pre-translationally, perhaps to change the stability of the *fliL* mRNA, as has been suggested by Lee et al (2013).

Table 10. Properties of the conserved FliM peptiode in wild-type and mutant

	LSQAEIDALL[2]	**LSQTEIDALL**[3]
Number of amino acids:	10	10
Molecular weight:	1072.2	1102.2
Theoretical pI:	3.67	3.67
Total number of negatively charged residues (Asp + Glu):	2	2
Total number of positively charged residues (Arg + Lys):	0	0
Formula:	$C_{47}H_{81}N_{11}O_{17}$	$C_{48}H_{83}N_{11}O_{18}$
Total number of atoms:	156	160
Instability index:	47.52	66.78
Aliphatic index:	176	166
Grand average of hydropathicity (GRAVY):	0.82	0.57

[1]Data generated from ExPassy ProtParam (177)
[2]Wild-type FliM conserved peptide sequence
[3]Mutant FliM conserved peptide sequence

Because of this low rate of mutation, I designed a new screening assay using 24-well plates (Figure 33). With the use of the 24 well plates, I achieved 92% (22 out of 24 YL1003/pYL98 colonies were Swr^+ after 36 hours) complementation with YL1003/pYL98. This was consistently observed in 4 control experiments each done on separate occasion. This gave confidence in the assay. This time I used pYL98 mutated over a period of 10 days for an approximate 100 generations in XL1- Red, expecting a highly mutated plasmid. I screened 1008 colonies in forty-two 24-well plates and ended up with 400 putative Swr^- mutants. Selected strains for sequencing were streaked on 0.9% LB agar plus Cm 40 and Kan 50 to isolate single colonies and measure swarming. There were three types of phenotypes observed: (1) Swr^+; these are false positives; (2) Swr^-, isolated colonies that were Swr^+ in dense areas; and, (3) Swr^- in all areas. Upon further analysis, the second phenotype were false positives, as when they were restreaked, they remained Swr^+. This could result from a mutation in a gene that interacts with *fliL*; however, the frequency of obtaining these mutants makes this unlikely, and the true cause for colonies with the second phenotype remains unknown.

I isolated and sequenced 54 plasmids from 27 Swr^- colonies each of phenotypes 2 and 3. Only one of the 54 Swr^- colonies had a mutation in *fliL* (Fig. 34). This plasmid was highly mutated. There was a substitution from C to A at position 277 that lead to a change from an arginine to serine. There was also an insertion of A at position 291 that change histidine from glutamine and shifted the coding region to introduce a stop codon resulting in a truncated protein due to a nonsense mutation. This proves that the assay can detect *fliL* mutations on pYL98. I have also tested different hypothesis on where the

mutations on pYL98 were but were unable to find additional mutations in *fliL*. In the Discussion section that follows, I elaborate all our attempts in finding other mutations

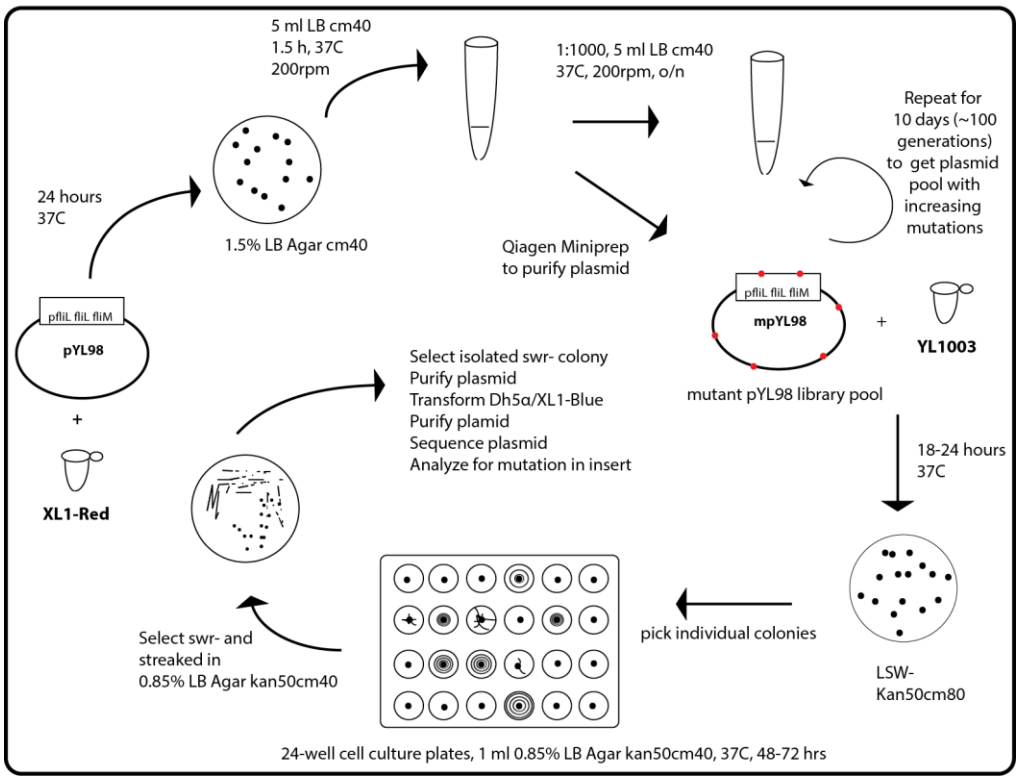

Fig. 33. Schematic Diagram of XL1-Red Mutageneis of pYL98 and succeeding screens for swarming. XL1-Red competent cells (Agilent Technology) were used to intoduce random mutations in plasmid pYL98. It was allowed to propogate for about 100 generations. Mutated plasmid pool were extracted and electroporated into YL1003. Colonies were picked into a 24 well plate with 0.85% LB agar with Kan50 and Cm 40 and incubated for 48-72 h. Colonies that were Swr^- were re-inoculated into another 24-well culture plate. Putative Swr^- mutant were then streaked into 0.85% LB agar with selection. Colonies that were not swarming were selected. Prior to sequencing, plasmid were purified into an *E. coli* strain (DH5α or XL1-Blue).

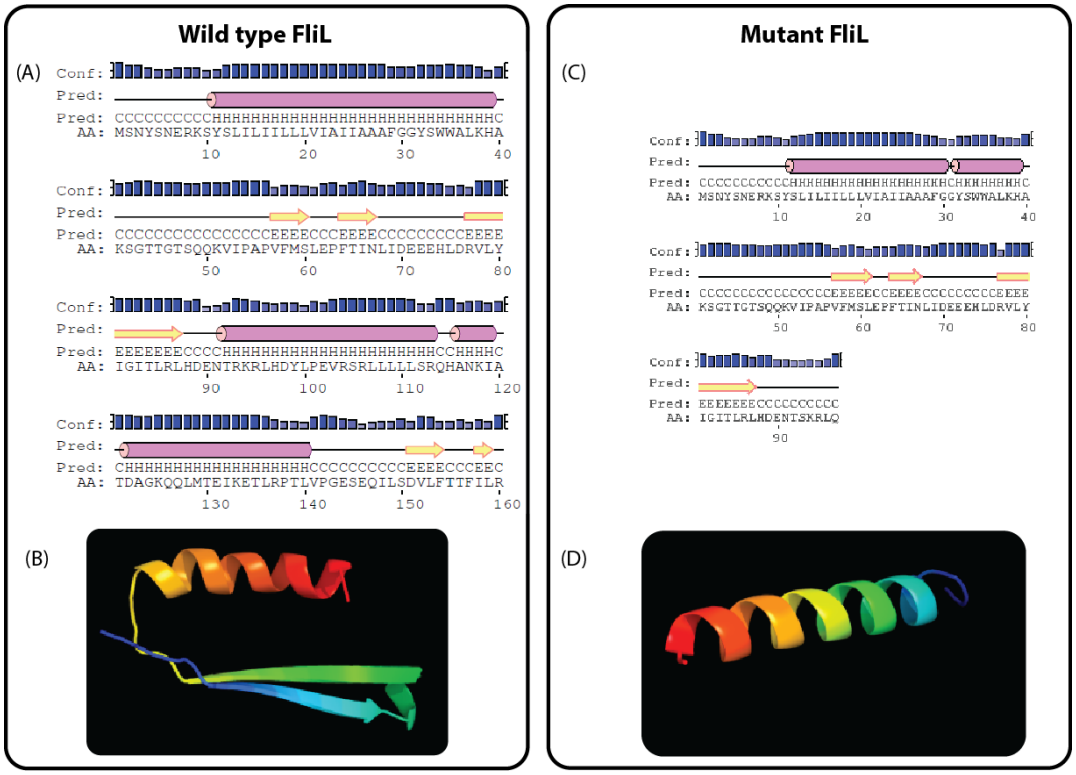

.

Fig. 34. Mutated FliL from XL1-Red Mutagenesis. Predicted (A) secondary and (B) tertiary structure for wildtype FliL and (C) secondry and (D) tertiary structure for mutant FliL. resulting to a truncated protein. (Image data generated from (A, C) PsiPred ((http://bioinf.cs.ucl.ac.uk/psipred/; 178) and (B, D) Phyre2 (http://www.sbg.bio.ic.ac.uk/phyre2/html/page.cgi?id=index; 179).

Discussion

There are *P. mirabilis fliL* mutant reported: - BB2204 (*fliL*::Tn*5*-*Cm*), which is non-motile; YL1001, which is a motile revertant of BB2204; and YL1003 (*fliL::kan-nt30*), which swims but does not swarm (18, 19, 63). All three produce pseudoswarmer

cells in broth, and all three can be complemented by *fliL* expressed *in trans.* The non-motile phenotype of BB2204 was attributed to polar effects, as shown in YL1001; however, both strains showed an alteration of the C terminus of FliL suggesting that it may be responsible for the pseudoswarmer cell phenotype. YL1003 on the other hand has an insertion in nt 30 generating a protein that is truncated and plasmid pYL98 can complement the Swr^- phenotype.

The goal of this study was to determine the functional domain of FliL required for swarming by generating random single base mutation that would result to a Swr^- phenotype. The prediction was that mutations would be concentrated in the promoter region and in the transmembrane domain of FliL. In addition, I expected to find nonsense mutation that can result in a truncated/nonfunctional protein. Based on my bioinformatics analysis, I also predicted mutations to be found on positions 76-160.

The complementation of the Swr^- phenotype of the *fliL* YL1003 is peculiar because it requires extra DNA aside from the *fliL* coding region (18). It requires at least the first 200 nucleotides upstream of the *fliL* start codon, where the promoter is speculated to be located. It also requires at least 400 nucleotides downstream of *fliL,* which is part of the 5' portion of *fliM*. Even then, this DNA does not complement YL1003 to a wild-type level swarming. I also found that the Swr^+ phenotype was not always manifested, possibly because the conditions for swarming of this mutant are more stringent. In any case, this presented obstacles in screening for mutated pYL98 because of the high frequency of false-positives. I have also shown that this complementation generated an interesting phenotype. YL1003/pYL98 showed better swarming than wild-type in 0.8% agar, an environment where active swarming is usually inhibited.

Additionally, swarming migration is also characterize by a thin filament of swarming without the consolidation zones that *P. mirabilis* is famous for. I used this difference between the complemented strain and BB2000 to improve my screening assay.

I have sequenced 94 putative Swr$^-$ *fliL* mutants, 40 from the the initial screening using 7x7 grid plates and 54 from the 24-well plate screening, but only two have a mutation in their respective sequences. The first mutation is in the conserved N-terminal region of *fliM* and the other one is in the *fliL* coding region resulting in a truncated protein. Only the first 400 bp from the 5' end of FliM was included in pYL98. The requirement for this extragenic sequence in *fliL*- YL1003 Swr$^-$ complementation is peculiar, and is suggested to be needed to stabilize the mRNA (18). It is possible that even though wild-type FliM exist in YL1003, the greater number of mutated FliM expressed from the plasmid caused the Swr$^-$ phenotype. The mutation is in the conserved FliM N-terminal peptide (LSQXEIDALL) contained on the N-terminal domain of FliM where CheY-P directly binds to switch rotational direction (39). With the change from alanine to threonine the net charge of the peptide was not changed (-2 at pH 7) but it lowered the hydropathicity from 0.82 to 0.57. Reduced hydrophaticity can make the peptide less hydrophobic and thus has the potentialto change its structure and interaction. Electrostatic interaction was already suggested to play an important role in FliM switching and it has been shown that even though rare, a Mot$^-$ phenotype can occur even with just an amino acid change in *Salmonella* (38). However, only a peptide was expressed from the *fliM* sequence in the plasmid and not a full protein. Nonetheless, this result showed that there is more to the extragenic requirement in YL1003 complementation than just for stability.

This low rate of mutation was unexpected, given the result from our control experiment (24% mutation rate) and the obvious phenotypic change in YL1003 when transformed with a XL1-Red mutated plasmid pool. I hypothesized that YL1003, because it contains essentially all of *fliL*, is somehow interfering with the mutation. I tested this by electroporating mutated pYL98 into *E. coli* DH5α and randomly screening 18 plasmids by sequencing. The prediction was that at least 20% of the plasmids (about 3 or 4) should contain a mutation but none of the randomly isolated plasmid showed any mutation in *fliL*, in the promoter, or in the *fliM* region. This raised the possibility that the control experiment was not accurate and should have been repeated. The sample size used is small and could have been increased but any more than that would be impractical with in a population of 1000.

I then speculated that I probably was not looking at the right phenotype for *fliL* mutation. I was working under the assumption that a mutation in *fliL* would result to a Swr^- phenotype. However, it is possible that a single mutation could lead to reduced swarming instead of a complete loss. I hypothesize then that the mutation in *fliL* could be in non-wild-type swarming colonies. I isolated 18 such colonies, selected because they started swarming only after 48 h of incubation during the screening assay. But again, none of the plasmids showed any mutation in any part of the *fliLM* insert of pYL98.

Another possibility was that the Swr^- phenotype was caused by mutations in the plasmid *ori* or Cm^R gene that could affect *fliL* gene copy number. I have sequenced both genes from five representative Swr^- colonies but no mutation were found. The possibility that other parts of the plasmid were mutated was also considered, however, I cannot think of how any of them could affect swarming. I also considered sequencing the pool of

mutated pYL98; however, I do not have the kind of high-level sequencing that can detect base pair mutations in a plasmid pool, especially if they were randomly dispersed. It was also highly impractical at this point, not to mention an improbable hypothesis.

As was previously mentioned, because YL1003 has the whole *fliL* sequence, there is always the possibility of a homologous recombination between chromosomal *fliL* and plasmid-borne *fliL*. I hypothesized that a recombination event exchanging mutated *fliL* from the plasmid and the good *fliL* from the chromosome had occurred. Based on this hypothesis, I predicted that if I sequenced the chromosomal *fliLM* of the putative Swr$^-$ mutants, I might find a mutation in *fliL*. After isolating the genomic DNA of 20 representative Swr$^-$ (10 each for the true non-swarmers and non-swarmers with swarming in dense areas), I PCR amplified fragments that included 500 bp upstream of *fliL* and the whole of *fliM.* Again, none showed any type of mutation.

Despite my best efforts, I was not able to detect any mutations in the DNA sequence, aside from the two already discussed. My hypothesis and experimental design was very straightforward and I did not expect all the caveats that I encountered. The use of XL1-Red in generating single base-pair mutations is well documented (173, 174, 181). My control experiment with pUC18 and our screening assay clearly showed that a change in the swarming phenotype occurred. What, then, are the possible reasons why our phenotypic variations were not supported by genetic changes?

Belas and Suvanasuthi (19) found that over-expression of *fliL in trans* negatively affected swarming in BB2000 wildtype. Furthermore, FliL functionality in *Borrelia* is sensitive to *fliL* copy number (182). These suggest that a threshold on *fliL* copy number exist such that the amount of transcription of the gene can affect swarming. This may explain

why attempts to complement the swarming defect of *fliL* mutants are not achieved by *fliL* alone (18).. Lee *et al.* (18), tried to test this hypothesis by expressing P_{fliI}::*fliL* from an ectopic site in the chromosome of YL1003 at the PMI3101 locus (encoding the sole c-di-GMP GGDEF protein of *P. mirabilis*). Recombination at the native *fliL* region occurred, restoring wild-type *fliLMNOPQR*, in turn, restoring the Swr^+ phenotype (18). This was unexpected since the c-di-GMP DNA is 1.5 kb while that of *fliL* was only less than 500 bp; yet the recombination occurred with the less statistically favorable. This result highlighted the caveat in using YL1003 – recombination is always a possibility especially since *P. mirabilis* seemed to favor the restoration of *fliL* function.

While this study was on-going, an effort by Dr. Yi-Ying Lee to make a complete deletion of *fliL* was underway. This system would have been the most ideal in studying *fliL* function and towards the end of the study, Dr. Yi-Ying Lee was able to make a complete Δ*fliL* strain. However, based on personal communications with her, this strain (YL1006) had an unexpected phenotype: it is Swr^+. She had a similar finding in *E. coli*, in which a complete deletion of *fliL* was also Swr^+, in contrast to previous reports (82). It would seem that in *P. mirabilis* and *E. coli*, a defective copy of *fliL* can result in a Swr^- phenotype, however, once the gene is completely deleted, the cell can swarm. Dr. Yi-Ying Lee's results, once published, will challenge what is currently known about *fliL* function.

Relating her findings to the current study, it may have been better that the screen focused on *fliL* defects that result in wild-type swarming motility, rather than a complete loss of swarming, as I had originally predicted. It is possible that *fliL* does not directly function in swarming, and that the Swr^- phenotype is an indirect effect. This would

explain why only the production of pseudoswarmers can be complemented by *fliL in trans.* This has also been demonstrated in part by Cusick *et al.* (63) when they reported YL1001, a motile revertant of the *fliL*$^{-}$ BB2204. Both YL1001 and YL1006 are Swr^{+} and produces pseudoswarmers in broth. Relating again to the study, a screen for Elo^{-} (formation of pseudoswarmers in broth) could have been the more appropriate phenotypic screen to detect *fliL* mutations.

Recent evidence by Lele *et al.* (183) showed that FliL in *E. coli* is not directly involved in how flagella sense mechanical stress on the motors. They have demonstrated that the stators act as mechanosensors changing their structure in response to changes in external load. They also showed that in cells with a *fliL* deletion, the motors are the same as wild-type. However, the *fliL* mutant they used were not full deletion of *fliL* and our lab recently sent them an *E. coli* Δ*fliL* for analysis. This is supported by Dr. Lee's unpublished data that a complete *fliL* deletion in *E. coli* results to a Swr^{+} strain, although it was not determined if swarming was similar to that of wild-type.

Bioinformatics analysis of FliL showed that the 3D structure of its highly conserved region (61-107) is homologous to the C-terminal region of FliK (Appendix Table XXX), another flagellar protein that controls flagellar hook length. Similar to FliL, FliK is not incorporated into the flagellar structure, but has a bifunctional role: control of hook length and selection of secretion substrates the latter of which prevents premature export of late flagellar substrates (30). FliK consists of four domains: N-terminal region (1-180), a linker region (181-205), a stably folded C-terminal region (206-370) and a relatively unstable short C-terminal stretch (371-405) (184). The N-terminal region is responsible for FliK export. The C-terminal region, which is highly conserved, contains a

a conserved structural domain called the type III secretion substrate specificity switch or T3S4 domain that has been implicated in the control of the secretion-specificity switch (185). There are currently two models for the function of FliK in substrate-specificity switching: the measuring cup model (30) and the molecular ruler model (185).

Similar to the dual function of FliK, FliL is proposed to have two roles: (1) sensing a surface (attributed to the C-terminal) and (2) maintaining the integrity of the flagellar rod (18). Based on bioinformatics, FliL has conserved domains that are predicted to have "intolerable consequences" when mutated, i.e., mutations within this domain potentially could lead to a nonfunctional protein. This region (76-160) is predicted to be structurally homologous to the C-terminal domain of FliK. It is tempting to speculate that FliL also serves as some kind of molecular sensor, such that this region in FliL is responsible for maintaining the flagellar rod integrity by sensing changes in the proton motive-force or by interacting with other proteins or other signals. Mutations in this region render FliL insensitive to these changes and switch its interactions with membrane proteins.

Another possibility is that *fliL* and possibly the N-terminal of *fliM* play a role in the genetic switch that controls *Proteus* swarming. The bistable nature of microbial populations and phenotypic variability in homologous conditions are now being recognized (186). For *Proteus* to swarm, surface-induced swarmer cell differentiation is required. However, swarmer cells alone do not guarantee movement, which requires, among other things, that the population form a swarming raft that can facilitate its outward movement. (2, 187) As was mentioned previously, complementation of swarming in YL1003 is characterized by flares, rafts of motile cells that protrude outward

from the otherwise nonmotile colony. Also, cells from the same population can exhibit differential swarming capacity which becomes more evident in a viscosity dependent manner (Figure 30). Swarming is also affected by temperature and moisture content as was shown in this study. YL1003 contains a defective copy of *fliL*, and Swr^+ complementation requires extra DNA specifically the N-terminal region of FliM important in CW-CCW switch that possibly stabilized or enhance this complementation. YL1006, on the other hand, has no *fliL* but confers a Swr^+ phenotype. Taken together, it can be hypothesized that swarming in *Proteus* is controlled by a bistable switch and that *fliL* (probably through its FliK-homologous region) indirectly/directly affects its regulation by detecting environmental cues such as moisture, temperature, PMF dissipation etc, such that a defective copy can disrupt its balance.

Recommendations

This study was relatively simple and straightforward in its initial conceptualization: determine the nucleotides of *fliL* that are essential for swarming through the introduction of random mutations on a plasmid harboring *fliL* which complements the swarming defect in YL1003. The complementing plasmid (pYL98) containing *fliL*, its native promoter and the 400 bp 5` sequence of *fliM* (18) was already constructed, the use of XL-1 Red mutator strain (173, 174, 181) for introducing base pair mutations is already well-documented, and the screen was supposedly a simple Swr^+ or Swr^- on a standard 1.5% LB agar. However, this turned out not to be the case, and instead my study was confounded by a number of factors including: (1) A more stringent condition was needed for the Swr^+ complementation of pYL98 to be uniformly manifested; ; (2) after plasmid

mutation, the percentage of Swr$^-$ increase phenotypically but was not manifested in the genotype; and (3) pUC18 control yielded 20% mutation ,and (4) YL1003 contains essentially all of *fliL* sequence and thus occurrence of homologous recombination was always a possibility.

In attempts to circumvent these problems, I came up with a screening assay that showed uniform complementation with pYL98. Concerns 2 and 3 are somewhat inter-related. I expected high mutation rate because of the one-time control experiment that I did with pUC18 and *lacZ* indicated mutations at ca. 20% frequency, but this was solely based on the Lac phenotype, but a number of reasons can explain this. The most obvious possibility is contamination that could have increased the number of white colonies on the plate. However, this is unlikely, as the population seemed to be uniform. The second one is that the blue-white phenotype can be caused the natural fluctuation in *E. coli* population (186). In retrospect, sequencing at least some representative white colonies could actually give a more accurate and realistic expectation of false-positives and mutations per base pair. As was discussed previously, the phenotypic variability (Swr$^-$ and in this case white colony) could actually be a result of a mutation in the plasmid other than the gene of interest such as the origin of replication and the selection marker. Also, a higher mutation rate is to be expected from high copy pUC plasmid (173, 174), which has a mutation in the colE1 origin that removes the copy number limit for the plasmid (175). The mutation rate of XL1-Red for a colE1-based plasmid is 1 mutation/2kb of cloned DNA after 30 generations and increases proportionally with increase generation time in XL1-Red (173, 174). For a non-colE1 low copy plasmid such as pACYC184, as Greener et al (173, 174) noted in their original publication for XL1-Red, the generation time

needed for the same mutation is expected to be higher. However, because it uses DNA polymerase III instead of DNA polymerase I, the *mutD* mutation can actually enhance the mutation and thus the same rate can be expected. In a study by Rasila et al (181), they were able to obtain only 2% discernible mutants after 100 generations and sequencing shows 1 mutation/500 bp. Although my study cannot be directly compared to the Rasila (181) results, my experimental results of 2% mutation rate (not the 24% mutation for the control experiment) is actually consistent with published literature (173, 174, 181).

The biggest caveat then is still the screening assay and especially optimizing the condition for swarming and minimizing the effect of vector mutation. These mutations affect cell growth and cell number by affecting plasmid copy number and/or susceptibility to the antibiotic resistance (173, 174). This in turn can potentially increase or decrease swarming independent of *fliL*. Over-swarming is no longer an issue with the 24 well plate, thus, improving swarming conditions to further eliminate false-positives should be the focus. This can be done by lowering the concentration of Cm from the media used for the assay to promote growth of colonies with some mutations in the Cm^R gene. To eliminate effect of possible mutation in copy number, more cells could be inoculated for the assay. Instead of picking colonies using a toothpick, each colony can be resuspended in 2-3µl of 1% PBS and inoculating all in each well. This can be more time-consuming, but if it proved to be effective, it will lessen time and resources use by eliminating additional rounds of assay and false positives. Additional rounds of screening would certainly improve the chance of getting mutations. For the succeeding rounds, using a bigger diameter culture plate such as as 12-well or 6-well plate will not only screen for loss of *fliL* function mutants (Swr^-) but also for decrease or increase FliL

activity mutants (decrease/increase swarming). Also, a 6 well plate can be potentially use for motility assays that would be used as an added screen. Once the false-positive barrier can be overcome, more cells could be screened and the chances of getting mutants after sequencing would be higher. Given the low mutation rate for XL1-Red to generate random mutagenesis to a particular gene of interest indicated by published literature (173, 174, 181) it is important to get as much samples as possible, at the same time, be able to have a strong screen or stable phenotype to use.

Increasing the time the plasmid is in XL1-Red will also increase the chance of getting mutation in the *fliL* region. The initial concern was that multiple mutations, as oppose to single mutation, would be harder to analyze and interpret. As it stands now, getting any type of mutation in the region of interest is the priority. Also, aside from the use of XL1-Red, other methods to generate random mutations are available and may be more applicable to pYL98. These include the use of error-prone PCR protocols (use of Taq in mutagenic buffer, use of MutazymeII DNA polymerases) and chemical modifications (i.e. ethyl methane sulfonate (EMS) and hydroxylamine hydrochloride ($NH_2OH–HCl$)) which were compared and evaluated along with XL1-Red by Rasila *et al* (181).

There is also the possibility that the phenotype that should be screened is not just Swr^- but also Swr^+ that is not to pYL98 complementation level. Recent findings by Dr. Yi-Ying Lee (unpublished results) suggest that *fliL* mutation causes a change in swarming pattern in lower agar concentration. This is consistent with the observation in this study that some Swr^+ mutated pYL98 strains showed different swarming patterns. Also, unpublished results by Dr. Yi-Ying Lee showed that *fliL* mutant swarming is

temperature dependent. This is again consistent with the study's findings that the Swr^+ complementation of pYL98 is temperature dependent. With the recent results obtained from her work, this assay can be improved further.

The final concern, YL1003, can be addressed with the use of the new Δ*fliL* strain YL1006. This new strain is characterized by precocious swarming on 0.8% agar and based on communications with Dr. Yi-Ying Lee, expression of *fliL in trans* restores swarming to wild-type. If I use this strain to study *fliL* based on the protocol devised in this study, a hypothesis on *fliL* function should be put in place. One hypothesis is that *Proteus* can swarm with or without the FliL protein, but cannot swarm with a defective *fliL* gene. The prediction is that a mutated copy of *fliL* will cause YL1006 to not swarm and the screening would be, in theory, straightforward. Another hypothesis which can be link to the first one is that FliL interact and/or regulates itself such that function is dependent on the FliL level in the cell relative to the baseline.

Chapter 5: Summary and Conclusion

P. mirabilis swarmer cell differentiation is induced by physical conditions that inhibit rotation of vegetative swimmer cell flagella, and the protein FliL has been implicated in this induction although the molecular mechanism remains unknown (19). Defects in differentiation result from many different types of mutations, particularly in genes involved in cell wall formation (52, 53, 84). Recent transcriptomic analyses of swarmer cells and *fliL* pseudoswarmer cells indicate major changes in the expression of these genes as well as an increase in the expression of *umoA*, a regulator of *flhDC* (63). Defects in the Rcs cell envelope stress response genes results in precocious swarming behavior (68) and suggesting a link between cell envelope stress and swarmer cell differentiation. Both the Rcs system and the extracytoplasmic sigma factor RpoE was shown to negatively regulate *flhDC* in *P. mirabilis* (68, 143). Furthermore, work by the Rather group showed that O-antigen is important in surface sensing through the Rcs system and involves UmoB and UmoD (104). Based on these, I hypothesized that swimmer cells placed on an agar surface have torsional stress on their flagellar motors conveyed through FliL that then induces envelope stress, which transfers the signal to the Umo proteins (specifically UmoA and UmoD). Umo activity then increases transcription of *flhDC* and results in swarmer cell differentiation.

My results have shown that $cpxP_{Ec}$ expression changes over swarming migration with the highest levels at zones of initial inoculation and consolidation. The transcriptome of *P. mirabilis* also showed upregulation of *rcsB* and *umoA* during consolidation (155). I have proposed that *cpx* expression, i.e., cell wall stress, is highest when a swimmer cell is immobilized on the agar surface, and where torque on flagellar

motors is highest due to inhibition of filament rotation. Cell wall stress is relieved once the bacterium differentiates into a swarmer cell, with flagellar motors operating with less torsional constraint. The study also attempted to generate *P. mirabilis* mutants in the different cell envelope stress genes and UmoA. These could have given insights on the interplay between cell envelope stress, Umo proteins and FliL in swarmer cell differentiation.

FliL has a dual role in *P. mirabilis* – sensing the surface and maintaining the integrity of the flagellar rod (18). A mutation in *fliL* results to a Swr^- phenotype and the presence of pseudoswarmer cells in non-inducing condition (18, 19). The latter can be complemented by expressing *fliL in trans* but complementation of the Swr^- phenotype requires *fliL* and some exogenous DNA (18). I have shown in this study that this complementation is also viscosity-dependent, with an optimum on 0.85% agar, and it is temperature- and agar-hydration-sensitive. The *fliL* complemented phenotype is characterize by late swarming onset starting with flares. I have also shown for the first time that the complementation of YL1003 shows better swarming compared to wild-type in 0.8% agar. A thin film of active migration without the *P. mirabilis* characteristic consolidation zones characterizes the swarming pattern of YL1003/pYL98. Meanwhile wild-type BB2000 shows poor swarming with thick films of cells on LB with 0.8% agar. This result showed that a complemented strain acquired better swarming in condition that typically inhibits wild-type swarming.

Using bioinformatics, I predict that, aside from the promoter region and the predicted transmembrane domain of FliL, *fliL* mutations would be located in the region of the protein between amino acids 76-160. This region is conserved and is predicted to

have intolerable consequences when mutated. This region is predicted to be structurally homologous to the C-terminal domain of FliK. After XL-1 Red mutagenesis, only 2% of the putative Swr$^-$ mutants (2 out of a total of 100 mutants) had mutations in the *fliL-fliM* sequence. The rest of the putative mutants are most likely false-positives and/or mutants that have mutations in the *ori* and the Cm^R gene. One of the mutations is a single base change in the conserved N-terminal portion of *fliM* and the other is in the *fliL* coding and results in a truncated protein of 97 amino acid in length. In both cases, the expression of *fliM* was affected suggesting an important role of the extragenic *5' fliM* in swarming. It is also possible that the Swr$^-$ phenotype was caused by a condition where the flagella do not know which direction to turn because of the mixed FliM-CheY-P signal thus causing a stress response similar to a stalled motor.

I also tested the hypotheses that (1) Swr$^-$ resulted from mutations in the plasmid *ori* or Cm^R gene; (2) mutations in *fliL* resulted to crippled swarming but not complete loss (18 colonies sequenced); and (3) the mutated copy of *fliL* and the chromosomal copy of *fliL* had undergone homologous recombination. I have sequenced the *ori* and Cm^R genes of 5 Swr$^-$ colonies, the insert of 18 colonies that exhibited crippled swarming and the genomic *fliL* of 20 Swr$^-$ colonies. However, none of them showed mutations in the genetic sequence possibly because of the small number of samples sequenced considering that published rate of mutation using XL1-Red is 1 mutation/2 kb insert (173, 174).

Recent unpublished work by Dr. Yi-Ying Lee of the Belas Lab showed that a complete deletion of *fliL* conferred a Swr$^+$ phenotype though the swarming pattern is different from that of wild-type. The difference is clearly manifested in agar concentrations lower than 1.2%. Interestingly, the swarming pattern of YL1006 observed

by Dr. Yi-Ying Lee is similar to that of YL1003/pYL98 in lower agar concentration observed in this study. Also, I have observed different swarming pattern in some Swr^+ YL1003 with mutated pYL98. Dr Yi-Ying Lee also found that swarming of the *ΔfliL* strain is temperature dependent, which I have also observed in YL1003/pYL98. Although I cannot link these two strains directly, these parallel results can give insight on *fliL* function. The use of strain YL1006 would also be ideal for use in this study. It would be interesting to know CES and Umo expression in this mutant background. The use of XL1-Red to determine *fliL* function can also be explored in this system.

It seems that the true phenotype of *fliL* is the production of pseudoswarmers in non-inducing condition, which suggest that *fliL* is important in surface sensing. It is tempting to speculate that FliL also serve as some kind of molecular sensor, like FliK. That this region in FliL homologous to the C-terminal region of FliK is responsible for maintaining the flagellar rod integrity by sensing changes in the proton motive-force or by interacting with other proteins or other signals. Mutations in these regions render FliL insensitive to these changes and switch its interactions with membrane proteins.

Another possibility is that a genetic switch controls swarming in *Proteus*, and *fliL* could play a role in that switch by sensing stress in the cell membrane or the environment. The Swr^- phenotype could be an indirect effect brought about by the defective copy of *fliL*. The bistable nature of microbial populations and phenotypic variability in homologous condition are now being recognized (186). For *Proteus* to swarm, surface induce swarmer cell differentiation is required. However, a differentiated swarmer cells by itself does not guarantee movement. Rather, swarming requires, among others, cell-to-cell contact such that the population forms a raft of cells that facilitates its

outward movement. As was mentioned previously, complementation of swarming in YL1003 is characterized by flares, which are individual cells that started swarming ahead of the population. Also, cells from the same population can exhibit differential swarming capacity which becomes more evident in a viscosity dependent manner. YL1003 contains a defective copy of *fliL*, and Swr^+ complementation requires extra DNA, which included the N-terminal peptide in FliM important in switching that possibly stabilized and/or enhanced this complementation. YL1006, on the other hand, has no *fliL* but confers a Swr^+ phenotype in viscosity- and temperature-dependent manner similar (but not equivalent) to YL1003/pYL98. Results from *cpxP* induction showed that active swarming cells have increase *cpxP, umoA* and *rcsB* expression at the consolidation zones were torsional stress are highest for a vegetative cell about to undergo differentiation. However, as individual cells, differentiated swarmer cells have greater *cpxP* expression presumably from more flagella encountering the surface. A defect in *fliL* results in pseudoswarmer that have less flagella than wild-type swarmer cells (18). I speculate that Swr^- is a result of pseudoswarmer affecting cell wall stress induction. Taken together, this suggests that swarming in *Proteus* is controlled by a bistable switch and that *fliL* (probably through its FliK-homologous region) indirectly/directly affects its regulation by detecting environmental cues such as moisture, temperature, PMF dissipation, cell wall stress, such that a defective copy can disrupt its balance.

Appendix 1. SIFT BLINK prediction for *P. mirabilis* FliL

pos	A	C	D	E	F	G	H	I	K	L	M	N	P	Q	R	S	T	V	W	Y
1M 0.96	0	0	0	0	0	0	0	0	0	0	1	0	0	0	0	0	0	0	0	0
2S 0.96	0.05	0	0	0	0	0	0	0	0	0	0	0.01	0.09	0	0	1	0.52	0	0	0
3N 0.96	0.01	0	1	0.15	0	0.01	0	0	0.08	0	0	0.13	0.01	0.18	0.01	0.07	0.09	0	0	0
4Y 0.95	0.22	0.05	0.1	0.08	0.09	0.09	0.08	0.1	0.14	0.12	0.15	0.43	0.11	0.09	0.1	1	0.88	0.14	0.03	0.27
5S 0.99	1	0.01	0.03	0.04	0	0.02	0.01	0.01	0.14	0.02	0.01	0.05	0.02	0.26	0.13	0.76	0.48	0.02	0	0.01
6N 0.99	0.5	0.17	0.2	0.26	0.72	0.32	0.57	0.49	0.35	0.71	0.21	0.32	0.2	0.3	0.33	0.39	0.39	0.51	0.18	1
7E 0.99	0.76	0.01	0.13	0.55	0.01	0.08	0.03	0.04	0.2	0.06	0.02	0.41	1	0.33	0.3	0.82	0.41	0.06	0	0.01
8R 0.99	0.43	0.01	0.13	0.2	0.02	0.21	0.11	0.04	1	0.08	0.03	0.17	0.15	0.17	0.46	0.31	0.13	0.06	0.01	0.03
9K 0.99	0.23	0.01	0.15	0.19	0.01	0.35	0.03	0.04	1	0.06	0.02	0.16	0.07	0.11	0.13	0.34	0.13	0.05	0	0.01
10S 0.99	0.41	0.03	0.32	0.52	0.03	0.42	0.17	0.1	0.76	0.17	0.06	0.29	0.22	0.35	1	0.85	0.36	0.15	0.01	0.03
11Y 0.99	0.01	0	0	0.01	0	0.01	0.01	0.11	1	0.01	0	0.01	0.01	0.02	0.08	0.05	0.06	0.01	0	0.03
12S 0.99	0.02	0	0.04	0.02	0	0.04	0.01	0	0.04	0.01	0	0.29	0.08	0.02	1	0.27	0.03	0.01	0	0.01
13L 0.99	0.47	0.03	0.33	0.54	0.04	0.27	0.08	0.17	0.74	0.21	0.06	0.27	0.39	0.33	0.41	1	0.39	0.16	0.01	0.03
14I 1.00	0.1	0.02	0.02	0.02	0.14	0.19	0.03	1	0.08	0.83	0.07	0.02	0.02	0.02	0.03	0.03	0.04	0.44	0.05	0.07
15L 1.00	0.02	0.01	0	0.01	0.05	0.03	0	0.09	0.06	1	0.12	0.01	0.01	0.01	0.01	0.01	0.01	0.09	0.91	0.01
16I 1.00	0.02	0	0	0	0.01	0	0	1	0	0.58	0.13	0	0	0	0	0	0	0.38	0.06	0
17I 1.00	0.07	0.02	0.01	0.02	0.12	0.02	0.01	1	0.02	0.48	0.08	0.02	0.29	0.01	0.02	0.02	0.09	0.72	0.01	0.04
18L 1.00	0	0	0	0	0.01	0	0	0.34	0	1	0.03	0	0	0	0	0	0	0.13	0.05	0
19L 1.00	0	0	0	0	0.13	0	0	0.05	0	1	0.05	0	0	0	0	0	0	0.02	0	0
20L 1.00	0.21	0.01	0	0	0	0	0	0.28	0	0.42	0.01	0	0.01	0	0	0.09	0.04	1	0	0
21V 1.00	0.04	0	0	0	0.09	0	0	0.39	0	1	0.01	0	0	0	0	0	0	0.16	0	0
22I 1.00	0	0	0	0	0.09	0	0	1	0	0.19	0	0	0	0	0	0	0	0.34	0	0
23A 1.00	1	0.01	0.01	0.01	0.04	0.01	0	0.04	0.01	0.13	0.01	0.01	0.02	0.01	0.01	0.2	0.88	0.13	0	0
24I 0.99	0.07	0	0	0	0.01	0	0	0.38	0	1	0.01	0	0	0	0	0	0.01	0.45	0	0
25I 1.00	1	0.01	0.01	0.01	0.05	0.09	0	0.74	0.02	0.37	0.05	0.01	0.02	0.01	0.01	0.05	0.05	0.45	0.01	0.02
26A 1.00	1	0	0	0	0	0.19	0	0	0	0.05	0	0	0.04	0	0	0.2	0.01	0	0	0
27A 1.00	0.46	1	0.01	0.01	0	0.09	0	0	0.01	0.02	0	0.01	0.02	0.01	0.04	0.14	0.25	0.1	0	0
28A 1.00	1	0.13	0.01	0.01	0.07	0.48	0	0	0.01	0.01	0	0	0.05	0.01	0.01	0.19	0.01	0.01	0	0
29F 1.00	1	0.09	0.1	0.1	0.28	0.57	0.09	0.31	0.12	0.18	0.07	0.13	0.19	0.09	0.1	0.62	0.68	0.37	0.04	0.15
30G 1.00	1	0	0	0	0	0.52	0	0	0	0	0	0	0.01	0	0	0.01	0	0.08	0	0
31G 1.00	0.01	0	0	0	0	1	0	0	0	0	0	0	0	0	0	0.05	0	0	0	0
32Y 1.00	0.09	0	0	0	0.07	0	0	0	0	0.01	0	0	0	0	0	0	0.03	0	0.01	1
33S 1.00	0.33	0.03	0.04	0.05	0.21	0.12	0.18	0.14	0.05	0.12	0.06	0.06	0.04	0.05	0.06	1	0.14	0.09	0.03	0.23
34W 1.00	0.04	0.01	0.01	0.01	0.32	0.17	0	0.04	0.01	0.08	0.02	0.01	0.01	0	0.01	0.03	0.02	0.29	1	0.66
35W 1.00	0	0	0	0	0.06	0	0	0	0	0	0	0	0	0	0	0	0	0	1	0.01
36A 0.89	0.64	0.18	0.3	0.42	0.72	0.38	0.56	0.44	0.44	0.74	0.25	0.38	0.24	0.41	0.5	0.52	0.49	0.55	0.19	1
37L 0.89	0.17	0.02	0.02	0.03	0.11	0.03	0.05	0.04	0.14	1	0.74	0.03	0.02	0.03	0.07	0.12	0.11	0.05	0.02	0.17
38K 0.99	0.19	0.05	0.11	0.15	0.18	0.15	1	0.12	0.79	0.21	0.56	0.67	0.1	0.98	0.37	0.28	0.2	0.15	0.05	0.37
39H 1.00	0.01	0	0.03	0.02	0	0.03	0.12	0	0.36	0.01	0	0.2	0.01	1	0.05	0.11	0.01	0.01	0	0.1
40A 0.78	0.82	0.06	0.6	1	0.08	0.38	0.21	0.2	0.97	0.32	0.11	0.48	0.27	0.6	0.53	0.76	0.57	0.29	0.03	0.11
41K 0.97	0.41	0.02	0.3	0.48	0.02	0.17	0.21	0.17	1	0.13	0.05	0.23	0.38	0.73	0.23	0.38	0.25	0.12	0.01	0.02
42S 0.97	0.57	0.04	0.5	1	0.03	0.32	0.08	0.13	0.66	0.2	0.07	0.71	0.58	0.51	0.35	0.7	0.59	0.3	0.01	0.03
43G 0.99	0.88	0.05	0.7	1	0.05	0.61	0.12	0.19	0.91	0.3	0.1	0.51	0.32	0.62	0.52	0.9	0.89	0.3	0.02	0.04
44T 0.99	1	0.05	0.7	0.95	0.04	0.34	0.11	0.22	0.85	0.3	0.09	0.47	0.29	0.58	0.47	0.71	0.7	0.28	0.02	0.03
45T 0.99	0.84	0.03	0.42	0.7	0.03	0.19	0.1	0.09	0.77	0.15	0.11	0.47	0.26	0.57	0.26	0.58	1	0.14	0.01	0.02
46G 0.95	1	0.05	0.59	0.91	0.04	0.35	0.2	0.16	0.9	0.26	0.09	0.43	0.37	0.53	0.44	0.64	0.48	0.31	0.01	0.03
47T 0.97	0.83	0.04	0.59	1	0.04	0.31	0.1	0.18	0.95	0.25	0.09	0.4	0.22	0.52	0.43	0.62	0.58	0.31	0.01	0.03
48S 0.92	1	0.01	0.11	0.43	0.01	0.05	0.02	0.03	0.19	0.04	0.01	0.09	0.12	0.18	0.07	0.35	0.08	0.11	0	0.01
49Q 0.90	0.12	0	0.05	0.55	0	0.03	0.01	0.01	1	0.11	0.01	0.03	0.05	0.19	0.05	0.05	0.05	0.04	0	0
50Q 0.91	0.95	0.06	0.59	1	0.1	0.37	0.18	0.2	0.97	0.38	0.11	0.5	0.64	0.84	0.59	0.74	0.57	0.43	0.03	0.19
51K 0.90	0.87	0.04	0.51	1	0.04	0.31	0.1	0.19	0.84	0.38	0.09	0.4	0.48	0.57	0.55	0.6	0.51	0.26	0.01	0.03
52V 0.96	0.12	0.01	0.06	0.09	0.01	0.04	0.02	0.04	0.14	0.07	0.02	0.19	1	0.08	0.06	0.19	0.17	0.32	0	0.01
53I 1.00	0.47	0.08	0.02	0.06	0.12	0.01	0.02	0.79	0.06	0.79	0.21	0.03	0.84	0.05	0.04	0.06	0.27	1	0.02	0.02
54P 1.00	0.34	0.01	0.01	0.06	0	0.03	0	0.01	0.01	0.01	0	0.01	1	0.01	0.01	0.11	0.04	0.21	0	0
55A 0.99	1	0.04	0.23	0.52	0.04	0.14	0.06	0.35	0.34	0.27	0.15	0.19	0.15	0.33	0.2	0.37	0.34	0.39	0.01	0.04
56P 0.98	0.02	0	0	0	0	0	0	0	0	0	0	0	1	0	0	0	0	0	0	0
57V 1.00	0	0	0	0	0	0	0	0.17	0	0	0	0	0	0	0	0	0	1	0	0
58F 1.00	0	0	0	0	1	0	0	0	0	0	0	0	0	0	0	0	0	0	0	0
59M 1.00	0.01	0	0	0	0.52	0	0	0.02	0	0.09	1	0	0	0	0	0	0	0.01	0.02	0.31
60S 1.00	1	0.06	0.26	0.15	0.03	0.32	0.04	0.06	0.15	0.08	0.04	0.22	0.59	0.11	0.09	0.64	0.59	0.15	0.01	0.03
61L 1.00	0	0	0	0	0	0	0	0.04	0	1	0.04	0	0	0	0	0	0	0	0	0
62E 1.00	0	0	1	0.47	0	0	0	0	0	0	0	0	0	0	0	0	0	0	0	0
63P 1.00	0.06	0.01	0.04	0.02	0.01	0.03	0.01	0.02	0.03	0.02	0.01	0.08	0.33	0.02	0.02	0.18	1	0.03	0	0.01
64F 1.00	0	0	0	0	1	0	0	0	0	0	0	0	0	0	0	0	0	0	0	0
65T 1.00	0	0	0	0	0	0	0	0	0	0	0	0	0	0	0	0	1	0	0	0
66I 1.00	0	0	0	0	0	0	0	0.09	0	0	0	0	0	0	0	0	0	1	0	0
67N 1.00	0	0	0	0	0	0	0	0	0	0	0	1	0	0	0	0	0	0	0	0
68L 1.00	0	0	0	0	0	0	0	0	0	1	0	0	0	0	0	0	0	0	0	0
69I 1.00	0.08	0.02	0.01	0.02	0.18	0.08	0.01	0.94	0.03	1	0.21	0.02	0.05	0.04	0.03	0.03	0.06	0.78	0.02	0.04
70D 1.00	0.04	0.01	1	0.07	0.01	0.31	0.04	0	0.05	0.01	0	0.73	0.03	0.03	0.03	0.45	0.54	0.01	0	0.02
71E 0.99	0.99	0.05	0.25	0.33	0.27	0.14	0.13	0.12	0.23	0.25	0.14	0.46	1	0.17	0.16	0.22	0.24	0.16	0.04	0.2
72E 0.65	0.01	0	1	0.19	0	0.15	0.01	0	0.01	0	0	0.24	0	0.01	0	0.01	0.01	0	0	0
73E 0.65	0.01	0	0.29	0.37	0	0.03	0.01	0	0.02	0	0	1	0.01	0.01	0.01	0.02	0.01	0	0	0
74H 0.65	0.04	0.01	1	0.06	0.01	0.22	0.26	0	0.15	0.01	0	0.73	0.03	0.04	0.03	0.17	0.04	0.01	0	0.14
75L 0.65	0.45	0.09	0.09	0.13	0.43	0.19	0.2	0.41	0.17	1	0.21	0.14	0.83	0.15	0.29	0.33	0.25	0.42	0.08	0.37
76D 1.00	0	0	1	0	0	0	0	0	0	0	0	0	0	0	0	0	0	0	0	0
77R 1.00	0	0	0	0	0	0	0	0	0.01	0	0	0.05	0	0	1	0	0	0	0	0

pos	A	C	D	E	F	G	H	I	K	L	M	N	P	Q	R	S	T	V	W	Y
78V 1.00	0	0	0	0	0	0	0	0	0	0	0	0	0	0	0	0	0	1	0	0
79L 1.00	0	0	0	0	0	0	0	0	0	1	0	0	0	0	0	0	0	0	0	0
80Y 1.00	0	0	0	0	0	0	0	0	0	0	0	0	0	0	0	0	0	0	0	1
81I 1.00	0	0	0	0	0	0	0	1	0	0.01	0	0	0	0	0	0	0	0.67	0	0
82G 1.00	0	0	0.15	0	0	1	0	0	0	0	0	0.04	0	0	0	0.01	0	0	0	0
83I 1.00	0.01	0	0	0	0.55	0	0	1	0	0.66	0.1	0	0	0	0	0	0.01	0.39	0	0
84T 1.00	0	0	0	0	0	0	0	0	0	0	0	0	0	0	0	0	1	0	0	0
85L 1.00	0	0	0	0	0	0	0	0	0	1	0	0	0	0	0	0	0	0	0	0
86R 1.00	0	0	0	0	0	0	0	0	0	0	0	0	0	0	1	0	0	0	0	0
87L 1.00	0	0	0	0	0	0	0	0	0	1	0.02	0	0	0	0	0	0	0	0	0
88H 1.00	0.36	0	0.01	0.01	0	0.01	0.06	0	0.42	0.01	0	0.01	1	0.01	0.02	0.07	0.11	0.01	0	0
89D 1.00	0	0	1	0.02	0	0.01	0	0	0	0	0	0.1	0	0	0	0.05	0	0	0	0
90E 1.00	0	0	0.1	1	0	0	0	0	0	0	0	0	0	0	0	0	0	0	0	0
91N 1.00	1	0.04	0.53	0.87	0.03	0.31	0.08	0.13	0.79	0.23	0.07	0.44	0.19	0.43	0.41	0.61	0.46	0.2	0.01	0.03
92T 1.00	0	0	0	0	0	0	0	0	0	0	0	0.04	0	0	0	0.14	1	0	0	0
93R 1.00	0	0	0	0	0	0	0	0	0.03	0	0	0	0	0	1	0	0	0	0	0
94K 1.00	0.73	0.02	0.22	0.37	0.02	0.19	0.06	0.07	1	0.18	0.04	0.19	0.11	0.46	0.71	0.51	0.42	0.11	0.01	0.02
95R 1.00	0.02	0	0	0	0	0	0	0	0.2	0	0	0	0	0.21	1	0	0.05	0	0	0
96L 1.00	0	0	0	0	0.22	0	0	0.07	0	1	0.18	0	0	0	0	0	0	0.01	0	0
97H 1.00	0.01	0	0.02	0.01	0	0.02	0.45	0	0.01	0	0	1	0.01	0.01	0.01	0.34	0.22	0	0	0
98D 1.00	0	0	1	0.39	0	0.01	0	0	0	0	0	0.13	0	0	0.03	0	0	0	0	0
99Y 1.00	0	0	0	0	0.27	0	0	0	0	0	0	0	0	0	0	0	0	0	0	1
100L 1.00	0	0	0	0	0	0	0	0	0	1	0.04	0	0	0	0	0	0	0	0	0
101P 1.00	0	0	0	0	0	0	0	0	0	0	0	0	1	0	0	0	0	0	0	0
102E 1.00	0	0	0	1	0	0	0	0	0	0	0	0	0	0	0	0	0	0	0	0
103V 1.00	0	0	0	0	0	0	0	0.11	0	0	0.04	0	0	0	0	0	0	1	0	0
104R 1.00	0	0	0	0	0	0	0	0	0	0	0	0	0	0	1	0	0	0	0	0
105S 1.00	0	0	0	0	0	0	0	0	0	0	0	0	0	0	0	1	0	0	0	0
106R 1.00	0	0	0	0	0	0	0	0	0	0	0	0	0	0	1	0	0	0	0	0
107L 1.00	0	0	0	0	0	0	0	0.05	0	1	0.08	0	0	0	0	0	0	0.06	0	0
108L 1.00	0	0	0	0	0	0	0	0.03	0	1	0	0	0	0	0	0	0	0	0	0
109L 1.00	0	0	0	0	0	0	0	0.01	0	1	0.22	0	0	0	0	0	0	0	0	0
110L 0.99	0	0	0	0	0	0	0	0	0	1	0	0	0	0	0	0	0	0	0	0
111L 0.99	0	0	0	0	0.36	0	0	0.01	0	1	0.01	0	0	0	0	0	0	0.01	0	0.01
112S 1.00	0	0	0	0	0	0	0	0	0	0	0	0	0	0	0	1	0	0	0	0
113R 1.00	0	0	0	0.03	0	0	0	0	0.01	0	0	0.06	0	0.04	1	0	0	0	0	0
114Q 1.00	0	0	0	0	0	0	0	0	0	0	0	0	0	1	0	0	0	0	0	0
115H 1.00	0.15	0.01	0.93	0.56	0.01	0.09	0.25	0.04	0.7	0.06	0.02	0.98	0.06	0.34	0.1	1	0.42	0.05	0	0.01
116A 1.00	1	0	0	0	0	0.01	0	0	0	0	0	0	0.07	0	0	0.1	0.03	0.03	0	0
117N 1.00	1	0.02	0.43	0.46	0.02	0.26	0.05	0.2	0.55	0.15	0.05	0.3	0.12	0.33	0.23	0.59	0.43	0.16	0.01	0.02
118K 1.00	1	0.04	0.6	0.98	0.06	0.28	0.12	0.21	0.74	0.23	0.09	0.37	0.2	0.66	0.39	0.96	0.66	0.37	0.01	0.04
119I 1.00	0	0	0	0	0	0	0	0.03	0	1	0	0	0	0	0	0	0	0	0	0
120A 1.00	1	0	0	0	0	0.1	0	0	0	0	0	0	0	0	0	0.36	0.02	0.03	0	0
121T 1.00	0.02	0	0.02	0.01	0	0.01	0.06	0	0.08	0	0	0.47	0.01	0.01	0.01	0.38	1	0.01	0	0
122D 1.00	0.01	0	0.31	1	0	0	0.16	0	0.01	0	0	0.03	0	0.04	0	0	0	0	0	0
123A 1.00	0.4	0.01	0.41	0.74	0.01	0.08	0.06	0.04	0.19	0.06	0.02	0.14	0.06	1	0.1	0.18	0.2	0.12	0	0.01
124G 1.00	0	0	0	0	0	1	0	0	0	0	0	0	0	0	0	0	0	0	0	0
125K 1.00	0	0	0	0	0	0	0	0	1	0	0	0	0	0	0	0	0	0	0	0
126Q 1.00	0.09	0.01	0.02	0.09	0.02	0.03	0.03	0.07	0.37	0.31	0.08	0.04	0.04	1	0.18	0.04	0.12	0.18	0.01	0.02
127Q 1.00	0.39	0	0.02	0.1	0.01	0.04	0.13	0.02	0.86	0.08	0.02	0.19	0.04	1	0.54	0.05	0.05	0.03	0.01	0.02
128L 1.00	0	0	0	0	0	0	0	0	0	1	0	0	0	0	0	0	0	0	0	0
129M 1.00	0.03	0	0	0	0	0	0	0.51	0	0.02	0.65	0	0	0	0	0	0.01	1	0	0
130T 1.00	0.81	0.05	0.64	1	0.04	0.36	0.11	0.17	0.86	0.27	0.09	0.46	0.24	0.58	0.47	0.69	0.57	0.25	0.02	0.03
131E 1.00	0.43	0	0.54	1	0.01	0.05	0.03	0.02	0.13	0.03	0.01	0.05	0.08	0.49	0.03	0.06	0.06	0.03	0.01	0.02
132I 1.00	0	0	0	0	0	0	0	1	0	0	0	0	0	0	0	0	0	0.06	0	0
133K 1.00	0	0	0	0	0	0	0	0	1	0	0	0	0	0	0	0	0	0	0	0
134E 1.00	0.3	0.01	0.26	0.49	0.01	0.07	0.02	0.04	0.24	0.06	0.02	0.25	0.05	1	0.14	0.22	0.4	0.05	0	0.01
135T 1.00	0.18	0.01	0	0.01	0.01	0	0	0.1	0.01	0.04	0.01	0	0.01	0.01	0	0.01	1	0.89	0	0
136L 1.00	0	0	0	0	0	0	0	0	0	1	0	0	0	0	0	0	0	0	0	0
137R 1.00	0.59	0	0.1	0.07	0.01	0.03	0.05	0.01	0.14	0.02	0.07	0.04	0.02	0.04	0.22	1	0.14	0.02	0	0.01
138P 1.00	0.27	0	0	0	0	0.02	0	0	0	0	0	0	1	0.09	0	0.02	0.22	0.01	0	0
139T 1.00	0.04	0	0	0	0	0.01	0	0	0	0	0	0	1	0.02	0	0.02	0.34	0.01	0	0
140L 1.00	0	0	0	0	0.06	0	0	0.06	0	1	0.24	0	0	0	0	0	0	0.17	0	0
141V 1.00	0.05	0	0	0.05	0	0	0	0.13	0	0.01	0	0	0	0	0	0	0.07	1	0	0
142P 1.00	0.58	0.01	0.14	0.23	0.02	0.09	0.05	0.05	1	0.18	0.03	0.31	0.93	0.43	0.14	0.28	0.14	0.13	0.01	0.02
143G 1.00	0	0	0.06	0.05	0	1	0	0	0	0	0	0.01	0	0	0	0	0	0	0	0
144E 1.00	0	0	0.01	0.23	0	0	0	0	0.07	0	0	0	0	1	0	0	0	0	0	0
145S 1.00	0.03	0	0	0	0	0.01	0	0	0	0	0	0.03	1	0	0	0.08	0	0	0	0
146E 1.00	0.44	0.02	0.6	0.69	0.02	0.33	0.06	0.08	1	0.13	0.04	0.61	0.29	0.43	0.22	0.32	0.25	0.12	0.01	0.02
147Q 1.00	0	0	0	0	0	0	0	0	0	0	0	0	0	1	0	0	0	0	0	0
148I 1.00	0.28	0.04	0.1	0.21	0.02	0.01	0.01	0.31	0.05	0.14	0.08	0.07	0.05	0.04	0.02	0.04	0.14	1	0	0.01
149L 1.00	0	0	0	0	0	0	0	0.31	0	0.04	0	0	0	0	0	0	0	1	0	0
150S 1.00	0.01	0	0.02	0	0	0.01	0	0	0	0	0	0.33	0.01	0	0	0.84	1	0	0	0
151D 1.00	0	0	1	0	0	0	0	0	0	0	0	0	0	0	0	0	0	0	0	0
152V 1.00	0	0	0	0	0	0	0	0	0	0	0	0	0	0	0	0	0	1	0	0
153L 1.00	0	0	0	0	0	0	0	0	0	1	0.06	0	0	0	0	0	0	0	0	0
154F 1.00	0	0	0	0	1	0	0	0	0	0	0	0	0	0	0	0	0	0	0	0.3
155T 1.00	0	0	0	0	0	0	0	0	0	0	0	0	0	0	0	0	1	0	0	0
156T 1.00	1	0	0	0	0	0.01	0	0	0	0	0	0	0	0	0	0.01	0.32	0	0	0
157F 1.00	0	0	0	0	1	0	0	0	0	0	0	0	0	0	0	0	0	0	0	0
158I 1.00	0	0	0	0	0	0	0	1	0	0	0	0	0	0	0	0	0	0	0	0
159L 1.00	0	0	0	0	0	0	0	0	0	1	0	0	0	0	0	0	0	0	0	0
160R 1.00	0	0	0	0	0	0	0	0	0	0	0	0	0	0	1	0	0	0	0	0

[1]Each row represent *P. mirabilis* FliL amino acid residue in each position and its degree of conservancy relative to other FliL protein in literature

[2]Each column represent each of the 20 amino acid and a score less than 0.05 means that the substitution is possibly not tolerated by the cell.

Appendix 2. Phyre2 Tertiary Structure Prediction for FliL

Phyre2

Top model

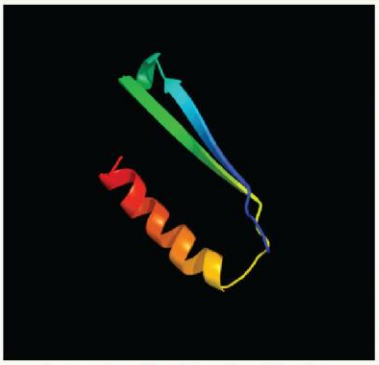

Image coloured by rainbow N → C terminus

Model dimensions (Å): **X**:19.384 **Y**:45.423 **Z**:27.573

Model (left) based on template c2rrlA_

Top template information

PDB header:protein transport
Chain: A: **PDB Molecule:**flagellar hook-length control protein;
PDBTitle: solution structure of the c-terminal domain of the flik

Confidence and coverage

Confidence: 69.3% Coverage: 26%

41 residues (26% of your sequence) have been modelled with 69.3% confidence by the single highest scoring template.

Phyre alarm

You may wish to submit your sequence to Phyrealarm. This will automatically scan your sequence every week for new potential templates as they appear in the Phyre2 library.

Please note: You must be registered and logged in to use Phyrealarm.

3D viewing

Interactive 3D view in Jmol

For other options to view your downloaded structure offline see the FAQ

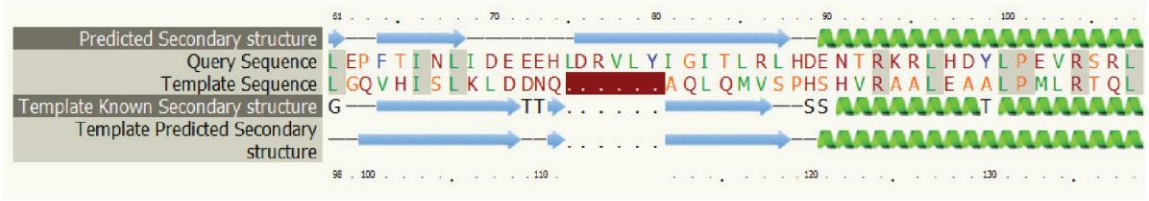

#	Template	Alignment Coverage	3D Model	Confidence	% I.d.	Template Information
1	c2rrlA_	Alignment	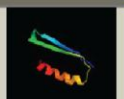	69.3	22	**PDB header:**protein transport **Chain:** A: **PDB Molecule:**flagellar hook-length control protein; **PDBTitle:** solution structure of the c-terminal domain of the flik
2	c3gxqB_	Alignment		45.3	13	**PDB header:**dna binding protein/dna **Chain:** B: **PDB Molecule:**putative regulator of transfer genes arta; **PDBTitle:** structure of arta and dna complex
3	c3j20A_	Alignment		42.7	7	**PDB header:**ribosome **Chain:** A: **PDB Molecule:**30s ribosomal protein s3ae; **PDBTitle:** promiscuous behavior of proteins in archaeal ribosomes revealed by2 cryo-em: implications for evolution of eukaryotic ribosomes (30s3 ribosomal subunit)
4	c4fvjB_	Alignment	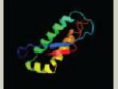	42.0	10	**PDB header:**membrane protein **Chain:** B: **PDB Molecule:**stomatin; **PDBTitle:** spfh domain of the mouse stomatin (crystal form 2)
5	c2rpbA_	Alignment	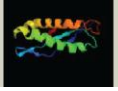	40.0	12	**PDB header:**membrane protein **Chain:** A: **PDB Molecule:**hypothetical membrane protein; **PDBTitle:** the solution structure of membrane protein

References

1. **Aldridge P, Hughes KT.** 2001. How and when are substrates selected for type III secretion? Trends Microbiol **9:**209-214.

2. **Hoeniger JFM.** 1965. Development of Flagella by *Proteus mirabilis*. Journal of General Microbiology **40:**29-42.

3. **Hauser G.** 1885. Uber Fäulnissbacterien und deren Beziehungen zur Septicämie. In *Ein Beitrag zur Morphologie der Speltpilze*. p. 12 Leipzig: Vogel.

4. **O'Hara CM, Brenner FW, Steigerwalt AG, Hill BC, Holmes B, Grimont PA, Hawkey PM, Penner JL, Miller JM, Brenner DJ.** 2000. Classification of *Proteus vulgaris* biogroup 3 with recognition of *Proteus hauseri* sp. nov., nom. rev. and unnamed *Proteus* genomospecies 4, 5 and 6. Int J Syst Evol Microbiol **50:**1869-1875.

5. **Wazait HD, Patel HR, Veer V, Kelsey M, Van Der Meulen JH, Miller RA, Emberton M.** 2003. Catheter-associated urinary tract infections: prevalence of uropathogens and pattern of antimicrobial resistance in a UK hospital (1996-2001). BJU Int **91:**806-809.

6. **Stickler DJ, Feneley RC.** 2010. The encrustation and blockage of long-term indwelling bladder catheters: a way forward in prevention and control. Spinal Cord **48:**784-790.

7. **Macleod SM, Stickler DJ.** 2007. Species interactions in mixed-community crystalline biofilms on urinary catheters. J Med Microbiol **56:**1549-1557.

8. **Stickler DJ, King JB, Winters C, Morris SL.** 1993. Blockage of urethral catheters by bacterial biofilms. J Infect **27:**133-135.

9. **Morris NS, Stickler DJ, Winters C.** 1997. Which indwelling urethral catheters resist encrustation by *Proteus mirabilis* biofilms? Br J Urol **80:**58-63.

10. **Stickler DJ, Lear JC, Morris NS, Macleod SM, Downer A, Cadd DH, Feast WJ.** 2006. Observations on the adherence of *Proteus mirabilis* onto polymer surfaces. J Appl Microbiol **100:**1028-1033.

11. **Armbruster CE, Mobley HL.** 2012. Merging mythology and morphology: the multifaceted lifestyle of *Proteus mirabilis*. Nat Rev Microbiol **10:**743-754.

12. **Jacobsen SM, Stickler DJ, Mobley HL, Shirtliff ME.** 2008. Complicated catheter-associated urinary tract infections due to *Escherichia coli* and *Proteus mirabilis*. Clin Microbiol Rev **21:**26-59.

13. **Sabbuba N, Hughes G, Stickler DJ.** 2002. The migration of *Proteus mirabilis* and other urinary tract pathogens over Foley catheters. BJU Int **89:**55-60.

14. **Stickler DJ, Evans A, Morris N, Hughes G.** 2002. Strategies for the control of catheter encrustation. Int J Antimicrob Agents **19:**499-506.

15. **Jones BV, Young R, Mahenthiralingam E, Stickler DJ.** 2004. Ultrastructure of *Proteus mirabilis* swarmer cell rafts and role of swarming in catheter-associated urinary tract infection. Infect Immun **72:**3941-3950.

16. **Schneider R, Lockatell CV, Johnson D, Belas R.** 2002. Detection and mutation of a *luxS*-encoded autoinducer in *Proteus mirabilis*. Microbiol **148:**773-782.

17. **Allison C, Coleman N, Jones PL, Hughes C.** 1992. Ability of *Proteus mirabilis* to invade human urothelial cells is coupled to motility and swarming differentiation. Infect Immun **60:**4740-4746.

18. **Lee YY, Patellis J, Belas R.** 2013. Activity of *Proteus mirabilis* FliL is viscosity dependent and requires extragenic DNA. J Bacteriol **195:**823-832.

19. **Belas R, Suvanasuthi R.** 2005. The ability of *Proteus mirabilis* to sense surfaces and regulate virulence gene expression involves FliL, a flagellar basal body protein. J Bacteriol **187:**6789-6803.

20. **Jarrell KF, McBride MJ.** 2008. The surprisingly diverse ways that prokaryotes move. Nat Rev Microbiol **6:**466-476.

21. **McBride MJ.** 2001. Bacterial gliding motility: multiple mechanisms for cell movement over surfaces. Annu Rev Microbiol **55:**49-75.

22. **Harshey RM.** 2003. Bacterial motility on a surface: many ways to a common goal. Annu Rev Microbiol **57:**249-273.

23. **Silverman M, Simon M.** 1974. Flagellar rotation and the mechanism of bacterial motility. Nature **249:**73-74.

24. **Ueno T, Oosawa K, Aizawa S.** 1992. M ring, S ring and proximal rod of the flagellar basal body of *Salmonella Typhimurium* are composed of subunits of a single protein, FliF. J Mol Biol **227:**672-677.

25. **Homma M, Aizawa S, Dean GE, Macnab RM.** 1987. Identification of the M-ring protein of the flagellar motor of *Salmonella Typhimurium*. Proc Natl Acad Sci U S A **84:**7483-7487.

26. **Schoenhals GJ, Macnab RM.** 1996. Physiological and biochemical analyses of FlgH, a lipoprotein forming the outer membrane L ring of the flagellar basal body of *Salmonella Typhimurium*. J Bacteriol **178:**4200-4207.

27. **Terashima H, Kojima S, Homma M.** 2008. Flagellar Motility in Bacteria: Structure and Function of Flagellar Motor. Int Rev Cell Mol Biol **270**:39-85.

28. **Macnab RM.** 1999. The bacterial flagellum: reversible rotary propellor and type III export apparatus. J Bacteriol **181:**7149-7153.

29. **Hirano T, Yamaguchi S, Oosawa K, Aizawa S.** 1994. Roles of FliK and FlhB in determination of flagellar hook length in *Salmonella Typhimurium*. J Bacteriol **176:**5439-5449.

30. **Aizawa S.** 2012. Mystery of fliK in length control of the flagellar hook. J Bacteriol **194:**4798-4800.

31. **Fahrner KA, Block SM, Krishnaswamy S, Parkinson JS, Berg HC.** 1994. A mutant hook-associated protein (HAP3) facilitates torsionally induced transformations of the flagellar filament of *Escherichia coli*. J Mol Biol **238:**173-186.

32. **Francis NR, Sosinsky GE, Thomas D, DeRosier DJ.** 1994. Isolation, characterization and structure of bacterial flagellar motors containing the switch complex. J Mol Biol **235:**1261-1270.

33. **Thomas DR, Morgan DG, DeRosier DJ.** 1999. Rotational symmetry of the C ring and a mechanism for the flagellar rotary motor. Proc Natl Acad Sci U S A **96:**10134-10139.

34. **Zhao R, Pathak N, Jaffe H, Reese TS, Khan S.** 1996. FliN is a major structural protein of the C-ring in the *Salmonella Typhimurium* flagellar basal body. J Mol Biol **261:**195-208.

35. **Zhao R, Amsler CD, Matsumura P, Khan S.** 1996. FliG and FliM distribution in the *Salmonella Typhimurium* cell and flagellar basal bodies. J Bacteriol **178:**258-265.

36. **Yamaguchi S, Aizawa S, Kihara M, Isomura M, Jones CJ, Macnab RM.** 1986. Genetic evidence for a switching and energy-transducing complex in the flagellar motor of *Salmonella Typhimurium*. J Bacteriol **168:**1172-1179.

37. **Yamaguchi S, Fujita H, Ishihara A, Aizawa S, Macnab RM.** 1986. Subdivision of flagellar genes of *Salmonella Typhimurium* into regions responsible for assembly, rotation, and switching. J Bacteriol **166:**187-193.

38. **Sockett H, Yamaguchi S, Kihara M, Irikura VM, Macnab RM.** 1992. Molecular analysis of the flagellar switch protein FliM of *Salmonella Typhimurium*. J Bacteriol **174:**793-806.

39. **Bren A, Eisenbach M.** 1998. The N terminus of the flagellar switch protein, FliM, is the binding domain for the chemotactic response regulator, CheY. J Mol Biol **278:**507-514.

40. **Welch M, Oosawa K, Aizawa SI, Eisenbach M.** 1994. Effects of phosphorylation, Mg^{2+}, and conformation of the chemotaxis protein CheY on its binding to the flagellar switch protein FliM. Biochem **33:**10470-10476.

41. **Brown PN, Mathews MAA, Joss LA, Hill CP, Blair DF.** 2005. Crystal structure of the flagellar rotor protein FliN from *Thermotoga maritima*. J Bacteriol **187:**2890-2902.

42. **Vogler AP, Homma M, Irikura VM, Macnab RM.** 1991. *Salmonella Typhimurium* mutants defective in flagellar filament regrowth and sequence similarity of FliI to F0F1, vacuolar, and archaebacterial ATPase subunits. J Bacteriol **173:**3564-3572.

43. **Kojima S, Blair DF.** 2004. The bacterial flagellar motor: structure and function of a complex molecular machine. Int Rev Cytol **233:**93-134.

44. **Kojima S, Blair DF.** 2004. Solubilization and purification of the MotA/MotB complex of *Escherichia coli*. Biochem **43:**26-34.

45. **Dean GE, Macnab RM, Stader J, Matsumura P, Burks C.** 1984. Gene sequence and predicted amino acid sequence of the MotA protein, a membrane-associated protein required for flagellar rotation in *Escherichia coli*. J Bacteriol **159:**991-999.

46. **Lloyd SA, Tang H, Wang X, Billings S, Blair DF.** 1996. Torque generation in the flagellar motor of *Escherichia coli*: evidence of a direct role for FliG but not for FliM or FliN. J Bacteriol **178:**223-231.

47. **Zhou J, Lloyd SA, Blair DF.** 1998. Electrostatic interactions between rotor and stator in the bacterial flagellar motor. Proc Natl Acad Sci U S A **95:**6436-6441.

48. **Oosawa K, Ueno T, Aizawa S.** 1994. Overproduction of the bacterial flagellar switch proteins and their interactions with the MS ring complex in vitro. J Bacteriol **176:**3683-3691.

49. **Mitchell JG, Kogure K.** 2006. Bacterial motility: links to the environment and a driving force for microbial physics. FEMS Microbiol Ecol **55:**3-16.

50. **Matz C, Jurgens K.** 2005. High motility reduces grazing mortality of planktonic bacteria. Appl Environ Microbiol **71:**921-929.

51. **Harshey RM.** 1994. Bees aren't the only ones: swarming in gram-negative bacteria. Mol Microbiol **13:**389-394.

52. **Belas R, Erskine D, Flaherty D.** 1991. *Proteus mirabilis* mutants defective in swarmer cell differentiation and multicellular behavior. J Bacteriol **173:**6279-6288.

53. **Belas R, Erskine D, Flaherty D.** 1991. Transposon mutagenesis in *Proteus mirabilis*. J Bacteriol **173:**6289-6293.

54. **Kearns DB.** 2010. A field guide to bacterial swarming motility. Nat Rev Microbiol **8:**634-644.

55. **Belas R, Simon M, Silverman M.** 1986. Regulation of lateral flagella gene transcription in *Vibrio parahaemolyticus*. J Bacteriol **167:**210-218.

56. **Wang Q, Suzuki A, Mariconda S, Porwollik S, Harshey RM.** 2005. Sensing wetness: a new role for the bacterial flagellum. EMBO J **24:**2034-2042.

57. **Gygi D, Bailey MJ, Allison C, Hughes C.** 1995. Requirement for FlhA in flagella assembly and swarm-cell differentiation by *Proteus mirabilis*. Mol Microbiol **15:**761-769.

58. **Hay NA, Tipper DJ, Gygi D, Hughes C.** 1997. A nonswarming mutant of *Proteus mirabilis* lacks the Lrp global transcriptional regulator. J Bacteriol **179:**4741-4746.

59. **Rahman MM, Guard-Petter J, Asokan K, Hughes C, Carlson RW.** 1999. The structure of the colony migration factor from pathogenic *Proteus mirabilis*. A capsular polysaccharide that facilitates swarming. J Biol Chem **274:**22993-22998.

60. **Neu TR.** 1996. Significance of bacterial surface-active compounds in interaction of bacteria with interfaces. Microbiol Rev **60:**151-166.

61. **Mobley HL, Belas R.** 1995. Swarming and pathogenicity of *Proteus mirabilis* in the urinary tract. Trends Microbiol **3:**280-284.

62. **Alavi M, Belas R.** 2001. Surface sensing, swarmer cell differentiation, and biofilm development. Methods Enzymol **336:**29-40.

63. **Cusick K, Lee YY, Youchak B, Belas R.** 2012. Perturbation of FliL interferes with *Proteus mirabilis* swarmer cell gene expression and differentiation. J Bacteriol **194:**437-447.

64. **Karlinsey JE, Tanaka S, Bettenworth V, Yamaguchi S, Boos W, Aizawa SI, Hughes KT.** 2000. Completion of the hook-basal body complex of the *Salmonella Typhimurium* flagellum is coupled to FlgM secretion and *fliC* transcription. Mol Microbiol **37:**1220-1231.

65. **Wang S, Fleming RT, Westbrook EM, Matsumura P, McKay DB.** 2006. Structure of the *Escherichia coli* FlhDC complex, a prokaryotic heteromeric regulator of transcription. J Mol Biol **355:**798-808.

66. **Chevance FF, Hughes KT.** 2008. Coordinating assembly of a bacterial macromolecular machine. Nat Rev Microbiol **6:**455-465.

67. **Smith TG, Hoover TR.** 2009. Deciphering bacterial flagellar gene regulatory networks in the genomic era. Adv Appl Microbiol **67:**257-295.

68. **Belas R, Schneider R, Melch M.** 1998. Characterization of *Proteus mirabilis* precocious swarming mutants: identification of *rsbA*, encoding a regulator of swarming behavior. J Bacteriol **180:**6126-6139.

69. **Calvo JM, Matthews RG.** 1994. The leucine-responsive regulatory protein, a global regulator of metabolism in *Escherichia coli*. Microbiol Rev **58:**466-490.

70. **Furness RB, Fraser GM, Hay NA, Hughes C.** 1997. Negative feedback from a *Proteus* class II flagellum export defect to the *flhDC* master operon controlling cell division and flagellum assembly. J Bacteriol **179:**5585-5588.

71. **Bange G, Kummerer N, Engel C, Bozkurt G, Wild K, Sinning I.** 2010. FlhA provides the adaptor for coordinated delivery of late flagella building blocks to the type III secretion system. Proc Natl Acad Sci U S A **107:**11295-11300.

72. **Wei BL, Brun-Zinkernagel AM, Simecka JW, Pruss BM, Babitzke P, Romeo T.** 2001. Positive regulation of motility and *flhDC* expression by the RNA-binding protein CsrA of *Escherichia coli*. Mol Microbiol **40:**245-256.

73. **Claret L, Hughes C.** 2000. Rapid turnover of FlhD and FlhC, the flagellar regulon transcriptional activator proteins, during *Proteus* swarming. J Bacteriol **182:**833-836.

74. **Stevenson LG, Rather PN.** 2006. A novel gene involved in regulating the flagellar gene cascade in *Proteus mirabilis*. J Bacteriol **188:**7830-7839.

75. **Stevenson LG, Szostek BA, Clemmer KM, Rather PN.** 2013. Expression of the DisA amino acid decarboxylase from *Proteus mirabilis* inhibits motility and class 2 flagellar gene expression in *Escherichia coli*. Res Microbiol **164:**31-37.

76. **Dufour A, Furness RB, Hughes C.** 1998. Novel genes that upregulate the *Proteus mirabilis* flhDC master operon controlling flagellar biogenesis and swarming. Mol Microbiol **29:**741-751.

77. **Aldridge P, Karlinsey J, Hughes KT.** 2003. The type III secretion chaperone FlgN regulates flagellar assembly via a negative feedback loop containing its chaperone substrates FlgK and FlgL. Mol Microbiol **49:**1333-1345.

78. **Kihara M, Homma M, Kutsukake K, Macnab RM.** 1989. Flagellar switch of *Salmonella Typhimurium*: gene sequences and deduced protein sequences. J Bacteriol **171:**3247-3257.

79. **Jenal U, White J, Shapiro L.** 1994. *Caulobacter* flagellar function, but not assembly, requires FliL, a non-polarly localized membrane protein present in all cell types. J Mol Biol **243:**227-244.

80. **Belas R, Horikawa E, Aizawa S-I, Suvanasuthi R.** 2009. Genetic determinants of *Silicibacter* sp. TM1040 motility. J Bacteriol **191:**4502-4512.

81. **Suaste-Olmos F, Domenzain C, Mireles-Rodriguez JC, Poggio S, Osorio A, Dreyfus G, Camarena L.** 2010. The flagellar protein FliL is essential for swimming in *Rhodobacter sphaeroides*. J Bacteriol **192:**6230-6239.

82. **Attmannspacher U, Scharf BE, Harshey RM.** 2008. FliL is essential for swarming: motor rotation in absence of FliL fractures the flagellar rod in swarmer cells of *Salmonella enterica*. Mol Microbiol **68:**328-341.

83. **Raha M, Sockett H, Macnab RM.** 1994. Characterization of the fliL gene in the flagellar regulon of *Escherichia coli* and *Salmonella Typhimurium*. J Bacteriol **176:**2308-2311.

84. **Belas R, Goldman M, Ashliman K.** 1995. Genetic analysis of *Proteus mirabilis* mutants defective in swarmer cell elongation. J Bacteriol **177:**823-828.

85. **Kuhn HM, Meier-Dieter U, Mayer H.** 1988. ECA, the enterobacterial common antigen. FEMS Microbiol Rev **4:**195-222.

86. **Reeves PP, Wang L.** 2002. Genomic organization of LPS-specific loci. Curr Top Microbiol Immunol **264:**109-135.

87. **Bowden MG, Kaplan HB.** 1998. The *Myxococcus xanthus* lipopolysaccharide O-antigen is required for social motility and multicellular development. Mol Microbiol **30:**275-284.

88. **Toguchi A, Siano M, Burkart M, Harshey RM.** 2000. Genetics of swarming motility in *Salmonella enterica* serovar *Typhimurium*: critical role for lipopolysaccharide. J Bacteriol **182:**6308-6321.

89. **Girgis HS, Liu Y, Ryu WS, Tavazoie S.** 2007. A comprehensive genetic characterization of bacterial motility. PLoS Genet **3:**1644-1660.

90. **Morgenstein RM, Clemmer KM, Rather PN.** 2010. Loss of the *waaL* O-antigen ligase prevents surface activation of the flagellar gene cascade in *Proteus mirabilis*. J Bacteriol **192:**3213-3221.

91. **Castelli ME, Vescovi EG.** 2011. The Rcs signal transduction pathway is triggered by enterobacterial common antigen structure alterations in Serratia marcescens. J Bacteriol **193:**63-74.

92. **Chang C, Stewart RC.** 1998. The two-component system. Regulation of diverse signaling pathways in prokaryotes and eukaryotes. Plant Physiol **117:**723-731.

93. **Bury-Mone S, Nomane Y, Reymond N, Barbet R, Jacquet E, Imbeaud S, Jacq A, Bouloc P.** 2009. Global analysis of extracytoplasmic stress signaling in *Escherichia coli*. PLoS Genet **5:**e1000651.

94. **Majdalani N, Gottesman S.** 2005. The Rcs phosphorelay: a complex signal transduction system. Annu Rev Microbiol **59:**379-405.

95. **Stout V, Gottesman S.** 1990. RcsB and RcsC: a two-component regulator of capsule synthesis in *Escherichia coli*. J Bacteriol **172:**659-669.

96. **Francez-Charlot A, Laugel B, Van Gemert A, Dubarry N, Wiorowski F, Castanie-Cornet MP, Gutierrez C, Cam K.** 2003. RcsCDB His-Asp phosphorelay system negatively regulates the *flhDC* operon in *Escherichia coli*. Mol Microbiol **49:**823-832.

97. **Delgado MA, Mouslim C, Groisman EA.** 2006. The PmrA/PmrB and RcsC/YojN/RcsB systems control expression of the *Salmonella* O-antigen chain length determinant. Mol Microbiol **60:**39-50.

98. **Cano DA, Martinez-Moya M, Pucciarelli MG, Groisman EA, Casadesus J, Garcia-Del Portillo F.** 2001. *Salmonella enterica* serovar *Typhimurium* response involved in attenuation of pathogen intracellular proliferation. Infect Immun **69:**6463-6474.

99. **Laubacher ME, Ades SE.** 2008. The Rcs phosphorelay is a cell envelope stress response activated by peptidoglycan stress and contributes to intrinsic antibiotic resistance. J Bacteriol **190:**2065-2074.

100. **Erickson KD, Detweiler CS.** 2006. The Rcs phosphorelay system is specific to enteric pathogens/commensals and activates *ydeI*, a gene important for persistent *Salmonella* infection of mice. Mol Microbiol **62:**883-894.

101. **Huang YH, Ferrieres L, Clarke DJ.** 2006. The role of the Rcs phosphorelay in *Enterobacteriaceae*. Res Microbiol **157:**206-212.

102. **Chen MH, Takeda S, Yamada H, Ishii Y, Yamashino T, Mizuno T.** 2001. Characterization of the RcsC-->YojN-->RcsB phosphorelay signaling pathway involved in capsular synthesis in *Escherichia coli*. Biosci Biotechnol Biochem **65:**2364-2367.

103. **Rogov VV, Schmoe K, Lohr F, Rogova NY, Bernhard F, Dotsch V.** 2008. Modulation of the Rcs-mediated signal transfer by conformational flexibility. Biochem Soc Trans **36:**1427-1432.

104. **Morgenstein RM, Rather PN.** 2012. Role of the Umo proteins and the Rcs phosphorelay in the swarming motility of the wild type and an O-antigen (*waaL*) mutant of *Proteus mirabilis*. J Bacteriol **194:**669-676.

105. **Majdalani N, Chen S, Murrow J, St John K, Gottesman S.** 2001. Regulation of RpoS by a novel small RNA: the characterization of RprA. Mol Microbiol **39:**1382-1394.

106. **Majdalani N, Hernandez D, Gottesman S.** 2002. Regulation and mode of action of the second small RNA activator of RpoS translation, RprA. Mol Microbiol **46:**813-826.

107. **Majdalani N, Heck M, Stout V, Gottesman S.** 2005. Role of RcsF in signaling to the Rcs phosphorelay pathway in *Escherichia coli*. J Bacteriol **187:**6770-6778.

108. **Oshima T, Aiba H, Masuda Y, Kanaya S, Sugiura M, Wanner BL, Mori H, Mizuno T.** 2002. Transcriptome analysis of all two-component regulatory system mutants of *Escherichia coli* K-12. Mol Microbiol **46:**281-291.

109. **Bereswill S, Geider K.** 1997. Characterization of the *rcsB* gene from *Erwinia amylovora* and its influence on exoploysaccharide synthesis and virulence of the fire blight pathogen. J Bacteriol **179:**1354-1361.

110. **Cano DA, Dominguez-Bernal G, Tierrez A, Garcia-Del Portillo F, Casadesus J.** 2002. Regulation of capsule synthesis and cell motility in *Salmonella enterica* by the essential gene *igaA*. Genetics **162:**1513-1523.

111. **Mariscotti JF, Garcia-del Portillo F.** 2009. Genome expression analyses revealing the modulation of the *Salmonella* Rcs regulon by the attenuator IgaA. J Bacteriol **191:**1855-1867.

112. **Price NL, Raivio TL.** 2009. Characterization of the Cpx regulon in *Escherichia coli* strain MC4100. J Bacteriol **191:**1798-1815.

113. **Raivio TL, Silhavy TJ.** 1999. The σE and Cpx regulatory pathways: overlapping but distinct envelope stress responses. Curr Opin Microbiol **2:**159-165.

114. **Raivio TL, Popkin DL, Silhavy TJ.** 1999. The Cpx envelope stress response is controlled by amplification and feedback inhibition. J Bacteriol **181:**5263-5272.

115. **Raivio TL, Silhavy TJ.** 1997. Transduction of envelope stress in *Escherichia coli* by the Cpx two-component system. J Bacteriol **179:**7724-7733.

116. **Danese PN, Snyder WB, Cosma CL, Davis LJ, Silhavy TJ.** 1995. The Cpx two-component signal transduction pathway of *Escherichia coli* regulates transcription of the gene specifying the stress-inducible periplasmic protease, DegP. Genes Dev **9:**387-398.

117. **Miot M, Betton JM.** 2007. Optimization of the inefficient translation initiation region of the *cpxP* gene from *Escherichia coli*. Protein Sci **16:**2445-2453.

118. **Rowley G, Spector M, Kormanec J, Roberts M.** 2006. Pushing the envelope: extracytoplasmic stress responses in bacterial pathogens. Nat Rev Microbiol **4:**383-394.

119. **Danese PN, Silhavy TJ.** 1998. CpxP, a stress-combative member of the Cpx regulon. J Bacteriol **180:**831-839.

120. **Thede GL, Arthur DC, Edwards RA, Buelow DR, Wong JL, Raivio TL, Glover JN.** 2011. Structure of the periplasmic stress response protein CpxP. J Bacteriol **193:**2149-2157.

121. **Kwon E, Kim DY, Gross CA, Gross JD, Kim KK.** 2010. The crystal structure *Escherichia coli* Spy. Protein Sci **19:**2252-2259.

122. **Weiner L, Brissette JL, Model P.** 1991. Stress-induced expression of the *Escherichia coli* phage shock protein operon is dependent on σ54 and modulated by positive and negative feedback mechanisms. Genes Dev **5:**1912-1923.

123. **Bergler H, Abraham D, Aschauer H, Turnowsky F.** 1994. Inhibition of lipid biosynthesis induces the expression of the *pspA* gene. Microbiol **140 (Pt 8):**1937-1944.

124. **Kleerebezem M, Crielaard W, Tommassen J.** 1996. Involvement of stress protein PspA (phage shock protein A) of *Escherichia coli* in maintenance of the protonmotive force under stress conditions. EMBO J **15:**162-171.

125. **Brissette JL, Russel M, Weiner L, Model P.** 1990. Phage shock protein, a stress protein of *Escherichia coli*. Proc Natl Acad Sci U S A **87:**862-866.

126. **Model P, Jovanovic G, Dworkin J.** 1997. The *Escherichia coli* phage-shock-protein (*psp*) operon. Mol Microbiol **24:**255-261.

127. **Darwin AJ.** 2005. The phage-shock-protein response. Mol Microbiol **57:**621-628.

128. **Elderkin S, Jones S, Schumacher J, Studholme D, Buck M.** 2002. Mechanism of action of the *Escherichia coli* phage shock protein PspA in repression of the AAA family transcription factor PspF. J Mol Biol **320:**23-37.

129. **Green RC, Darwin AJ.** 2004. PspG, a new member of the Yersinia enterocolitica phage shock protein regulon. J Bacteriol **186:**4910-4920.

130. **Huvet M, Toni T, Sheng X, Thorne T, Jovanovic G, Engl C, Buck M, Pinney JW, Stumpf MP.** 2011. The evolution of the phage shock protein response system: interplay between protein function, genomic organization, and system function. Mol Biol Evol **28:**1141-1155.

131. **Darwin AJ.** 2013. Stress relief during host infection: the phage shock protein response supports bacterial virulence in various ways. PLoS Pathog **9:**e1003388.

132. **Beloin C, Valle J, Latour-Lambert P, Faure P, Kzreminski M, Balestrino D, Haagensen JA, Molin S, Prensier G, Arbeille B, Ghigo JM.** 2004. Global impact of mature biofilm lifestyle on *Escherichia coli* K-12 gene expression. Mol Microbiol **51:**659-674.

133. **Raffa RG, Raivio TL.** 2002. A third envelope stress signal transduction pathway in *Escherichia coli*. Mol Microbiol **45:**1599-1611.

134. **Leblanc SK, Oates CW, Raivio TL.** 2011. Characterization of the induction and cellular role of the BaeSR two-component envelope stress response of *Escherichia coli*. J Bacteriol **193:**3367-3375.

135. **Missiakas D, Raina S.** 1998. The extracytoplasmic function sigma factors: role and regulation. Mol Microbiol **28:**1059-1066.

136. **Missiakas D, Mayer MP, Lemaire M, Georgopoulos C, Raina S.** 1997. Modulation of the *Escherichia coli* σE (RpoE) heat-shock transcription-factor activity by the RseA, RseB and RseC proteins. Mol Microbiol **24:**355-371.

137. **Raina S, Missiakas D, Georgopoulos C.** 1995. The *rpoE* gene encoding the σE (σ24) heat shock sigma factor of *Escherichia coli*. EMBO J **14:**1043-1055.

138. **Rouviere PE, De Las Penas A, Mecsas J, Lu CZ, Rudd KE, Gross CA.** 1995. *rpoE*, the gene encoding the second heat-shock sigma factor, σE, in *Escherichia coli*. EMBO J **14:**1032-1042.

139. **Miticka H, Rowley G, Rezuchova B, Homerova D, Humphreys S, Farn J, Roberts M, Kormanec J.** 2003. Transcriptional analysis of the *rpoE* gene encoding extracytoplasmic stress response sigma factor σE in *Salmonella enterica* serovar *Typhimurium*. FEMS Microbiol Lett **226:**307-314.

140. **Raivio TL.** 2005. Envelope stress responses and Gram-negative bacterial pathogenesis. Mol Microbiol **56:**1119-1128.

141. **Paget MS, Chamberlin L, Atrih A, Foster SJ, Buttner MJ.** 1999. Evidence that the extracytoplasmic function sigma factor σE is required for normal cell wall structure in *Streptomyces coelicolor* A3(2). J Bacteriol **181:**204-211.

142. **De Las Penas A, Connolly L, Gross CA.** 1997. The σE-mediated response to extracytoplasmic stress in *Escherichia coli* is transduced by RseA and RseB, two negative regulators of σE. Mol Microbiol **24:**373-385.

143. **Jiang SS, Lin TY, Wang WB, Liu MC, Hsueh PR, Liaw SJ.** 2010. Characterization of UDP-glucose dehydrogenase and UDP-glucose pyrophosphorylase mutants of *Proteus mirabilis*: defectiveness in polymyxin B resistance, swarming, and virulence. Antimicrob Agents Chemother **54:**2000-2009.

144. **Du H, Sheng X, Zhang H, Zou X, Ni B, Xu S, Zhu X, Xu H, Huang X.** 2011. RpoE may promote flagellar gene expression in *Salmonella enterica* serovar *typhi* under hyperosmotic stress. Curr Microbiol **62:**492-500.

145. **Hayden JD, Ades SE.** 2008. The extracytoplasmic stress factor, σE, is required to maintain cell envelope integrity in *Escherichia coli*. PLoS One **3:**e1573.

146. **Armitage JP, Rowbury RJ, Smith DG.** 1975. Indirect evidence for cell wall and membrane differences between filamentous swarming cells and short non-swarming cells of *Proteus mirabilis*. J Gen Microbiol **89:**199-202.

147. **Armitage JP, Smith DG, Rowbury RJ.** 1979. Alterations in the cell envelope composition of *Proteus mirabilis* during the development of swarmer cells. Biochim Biophys Acta **584:**389-397.

148. **Raivio TL, Laird MW, Joly JC, Silhavy TJ.** 2000. Tethering of CpxP to the inner membrane prevents spheroplast induction of the *cpx* envelope stress response. Mol Microbiol **37:**1186-1197.

149. **Castanie-Cornet MP, Cam K, Jacq A.** 2006. RcsF is an outer membrane lipoprotein involved in the RcsCDB phosphorelay signaling pathway in *Escherichia coli*. J Bacteriol **188:**4264-4270.

150. **Mecsas J, Rouviere PE, Erickson JW, Donohue TJ, Gross CA.** 1993. The activity of σE, an *Escherichia coli* heat-inducible sigma-factor, is modulated by expression of outer membrane proteins. Genes Dev **7:**2618-2628.

151. **Wang R-F, Kushner SR.** 1991. Construction of versatile low-copy-number vectors for cloning, sequencing and gene expression in *Escherichia coli*. Gene **100:**195-199.

152. **Simons RW, Houman F, Kleckner N.** 1987. Improved single and multicopy *lac*-based cloning vectors for protein and operon fusions. Gene **53:**85-96.

153. **Gruber AR, Lorenz R, Bernhart SH, Neubock R, Hofacker IL.** 2008. The Vienna RNA websuite. Nucleic Acids Res **36:**W70-74.

154. **Otto K, Silhavy TJ.** 2002. Surface sensing and adhesion of *Escherichia coli* controlled by the Cpx-signaling pathway. Proc Natl Acad Sci USA **99:**2287-2292.

155. **Pearson MM, Rasko DA, Smith SN, Mobley HL.** 2010. Transcriptome of swarming *Proteus mirabilis*. Infect Immun **78:**2834-2845.

156. **Yamamoto K, Ishihama A.** 2006. Characterization of copper-inducible promoters regulated by CpxA/CpxR in *Escherichia coli*. Biosci Biotechnol Biochem **70:**1688-1695.

157. **Miller VL, Mekalanos JJ.** 1988. A novel suicide vector and its use in construction of insertion mutations: osmoregulation of outer membrane proteins and virulence determinants in Vibrio cholerae requires *toxR*. J Bacteriol **170:**2575-2583.

158. **de Lorenzo V, Herrero M, Jakubzik U, Timmis KN.** 1990. Mini-Tn5 transposon derivatives for insertion mutagenesis, promoter probing, and chromosomal insertion of cloned DNA in gram-negative eubacteria. J Bacteriol **172:**6568-6572.

159. **Kaniga K, Delor I, Cornelis GR.** 1991. A wide-host-range suicide vector for improving reverse genetics in gram-negative bacteria: inactivation of the *blaA* gene of *Yersinia enterocolitica*. Gene **109:**137-141.

160. **Chang AC, Cohen SN.** 1978. Construction and characterization of amplifiable multicopy DNA cloning vehicles derived from the P15A cryptic miniplasmid. J Bacteriol **134:**1141-1156.

161. **Wolfe AJ, Parikh N, Lima BP, Zemaitaitis B.** 2008. Signal integration by the two-component signal transduction response regulator CpxR. J Bacteriol **190:**2314-2322.

162. **Nakamura H, Yoshiyama H, Takeuchi H, Mizote T, Okita K, Nakazawa T.** 1998. Urease plays an important role in the chemotactic motility of *Helicobacter pylori* in a viscous environment. Infect Immun **66:**4832-4837.

163. **Vincze T, Posfai J, Roberts RJ.** 2003. NEBcutter: a program to cleave DNA with restriction enzymes. Nucleic Acids Res **31:**3688-3691.

164. **Khasanov FK, Zvingila DJ, Zainullin AA, Prozorov AA, Bashkirov VI.** 1992. Homologous recombination between plasmid and chromosomal DNA in *Bacillus subtilis* requires approximately 70 bp of homology. Mol Gen Genet **234:**494-497.

165. **Vagner V, Dervyn E, Ehrlich SD.** 1998. A vector for systematic gene inactivation in *Bacillus subtilis*. Microbiol **144 (Pt 11):**3097-3104.

166. **Watt VM, Ingles CJ, Urdea MS, Rutter WJ.** 1985. Homology requirements for recombination in *Escherichia coli*. Proc Natl Acad Sci U S A **82:**4768-4772.

167. **Shen P, Huang HV.** 1986. Homologous recombination in *Escherichia coli*: dependence on substrate length and homology. Genetics **112:**441-457.

168. **Shen P, Huang HV.** 1989. Effect of base pair mismatches on recombination via the RecBCD pathway. Mol Gen Genet **218:**358-360.

169. **Zhou YN, Kusukawa N, Erickson JW, Gross CA, Yura T.** 1988. Isolation and characterization of *Escherichia coli* mutants that lack the heat shock sigma factor σ32. J Bacteriol **170:**3640-3649.

170. **Rhodius VA, Suh WC, Nonaka G, West J, Gross CA.** 2006. Conserved and variable functions of the σE stress response in related genomes. PLoS Biol **4:**e2.

171. **Nishino K, Honda T, Yamaguchi A.** 2005. Genome-wide analyses of *Escherichia coli* gene expression responsive to the BaeSR two-component regulatory system. J. Bacteriol. **187:**1763-1772.

172. **Hirakawa H, Inazumi Y, Masaki T, Hirata T, Yamaguchi A.** 2005. Indole induces the expression of multidrug exporter genes in *Escherichia coli*. Mol. Microbiol. **55:**1113-1126.

173. **Greener A, Callahan M, Jerpseth B.** 1996. An efficient random mutagenesis technique using an *E. coli* mutator strain. Methods Mol Biol **57:**375-385.

174. **Greener A, Callahan M, Jerpseth B.** 1997. An efficient random mutagenesis technique using an *E. coli* mutator strain. Mol Biotechnol **7:**189-195.

175. **Yanisch-Perron C, Vieira J, Messing J.** 1985. Improved M13 phage cloning vectors and host strains: nucleotide sequences of the M13mpl8 and pUC19 vectors. Gene **33:**103-119.

176. **Hall TA.** 1999. BioEdit: a user-friendly biological sequence alignment editor and analysis program for Windows 95/98/NT. Nucleic Acids Symposium Series **41:**95-98.

177. **Gasteiger E, Hoogland C, Gattiker A, Duvaud Se, Wilkins M, Appel R, Bairoch A.** 2005. Protein identification and analysis tools on the ExPASy Server, p. 571-607. *In* Walker J (ed.), The proteomics protocols handbook. Humana Press, Totowa, N.J.

178. **Ng PC, Henikoff S.** 2003. SIFT: Predicting amino acid changes that affect protein function. Nucleic Acids Res **31:**3812-3814.

179. **Jones DT.** 1999. Protein secondary structure prediction based on position-specific scoring matrices. J Mol Biol **292:**195-202.

180. **Kelley LA, Sternberg MJ.** 2009. Protein structure prediction on the Web: a case study using the Phyre server. Nat Protoc **4:**363-371.

181. **Rasila TS, Pajunen MI, Savilahti H.** 2009. Critical evaluation of random mutagenesis by error-prone polymerase chain reaction protocols, *Escherichia coli* mutator strain, and hydroxylamine treatment. Anal Biochem **388:**71-80.

182. **Motaleb MA, Pitzer JE, Sultan SZ, Liu J.** 2011. A novel gene inactivation system reveals altered periplasmic flagellar orientation in a *Borrelia burgdorferi fliL* mutant. J Bacteriol **193:**3324-3331.

183. **Lele PP, Hosu BG, Berg HC.** 2013. Dynamics of mechanosensing in the bacterial flagellar motor. Proc Natl Acad Sci U S A **110:**11839-11844.

184. **Ferris HU, Minamino T.** 2006. Flipping the switch: bringing order to flagellar assembly. Trends Microbiol **14:**519-526.

185. **Hughes KT.** 2012. Flagellar hook length is controlled by a secreted molecular ruler. J Bacteriol **194:**4793-4796.

186. **Veening JW, Smits WK, Kuipers OP.** 2008. Bistability, epigenetics, and bet-hedging in bacteria. Annu Rev Microbiol **62:**193-210.

187. **Rauprich O, Matsushita M, Weijer CJ, Siegert F, Esipov SE, Shapiro JA.** 1996. Periodic phenomena in *Proteus mirabilis* swarm colony development. J Bacteriol **178:**6525-6538.

VANESSA MERCEE D. VARGAS
3715 Gunston Rd, Alexandria, VA, 22302 | 201-4065904 | vmdvargas@gmail.com

EDUCATION

University of Maryland, College Park
MS Marine, Estuarine and Environmental Sciences **2013**

University of the Philippines, Diliman
MS Marine Science **2009**

University of the Philippines, DIliman
BS Molecular Biology and Biotechnology **2004**
Areas of concentration: Molecular Microbiology

AWARDS

Medical University of South Carolina, College of Graduate Studies **August 2009-July 2010**
Dean's Scholarship for Doctoral Studies, Biomedical Sciences

RESEARCH AND PROFESSIONAL EXPERIENCE

University of Maryland Baltimore County **August 2010- September 2013**
Graduate Research Assistant
-Research assistant performing molecular microbiology work, laboratory and web and literature- base research, data analysis, writing research reports and publication and constructing and delivering presentations

Marine Science Institute, University of the Philippines, Diliman
Senior Research Assistant/University Research Associate 1 **September 2004 – July 2009**
-Provided technical/laboratory and extension services as well as project management and communication.

- Involved with the following project in the Harmful Algal Blooms Laboratory: (1) Study of Bacteria-Algal-Seaweed interaction, (2) Scale-up of saxitoxin production from *Pyrodinium bahamense* var *compressum*, (3) Monitoring of harmful algal blooms in the Manila Bay (4) Maintenance of bacterial and algal cultures (5) Determination of PSP toxin production of bacterial endosymbiont from *Pyrodinium bahamense* var *compressum*.

- Performed laboratory and field research as well as web and literature base research. Collected and analyzed data, wrote and prepared mid-year and year-end reports, as well as other related technical publications and presentations such as progress and terminal reports, budget management and presentations

OTHER RELATED EXPERIENCE

First National Conference on Marine Plant Biodiversity and Its Natural Products
May 2009
Secretariat/Organizing Committee
The Marine Science Institute, UP Diliman, Philippines

Second National Conference on Harmful Algal Blooms
May 2008
Secretariat/Organizing Committee
The Marine Science Institute, UP DIliman, Philippines

Pacific Seaboard 2 **August-Oct 2006**
Research assistant
Developed genetic markers for different fish species and interviewed with fishermen and Local government agencies.

Pacific Seaboard Oceanographic Cruise **June 2006**
Graduate Student
Assisted in water sample collection and chemical and biological analysis

Seventh Asia Pacific Congress on Animal, Plant and Microbial Toxin **October 2005**
Secretariat/ Organizing Committee
Plantation Bay, Mactan Island, Cebu, Philippines

PUBLICATIONS

Azanza, RV., **VMD Vargas**, K. Fukami, K. Shashank, DF. Onda, and MPV Azanza. 2013. Culturable algalytic bacteria isolated from seaweeds in the Philippines and Japan. Journal of Environmental Science and Management 1-10 (Special Issue 1-2013)

Azanza, M.P.V., R.V. Azanza, **V.M.D. Vargas**, C.T. Hedreyda. 2006. Bacterial endosymbionts of *Pyrodinium bahamense* var. *compressum*. Microbial Ecology. Vol. 52, Number 4, November 2006.

PRESENTATIONS

Papers presented in International Conferences:

1. **Vargas, Vanessa Mercee D**. and Robert Belas. Poster Presentation. cpxP Expression Changes During Swarmer Cell Differentiation. The Gordon Research Conference on Sensory Transduction in Microorganisms. Ventura Beach, California, 15-20 January 2012
2. **Vargas, Vanessa Mercee D**. and Rhodora V. Azanza. Oral Presentation. Algicidal Bacteria from areas with incidence of *Pyrodinium* toxic blooms in Sorsogon and Samar, Philippines. 13th International Conference on Harmful Algae, Hong Kong, 3-7 November 2008

3. Azanza,R., C.Ferrera, **V.M.D.Vargas,** V.Borja, N.Gatdula, K.Furuya, T.Omura and Y.Fukuyo. Oral Presentation. Two Decades of Harmful Algal Blooms in Manila Bay, Philippines. 13th International Conference on Harmful Algae, Hong Kong, 3-7 November 2008
4. Azanza,R., K.Furuya, C.Ferrera, **V.M.D.Vargas**, V.Borja, N.Gatdula, T.Omura and Y.Fukuyo. Oral Presentation. Physical conditions during the predominance of *Noctiluca scintillans* in the 24-hour phytoplankton sampling at Manila Bay, Philippines. LIPI-JSPS Joint Seminar on Coastal Marine Science. Yogyakarta, Indonesia, 3-5 August 2007.
5. Azanza,R., K.Fukami and **V.M.D.Vargas**. Oral Presentation. Algicidal bacteria in natural and cultured seaweed beds in the Philippines: Can they help alleviate harmful algal blooms/red tides? LIPI-JSPS Joint Seminar on Coastal Marine Science. Yogyakarta, Indonesia, 3-5 August 2007
6. Azanza,R., K.Fukami and **V.M.D.Vargas**. Oral Presentation. Can Seaweed monoculture/polyculture help alleviate red tide/Harmful Algal blooms? 19th International Seaweed Symposium, Kobe, Japan, March 26-31, 2007.
7. **Vargas, V.M.D**, Azanza, M.P.V., R.V. Azanza, C.T. Hedreyda. Poster presentation. Determination of PSP toxin production of bacterial endosymbiont from *Pyrodinium bahamense* var *compressum*. 7th Asia Pacific Congress on Animal, Plant and Microbial Toxin. October 24-29 2005, Plantation Bay, Mactan Island, Cebu, Philippines
8. **Vargas, V.M.D**., Azanza, M.P.V., R.V. Azanza, D. Centeno Poster presentation. Isolated Bacterial Endosymbionts from *Pyrodinium bahamense* var *compressum*. Tenth International Congress for Culture collection (ICCC-10). October 10-15 2004, Epochal Tsukuba, Tsukuba, Japan

Papers presented in National Conferences:

1. **Vargas, V.M.D**., R.V. Azanza and K. Fukami. Poster presentation. Preliminary screening of potential algicidal bacteria from Bani and Bolinao, Pangasinan, after a fish kill event. 9th National Symposium in Marine Science, Punta Villa, Iloilo City, October 24-26 2007.
2. Azanza, RV and **V.M.D Vargas**. Oral presentation. Algicidal Bacteria in Coral Reef Areas: A Review of Research Efforts in the Philippines. Mini symposium on "Coral Diseases: Global Status and Updates on Current Research by the CDWG." The Marine Science Institute, UP Diliman, January 19-20, 2007.
3. **Vargas, V.M.D.**, B. San Luis and C.T. Hedryeda. Poster presentation. Additional Phenotypic and Molecular Data to Compare Vibrio Isolates From Reference *Vibrio harveyi* (IFO 15634) and *Vibrio campbellii* (IFO 15631). 33rd Philippine Society of Microbiology (PSM) Annual Convention. April 28-30 2004, Heritage Hotel Manila

LANGUAGES

English – speak fluently and read/write with high proficiency
Filipino – Native language

MEMBERSHIPS/AFFILIATIONS

PADI (Professional Association of Diving Instructors) certified Advanced Open Water SCUBA Diver
International Society for the Study of Harmful Algae
Philippine Association of Marine Scientist
Philippine Society of Microbiologist